2020

Toward the chemical modification of polyhydroxyalkanoates using click chemistry : an investigation of desirable reaction conditions

Benjamin J. Hession

TOWARD THE CHEMICAL MODIFICATION OF POLYHYDROXYALKANOATES USING CLICK CHEMISTRY: AN INVESTIGATION OF DESIRABLE REACTION CONDITIONS

by

Benjamin J. Hession

A THESIS

Submitted in partial fulfillment of the requirements for the degree of
Master of Science
in
The Department of Chemistry
to
The School of Graduate Studies
of
The University of Alabama in Huntsville

HUNTSVILLE, ALABAMA

2020

In presenting this thesis in partial fulfillment of the requirements for a master's degree from The University of Alabama in Huntsville, I agree that the Library of this University shall make it freely available for inspection. I further agree that permission for extensive copying for scholarly purposes may be granted by my advisor or, in his/her absence, by the Chair of the Department or the Dean of the School of Graduate Studies. It is also understood that due recognition shall be given to me and to The University of Alabama in Huntsville in any scholarly use which may be made of any material in this thesis.

08/05/2020

Student Signature

Date

THESIS APPROVAL FORM

Submitted by Benjamin Hession in partial fulfillment of the requirements for the degree of Master of Science in Chemistry and accepted on behalf of the Faculty of the School of Graduate Studies by the thesis committee.

We, the undersigned members of the Graduate Faculty of The University of Alabama in Huntsville, certify that we have advised and/or supervised the candidate on the work described in this thesis. We further certify that we have reviewed the thesis manuscript and approve it in partial fulfillment of the requirements for the degree of Master of Science in Chemistry.

Carmen Scholz 08/05/20
Committee Chair

Date

Luis R. Cruz-Vera 08/05/20

08/05/20

L. John R. Foster 08/11/2020
Department Chair

08.11.2020
College Dean

David Berkowitz 8/14/2020
Graduate Dean

ABSTRACT

The School of Graduate Studies
The University of Alabama in Huntsville

Degree: Master of Science College/Dept.: Science/Chemistry

Name of Candidate: Benjamin J. Hession

Title: Toward the Chemical Modification of Polyhydroxyalkanoates Using Click Chemistry: An Investigation of Desirable Reaction Conditions

Polyhydroxyalkanoates (PHAs) are polyesters produced by many microorganisms and are used as an energy and carbon storage material within the cell. PHAs are biocompatible, biodegradable, and applicable to many fields. The spectrum of applications of PHAs can be broadened by post-polymerization chemical modification of the polymer side chain. Copper Catalyzed Azide-Alkyne Cycloaddition ("click" chemistry) can be used to bind different functional groups to these side chains. Different catalysts, solvents, and chelating nitrogenous ligands were evaluated to determine the conditions that yield 100% conversion of the side chain terminus to propargyl benzoate and propargyl acetate. Polymer analogous click conversions were performed using a synthetic PHA structural analog, poly (methylacrylate-*co*-5-bromo-1-pentene). Typical click conditions include $CuSO_4$ and sodium-*L*-ascorbate in THF, which yields a 51.3% conversion to propargyl acetate and 60.1% conversion to propargyl benzoate. Using DMF as the solvent increases the degree of conversion by 15% for both click products. The presence of some nitrogenous ligands increases the degree of conversion by roughly 30%. Using the Cu(I) species $CuBr(PPh_3)_3$ in the presence of a nitrogenous ligand consistently yields 100.0% conversion for both click products.

Abstract Approval: Committee Chair _____ 8/5/20
Date

Department Chair L. John R. Foster 08/11/2020

Graduate Dean David Berkowitz 8/14/2020

Acknowledgements

I would like to thank my advisor, Dr. Carmen Scholz, first and foremost. Your guidance, support, and dedication to my success in all aspects of graduate life were fundamental. I am so grateful for the opportunity to work with you. To my committee members, Dr. Anusree Mukherjee and Dr. Roger Cruz-Vera, thank you for your time, critiques, and for being a part of this work. I would like to thank Dr. Bernhard Vogler for your essential and continued help with the many NMR experiments performed throughout this work. It seems that nearly every chemistry graduate student has depended on your knowledge and advice at some point during their time at UAH, and I am no exception. Thank you so much for all of your help. I'd like to thank Dr. Mukherjee and her group, especially Niharika Botcha, for your collaboration on this project, and providing catalysts for me to use in my experiments. This project could not have been done without you. I would like to thank James Wolfsberger for his help with the NMR experiments and for taking time to show me around the instrument when I was not yet able to operate it. Thank you as well to Jeff Champoux for all the administrative help you have provided. I am also grateful to Sam Nkrumah-Agyeefi, for selflessly giving your advice and guidance at all odd hours.

I would like to thank my family for their love and support throughout my undergraduate and graduate years, and for allowing me the opportunities that have led me to this accomplishment. I am everything I am today because of you.

Finally, to Allison, you are within every line of this work,

and I love you so very much.

Thank you.

Table of Contents

List of Figures

List of Tables

List of Schemes

1. Introduction

Polyhydroxyalkanoates (PHAs) are a class of biodegradable polyesters that are produced by many single-celled organisms (1). PHAs are synthesized by these microorganisms when metabolic precursors like oxygen, phosphorous, or nitrogen are depleted, but carbon is still available in excess (2). This excess carbon, often in the form of sugar, glycerol, molasses, or organic acids, is converted to PHAs and held by the microorganisms as a method of energy and carbon storage (3). Due to their insolubility in water, PHA intracellular inclusion bodies are coated with lipids and proteins and stored in the cytoplasm until conditions in the cell require their metabolism to produce energy (4).

PHAs are completely biodegradable, biocompatible, and are applicable to many fields (1, 5, 6). Efforts to create biodegradable commodity plastics from renewable resources are becoming much more crucial, and PHAs have been investigated as a possible alternative (2). In addition, PHAs are compatible with living organisms, and do not cause negative effects when used *in vivo*. Their versatility has led to their use in the fields of tissue repair and regeneration, nerve regeneration, drug delivery, and medical implants (2, 7).

PHAs can be chemically modified after biosynthesis in order to broaden their spectrum of applications. Copper catalyzed azide alkyne cycloaddition (CuAAC), a method of "click" chemistry, is a technique used to attach desired functional groups and other small molecules to specific targeted sites and is an important organic synthesis tool that has been widely used for nearly two decades. Functionalizing the aliphatic side chain of PHAs using click chemistry is a relatively simple method that can be used to broaden their spectrum of potential applications. However, the advertised high degree of conversion to the desired product (8, 9) is not always observed when functionalizing PHAs in this way (10). This

project was undertaken in order to address certain shortcomings of click reactions when functionalizing PHAs, and to determine the reaction conditions necessary to consistently achieve 100% conversion of the desired click product.

1.1 Biosynthesis

1.1.1 Microorganisms, PHA Structure, Synthetic Precursors

Bacteria are the most abundant producers of PHAs, but over 300 microorganisms are capable of producing these biopolyesters (11). Bacteria are most often used for large scale production, and genetically modified microorganisms have been introduced to increase production efficiency (11). All PHAs follow the same general structure shown in Figure 1. Any variation exhibited in the PHA structure occurs in the side chain (carbon #3 in Figure 1) (10). The composition of the PHA product is largely dependent on the microorganism that is used in the synthesis, as well as the carbon sources present for the fermentation.

The simplest PHA, polyhydroxybuturate (PHB), was discovered in 1926 by Maurice Lemoigne (13). PHAs are most often categorized by the size of the aliphatic side chain on carbon #3 (Fig. 1) and are designated: short chain length (scl), medium chain length (mcl), and long chain length (lcl). In addition, carbon #3 (Fig. 1) is a chiral center and is always found in the *R* configuration (10).

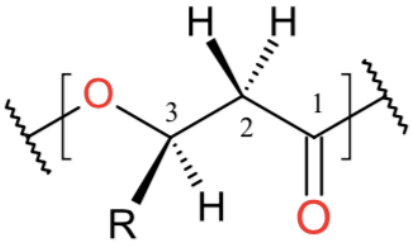

$R = (CH_2)_xCH_3$

X	PHA
0	PHB
0 -1	scl-PHA
2-10	mcl-PHA
>10	lcl-PHA

Figure 1: General structure of PHA backbone with examples of various chain lengths (10)

Several different compounds can be used as carbon sources for PHA synthesis. Usually, sugars such as glucose and sucrose are used because they are relatively inexpensive, but other substrates including fatty acids, glycerol, food and agricultural wastes like molasses and xylose, starch, cellulose, and carbon dioxide can be used (14). Over 150 monomers have been reported for use in PHA synthesis, however, the overall cost of production and polymer yield is determined by the carbon source that is used (12). Using renewable carbon sources is one of the most effective methods for decreasing production costs (6, 15).

1.1.2 Overview of Biosynthetic Pathways

The metabolic pathway used during PHA synthesis in bacteria depends on the carbon source that is used. The three most common pathways involve the metabolism of various sugars and fatty acids, while the fourth pathway, labeled "other pathways" in Fig. 2, illustrates the conversion of more complex carbon sources to PHAs (14).

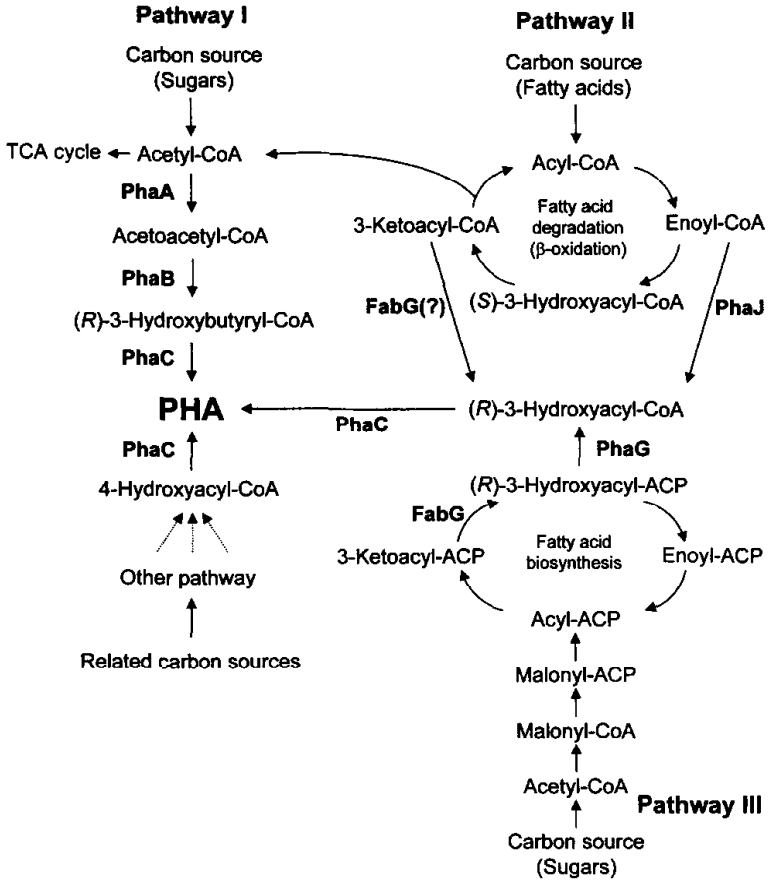

Figure 2: Common synthetic pathways involved in the production of PHAs (14)

There are several enzymes involved in PHA synthesis, but the most important is PhaC, also known as PHA synthase. This enzyme is responsible for catalyzing the polymerization of Coenzyme A-attached monomers (such as hydroxyacyl-CoA and hydroxybutyryl-CoA) into various PHAs. Due to the diversity of microorganisms that produce PHAs, there are several classes of PhaCs that have been discovered (16, 17). This PHA synthase family is divided into 4 distinct classes by their structure, substrate specificity, and subunit configurations (17). Class I PhaCs generally consist of a single subunit and produce scl polymers that are 3 to 5 carbons in length. Class I PhaCs are also capable of producing mcl polymers under certain conditions (17).

Class II PhaCs consist of one subunit but are responsible for producing medium chain length polymers from monomers produced from fatty acids and other organic acids. Two distinct members of this class are PhaC1, which has a relatively high catalytic rate, but tends to produce shorter chain length polymers, and PhaC2, which has a lower catalytic rate (17). Class III PhaCs are dimers made of one PhaC subunit and one subunit of PhaE, which greatly enhances the catalytic activity (17). Finally, Class IV PhaCs, are dimers composed of a PhaC and a PhaR subunit. These preferentially produce short chain length polymers, and also have the ability to cleave alcohols via alcoholysis, which helps regulate the chain length of the final PHA product (17, 18). Micro-organisms can also be genetically engineered to produce PHA synthases with increased catalytic activity, modified substrate specificity, and improved synthetic efficiency (19).

1.2 Biodegradation

The biodegradability of PHAs is an important factor in their role in medical applications and as potential substitutes for petroleum-based commodity plastics. PHAs are broken down to their monomeric components by PHA depolymerases, and do not require additional methods like radiation and photolysis (20). This biodegradation can take place both within and outside the cell.

Intracellular biodegradation typically occurs when the microorganism requires the metabolism of PHA inclusion bodies to produce energy. PHAs are insoluble in water and must be broken down to their water-soluble monomeric components by PHA depolymerase (21). These monomers are broken down further and converted into metabolic precursors such as acetyl-coA and are introduced into the cell's metabolic pathways (22).

Extracellular PHAs are too large to passively diffuse through the membrane of the microorganism, so they must be broken down into smaller monomeric and oligomeric components outside of the cell (23). PHA depolymerases are secreted by the microorganism into the environment, the polymer is hydrolyzed, the polymer fragments are moved from the environment into the cell, and they are metabolized to produce energy and biomass (24). Once the fragments are metabolized by the cell, they are ultimately converted to carbon dioxide and water (25).

The rate of PHA degradation in the environment depends on the microbial activity present in that environment, and microorganisms capable of degrading PHAs have been found in soil (26), lake water (27), sea water (28), and sewage sludge (29). Rates of extracellular PHA biodegradation are also dependent on the temperature, pH, and moisture level of the environment (30, 31). Sudesh and Ong have recently reported that the microbial

population in soil increases as PHAs are biodegraded, suggesting the presence of PHA is directly beneficial to the microorganisms in the environment (30).

1.3 Medical Applications

1.3.1 Overview of Medical Applications

Initially, PHAs were touted as possible alternatives for petroleum-based commodity plastics. However, there are many drawbacks and challenges that must be overcome before these PHAs become useful in this field. PHB is a very brittle and crystalline material. Its mechanical properties also tend to change with time due to secondary crystallization of the amorphous regions in the polymer, and it has a glass transition temperature near room temperature (32). Because of this, plasticizers and nucleating agents are introduced into the material to reduce the crystallinity (32). Nevertheless, PHAs are thermoplastic, and their structural and mechanical properties can be modified by changing the length of the aliphatic side chain, introducing terminal functional groups, or creating blends of different PHAs, which has led to applications in drug delivery, tissue repair and regeneration, and medical implants (7, 32-34).

Overall, the cost of production of PHAs is simply too high to validate their use as a petrol-plastic alternative (15), but their biocompatibility, biodegradability, and potential for chemical modification has led to an increase in research in its biomedical uses. (6, 7, 35).

1.3.2 Drug Delivery

The biodegradability of PHAs is a contributor to their success as drug carriers and drug delivery systems. PHAs are also hydrophobic, which allows them to be assembled into encapsulating micelles, nanoparticles, and implants. Several anticancer, contraceptive,

steroidal, antimicrobial, and anti-inflammatory drugs encapsulated in PHA particles have been developed (36). Notably, the anti-cancer drug lomustine released faster when encapsulated in a PHB microsphere compared to a poly (lactic acid) (PLA) microsphere (37). PHA microspheres were effective in the treatment of resistant bacterial infections by exhibiting sustained release of antibiotics at the site of infection in concentrations necessary to treat the infection (38). Drugs encapsulated in rod-shaped PHB and poly (3-hydroxybutyrate-co-3-hydroxyvalerate) (PHBV) implants also offer highly targeted release of medicines directly to the infection site (39).

Another method of modifiable targeted drug delivery is through the use of nanoparticles. The size of nanoparticles contributes to the ease of functionalization and modification of the particle surface, which leads to highly targeted drug delivery. Nanoparticles are also capable of delivering a wide spectrum of drugs, vaccines, proteins, and other macromolecules to these targeted sites (40). Notably, the hydrophobic and photodynamic cancer therapy agent 5,10,15,20-tetrakis(4-hydroxy-phenyl)-21H, 23H-porphine (pTHHP) was successfully encapsulated in PHA nanoparticles. These nanoparticles were assembled with diameters between 160-210 nm and loaded with 2-10% w/w pTHHP. The *in vitro* cytotoxicity of colon adenocarcinoma cells using pTHHP loaded PHA nanoparticles correlated highly to the cytotoxicity of free pTHHP (41). This result is notable because the ability to deliver drugs to highly specific target sites is a valuable attribute that increases the effectiveness and efficiency of the treatment and can limit the negative side effects of the drugs that are being administered (40).

1.3.3 Tissue Engineering

PHAs have proven to be very successful biomaterials for the regeneration and proliferation of cardiovascular, epidermal, osseous, and nerve tissue (7, 35, 42, 43). PHA scaffolds composed of PHB copolymers such as poly(3-hydroxybutyrate-*co*-3-hydroxyhexanoate) (PHBHHx) facilitate bone tissue regeneration and yield better proliferation of osteoblasts compared to PLA (44). PHBHHx blended with PHB also contributed to the increased proliferation of chondrocytes in rabbits (45). Heart valve scaffolds using porous PHA materials have been used to regenerate cardiovascular tissue, and the use of PHA scaffolds helps alleviate longer term side effects of cardiovascular implants because the polymer will eventually biodegrade and be replaced by cardiovascular tissue (46, 47).

PHAs have also been used as scaffold materials for nerve tissue regeneration. PHBHHx used as nerve regeneration conduits facilitated the cellular differentiation of bone marrow stem cells into nerve cells (48). PHB scaffolds were capable of regenerating human Schwann cells (49) and repairing peroneal nerve injuries up to 4 cm in length in rabbits (50). PHBHHx is desirable for nerve regeneration because its degradation products are non-toxic, it has high mechanical strength and flexibility, and it effectively facilitates nerve regeneration (42).

1.4 “Click” Chemistry

1.4.1 Copper Catalyzed Azide Alkyne Cycloaddition (CuAAC)

“Click” chemistry is a family of relatively simple organic reactions that are useful in synthetic chemistry. In general, click reactions involve the combination of subunits through a heteroatom linkage. By definition, all click reactions must be easy to perform under simple

reaction conditions. They must have very high yields and high selectivity with "in-offensive by-products" that can be removed without the use of chromatography (9). Also, they must be performed either without solvent or with solvent that can be easily removed. The final product must be easy to isolate and done so without the use of chromatography (9). Click chemistry was developed by Sharpless and coworkers, who described it as being "'spring-loaded' for a single trajectory" (9). The most widely used click reaction is copper(I) catalyzed azide alkyne cycloaddition (CuAAC) because it uses simple reaction conditions that yield highly regioselective products (Figure 3) (51-53).

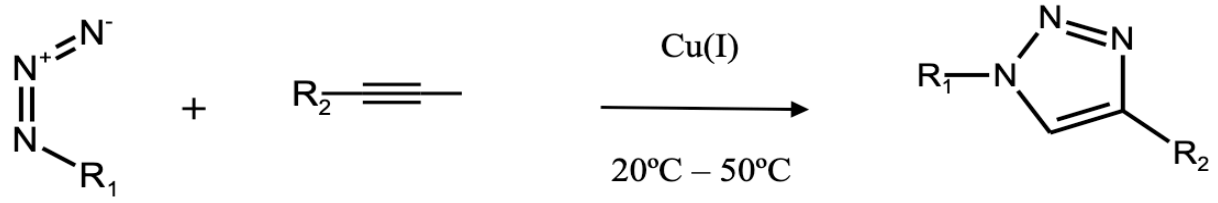

Figure 3: General reaction for Cu(I)-catalyzed azide alkyne cycloaddition (CuAAC) producing a 1,4-disubstituted 1,2,3-triazole ring as the heteroatom linkage.

The CuAAC mechanism proposed by Fokin and Finn (Figure 4) suggests the terminal alkyne is activated by Cu(I), which deprotonates the alkyne and produces Cu-acetylide. This acetylide species exists in both monomeric and dimeric forms with a second Cu(I) ion coordinating it. This second Cu(I) ion coordinates the terminal azide and activates it, causing a nucleophilic attack of the terminal nitrogen on the alkyne carbon opposite the covalently bound Cu(I) ion. A five-membered ring structure is formed. The ring contracts causing an interaction between the lone pair on the internal nitrogen and the two Cu(I) ions, liberating

one Cu ion, and producing a 1,4,5-trisubstituted triazole ring with one Cu ion still attached. The double bond at C4 (Figure 4) is then protonated, and the second Cu ion is liberated, yielding the 1,4-disubstituted 1,2,3-triazole ring and regenerating all catalyst species (54).

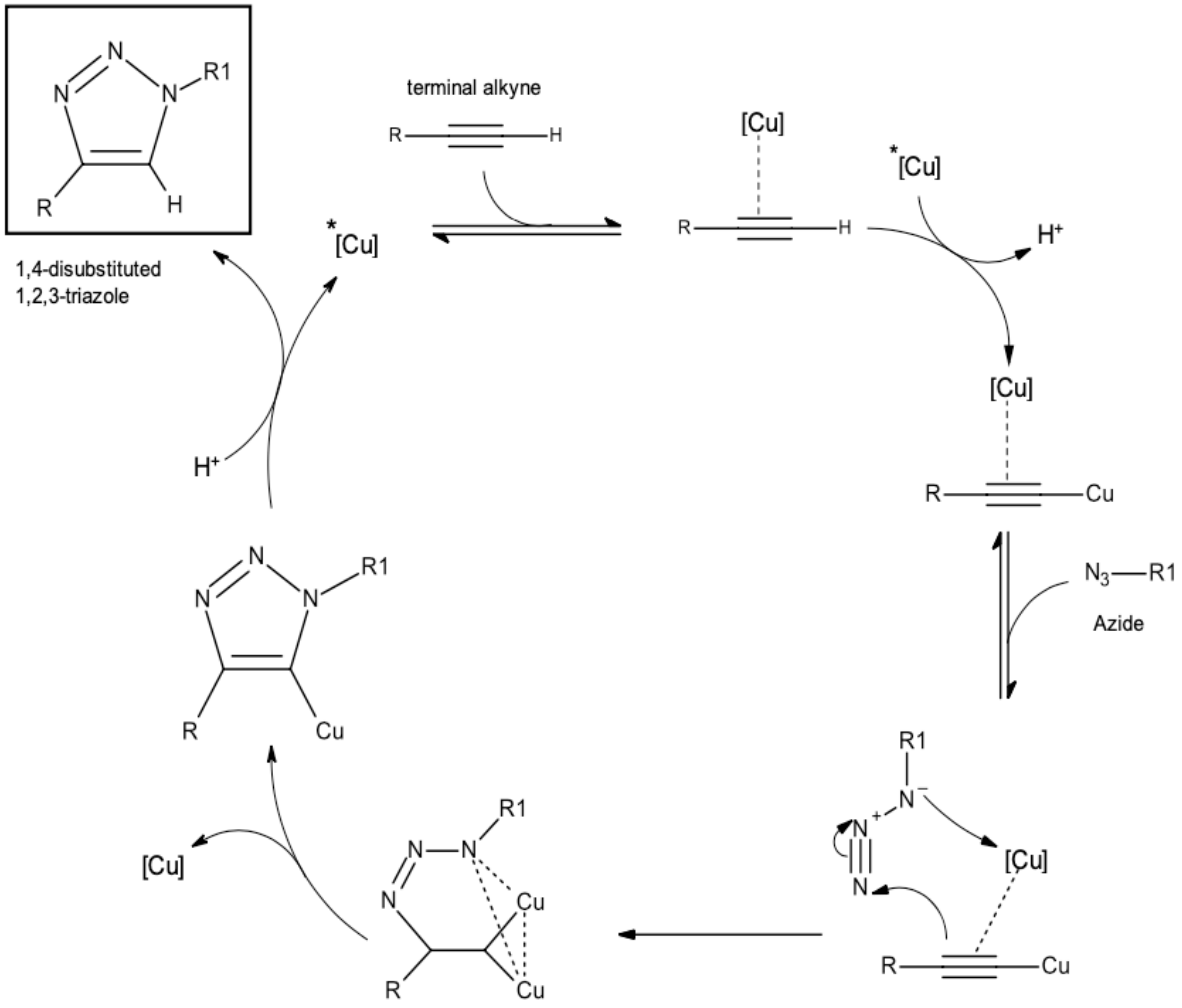

Figure 4: Proposed mechanism for the CuAAC reaction (Reproduced from Nkrumah-Agyeefi) (12)

Fokin and Finn also suggest that the rate of CuAAC reactions is accelerated by the presence of nitrogenous organic bases that function as chelating ligands, which stabilize the Cu(I) species (Figure 5) (55). The rate of reaction can increase up to $1x10^6$ times than the ligand-free reaction, but the rate increase depends on the nature and concentration of the ligand used (56). Using a concentration higher than a 1:1 ratio of ligand to copper can inhibit the reaction (56).

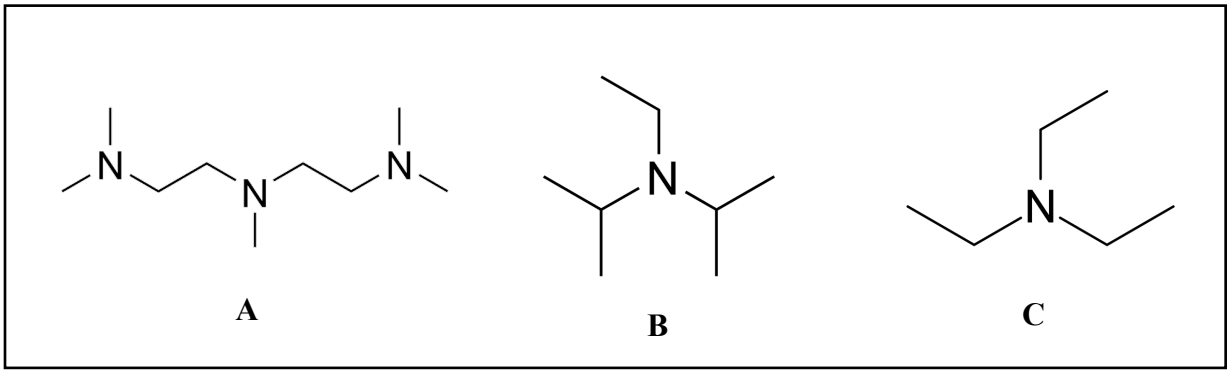

Figure 5: Structure of some chelating nitrogenous ligands used in CuAAC reactions including A) PMDETA, B) DIPEA, and C) Triethylamine

1.4.2 Chemical Modification of PHAs using "Click" Chemistry

As stated previously, most applications utilizing PHAs consist of either the pure polymer, PHA blends, or copolymers of natural PHA products. The spectrum of applications can be broadened by the addition of terminal functional groups to aliphatic side chains; however, this cannot be done during biosynthesis (57). This structural modification is important because it allows the chemical and physical properties of the polymer to be fine-tuned toward more specialized applications that cannot be achieved using the pure polymers

or blends (58). Click chemistry is considered an effective method of post-polymerization chemical modification of PHAs due to its simplicity, high yields, and high specificity. However, high conversion to the desired click product are not consistently reproducible (59). Typical click conditions include $CuSO_4 \bullet 5H_2O$ with sodium-*L*-ascorbate as a reducing agent, which is only capable of 100% conversion for certain functional groups (59).

Ultimately, the goal of this project is to investigate the click reaction conditions (solvent, catalyst, and ligand) that consistently produce 100% conversion to the desired click product regardless of the functional group that is used. This was achieved by using a structurally analogous synthetic mock copolymer, poly (methylacrylate-*co*-5-bromo-1-pentene), as the starting material. A mock copolymer was used because the biosynthesis of a click ready PHA is labor intensive and time consuming.

2. Materials

Tetrahydrofuran (THF), 5-bromo-1-pentene 96%, methanol (HPLC grade), dimethylformamide (DMF) 99%, dichloromethane (DCM) 99%, 1-propanol, hexanes 99%, 2,2'-azobis(2-methyl-propionitrile) (AIBN) 98%, (+)-sodium-*L*-ascorbate 99%, copper (II) sulfate pentahydrate 98% ($CuSO_4 \bullet 5H_2O$) , bromotris(triphenylphosphine) copper(I) 98% ($CuBr(PPh_3)_3$), N,N-diisopropylethylamine (DIPEA) 99%, triethylamine 99%, acrylic acid 99%, methyl acrylate 99%, propargyl benzoate 98%, propargyl acetate 97%, and Irgacure, were purchased from Fisher Scientific. N,N,N',N",N"-Pentamethyldiethylenetriamine (PMDETA) 98% was purchased from Tokyo Chemical Industry, America. Cu[N,N'-Dimethyl-N,N'-bis-(pyridine-2-ylmethyl)-1,2,diaminoethane]$(ClO_4)_2$ (CuBPMEN) was supplied by the Mukherjee group at UAH. All chemicals were used as received.

3. Methods

3.1 Synthesis of PHA mock copolymer, poly (methylacrylate-co-5-bromo-1-pentene) using Radical Polymerization

Methyl acrylate (0.0580 moles) and 5-bromo-1-pentene (0.0580 moles) were mixed in a round bottom flask with 30 mL of THF as the solvent. AIBN (0.1% by weight of monomers) was added to the reaction, and the mixture was stirred at 55ºC for 24 hr. THF was removed by rotary evaporation and the product was precipitated into stirred cold methanol. The polymer was re-dissolved in minimal THF, and precipitated into methanol once more, then washed with 50 mL of methanol while stirring. The polymer was allowed to dry in a fume hood and characterized by ^{1}H NMR Spectroscopy.

3.2 Bulk synthesis of PHA mock copolymer, poly (methylacrylate-co-5-bromo-1-pentene) using photoinitiated radical polymerization

Methyl acrylate (4.82 mmol) and 5-bromo-1-pentene (4.82 mmol) were combined in a 5 mL glass petri dish with 0.0071 g Irgacure. The solution was mixed and set 6 in. under a UV lamp for 1 hour. The product was visually assessed to determine if polymer had formed.

3.3 Synthesis of poly (5-bromo-1-pentene)

5-bromo-1-pentene (8.45 mmol) was placed in a round bottom flask with 15 mL THF and 5.0 mg AIBN. The solution was stirred overnight at 50ºC. The solvent was removed using rotary evaporation at 45ºC, and the product was precipitated into stirred cold methanol.

3.4 Synthesis of water soluble PHA mock copolymer, poly (acrylic acid-co-5-bromo-1-pentene)

Acrylic Acid (0.0580 moles) and 5-bromo-1-pentene (0.0580 moles) were mixed in a round bottom flask with 30 mL of THF as the solvent. AIBN (0.1% by weight of monomers) was added to the reaction, and the mixture was stirred at 55ºC for 24 hr. THF was removed by rotary evaporation and the product was precipitated into stirred cold chloroform. The polymer was re-dissolved in minimal THF, precipitated into chloroform once more, then washed with 50 mL of chloroform while stirring. The polymer was allowed to dry in a fume hood and characterized by ^{1}H NMR Spectroscopy.

3.5 Formation of azide-terminated mock copolymer, poly (methylacrylate-co-5-azido-1-pentene) by SN2 Nucleophilic Substitution of poly (methylacrylate-co-5-bromo-1-pentene)

For the conversion to the azide terminus, 400 mg of the brominated mock copolymer was dissolved in 50 mL DMF, and 100 mg (0.00153 moles) of sodium azide was added to the solution. The reaction was stirred at room temperature for 24 hr. DMF was removed by rotary evaporation using a vacuum pump at 45ºC. The product was dissolved in minimal DCM, and precipitated into stirred cold methanol, then washed with 50 mL cold methanol. The product was dried in a 60ºC oven overnight and stored in a fume hood.

3.6 Effect of Solvent, Catalyst, and Chelating Ligand on the CuAAC of the azido-mock copolymer, poly (methylacrylate-co-5-azido-1-pentene)

In a round bottom flask, 100 mg of azido-copolymer was dissolved in either 15 mL DMF or THF, and either 922.0 µL propargyl benzoate (0.00636 moles) or 809.0 µL propargyl acetate (0.00636 moles) was added. One of the following catalyst systems was used per reaction: **(1)** 1.25 mL $CuSO_4 \bullet 5H_2O$ (10 mM stock solution) and 2.5 mL sodium-*L*-ascorbate (20 mM stock solution), **(2)** 1.25 mL $[Cu(BPMEN)](ClO_4)_2$ (10 mM stock solution) and 2.5 mL sodium-*L*-ascorbate (20 mM stock solution), or **(3)** 46.5 mg $CuBr(PPh_3)_3$ (0.05 mmol) . One of the following ligands was used per reaction: **(1)** 56.7 µL DIPEA (0.00325 moles), **(2)** 45.4 µL triethylamine (0.00325 moles), **(3)** 67.9 µL PMDETA (0.00325 moles), or **(4)** no ligand was used.

Reactions were performed at 50ºC for 6 hr with vigorous stirring. DMF was removed by rotary evaporation using a vacuum pump at 45ºC. The product was washed with 50 mL hexanes to remove remaining alkyne reagent and $CuBr(PPh_3)_3$, if used. If necessary, 30 mL

of deionized water was used to wash any remaining sodium-*L*-ascorbate. The product was re-dissolved in minimal DCM and precipitated into stirred cold methanol. If no solid precipitated, then methanol was removed from this solution using rotary evaporation, the product was re-dissolved in minimal DCM, and precipitated into stirred cold 1-propanol. The product was dried in a 60ºC oven overnight and stored in a fume hood. Once dry, the click product was characterized by ^{1}H NMR Spectroscopy.

3.7 CuAAC of azido-copolymer, poly (methylacrylate-co-5-azido-1-pentene), using CuSO4•5H2O at different reaction times

In a round bottom flask, 100 mg of azido-copolymer was dissolved in 15 mL THF. Then 922.0 µL propargyl benzoate (0.00636 moles) was added, along with 1.25 mL $CuSO_4$•$5H_2O$ (10 mM stock solution), and 2.5 mL sodium-*L*-ascorbate (20 mM stock solution). The reaction was stirred vigorously for 3 hr at 50ºC. THF was removed by rotary evaporation at 45ºC. The product was washed with 50 mL hexanes to remove remaining alkyne reagent, and 30 mL of deionized water was used to wash any remaining sodium-*L*-ascorbate. The product was re-dissolved in minimal DCM and precipitated into stirred cold methanol. If no solid precipitated, then methanol was removed from this solution using rotary evaporation, the product was re-dissolved in minimal DCM, and precipitated into stirred cold 1-propanol. The product was dried in a 60ºC oven overnight and stored in a fume hood. Once dry, the click product was characterized by ^{1}H NMR Spectroscopy. This reaction was repeated using 14 hr and 22 hr reaction times.

3.8 CuAAC of azido-copolymer, poly (methylacrylate-co-5-azido-1-pentene), using CuBr(PPh3)3 at different reaction times

In a round bottom flask, 100 mg of azido-copolymer was dissolved in 15 mL DMF. Then 809.0 μL propargyl acetate (0.00636 moles) was added, along with 46.5 mg $CuBr(PPh_3)_3$ (0.05 mmol), and 56.7 μL DIPEA (0.00325 moles). The reaction was stirred vigorously for 3 hr or 6 hr at 50ºC. DMF was removed by rotary evaporation using a vacuum pump at 45ºC. The product was washed with 50 mL hexanes to remove remaining alkyne reagent and $CuBr(PPh_3)_3$. The product was re-dissolved in minimal DCM and precipitated into stirred cold methanol. If no solid precipitated, then methanol was removed from this solution using rotary evaporation, the product was re-dissolved in minimal DCM, and precipitated into stirred cold 1-propanol. The product was dried in a 60ºC oven overnight and stored in a fume hood. Once dry, the click product was characterized by ^1H NMR Spectroscopy.

3.9 Determination of cause of low yields in CuAAC reactions

100 mg of Azido-copolymer was dissolved in 15 mL DMF, and stirred for 6 hr. The solvent was removed by rotary evaporation at 45ºC using a vacuum pump. The product was re-dissolved in minimal DCM and precipitated into stirred cold methanol. The product was allowed to dry.

Azido-copolymer was placed in a glass vial loosely covered with the cap. The vial was stored overnight in a 60ºC oven to allow any remaining DCM, methanol, and any other solvents to evaporate. The total mass of the copolymer in the vial was measured. The vial

was stored in the oven overnight until the mass of polymer was constant. 100 mg of this dry azido-copolymer was then dissolved in 15 mL DMF, with 921.6 μL propargyl benzoate (0.00636 moles), along with 1.25 mL $CuSO_4 \bullet 5H_2O$ (10 mM stock solution), and 2.5 mL sodium-*L*-ascorbate (20 mM stock solution).

The reaction was stirred vigorously for 6 hr at 50ºC. DMF was removed by rotary evaporation using a vacuum pump at 45ºC. The product was washed with 50 mL hexanes to remove remaining alkyne reagent. The product was re-dissolved in minimal DCM and precipitated into stirred cold methanol. If no solid precipitated, then methanol was removed from this solution using rotary evaporation, the product was re-dissolved in minimal DCM, and precipitated into stirred cold propanol. This product was stored in a glass vial loosely covered with a cap and dried completely in a 60ºC oven to allow all solvents to evaporate. Once dry, the mass of the final click product was measured, and the polymer was characterized by H^1 NMR Spectroscopy.

3.10 Polymer Characterization using NMR Spectroscopy

All polymer products were analyzed using NMR spectroscopy and, all ^1H NMR experiments were performed in deuterated chloroform ($CDCl_3$) using a 500 MHz Varian INOVA Spectrometer with 32 scans and a relaxation delay of 1 second. All spectra were analyzed using MestReNova 14.0 software.

4. Results and Discussion

4.1 Synthesis of PHA mock copolymer, poly (methylacrylate-co-5-bromo-1-pentene) using Radical Polymerization

As mentioned previously, the biosynthesis of click-ready PHA is labor intensive and time consuming, therefore a structurally analogous synthetic mock copolymer, poly (methylacrylate-*co*-5-bromo-1-pentene), was used in the place of a brominated PHA biopolymer. The reaction for the synthesis of the mock copolymer is outlined in Scheme 1.

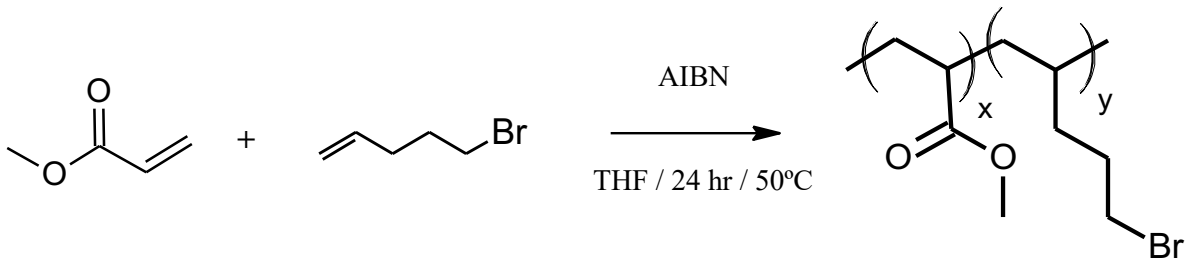

Scheme 1: Synthesis of mock polymer, poly (methylacrylate-*co*-5-bromo-1-pentene) by free radical polymerization

In order for a click reaction to be performed on a polymer it must contain either a terminal alkyne or terminal azide moiety (the conversion of poly (methylacrylate-*co*-5-bromo-1-pentene) to azide terminated poly (methylacrylate-co-5-azido-1-pentene) discussed in section 4.5). These functional groups can be present at the chain end or can form terminal side groups. In an effort to mimic the chemistries of a functionalized PHA, the mock polymer must contain a bromine at the terminus of the alkane side chain, which provides a site for the conversion from bromine to the click-ready terminal azide group by S_N2 nucleophilic substitution. The electronegativity of bromine yields a highly polar carbon-bromine bond,

and easily produces a bromide ion as a leaving group. Therefore, the bromine atom is substituted with the azide group, which establishes a click-ready reaction site at the terminus of the side chain (See section 4.5).

Several batches of the poly (methylacrylate-*co*-5-bromo-1-pentene) mock polymer were synthesized with an average polymer yield of 32.7% and an average percent bromination of 15.1% (Table 1). ^{1}H NMR spectroscopy was used to verify the polymer structure and to calculate the percent of side chains containing a terminal bromine group. Figure 6 shows an example ^{1}H NMR spectrum for the mock polymer. Peaks that correspond to the shielded methylene groups on the polymer backbone and alkane side chain are shown grouped upfield, and are distinctly separate from the methyl group adjacent to the oxygen on the methylacrylate side chain (peak D, Fig. 6, at δ=3.66 ppm), and the methylene group adjacent to the terminal bromine (peak e, Fig. 6, at δ=3.37 ppm) caused by the deshielding of the electronegative oxygen and bromine groups.

The percent of bromine-terminated alkane side chains was calculated using the integration of peak e (Fig. 6), which corresponds to 2 hydrogen atoms, and dividing by 2 to determine the total percent of brominated side chains present. The mock polymer contained an average of 15.1% brominated side chains, with a range of 13.4-17.0% (Table 1). . This result is comparable to biosynthesized brominated poly (3-hydroxynonanoate-co-3-hydroxy-11-bromoundecanoate) which contained 25% bromine-terminated side chains (59). Consequently, the remaining 85% of side chains on the polymer contain a methyl acrylate group

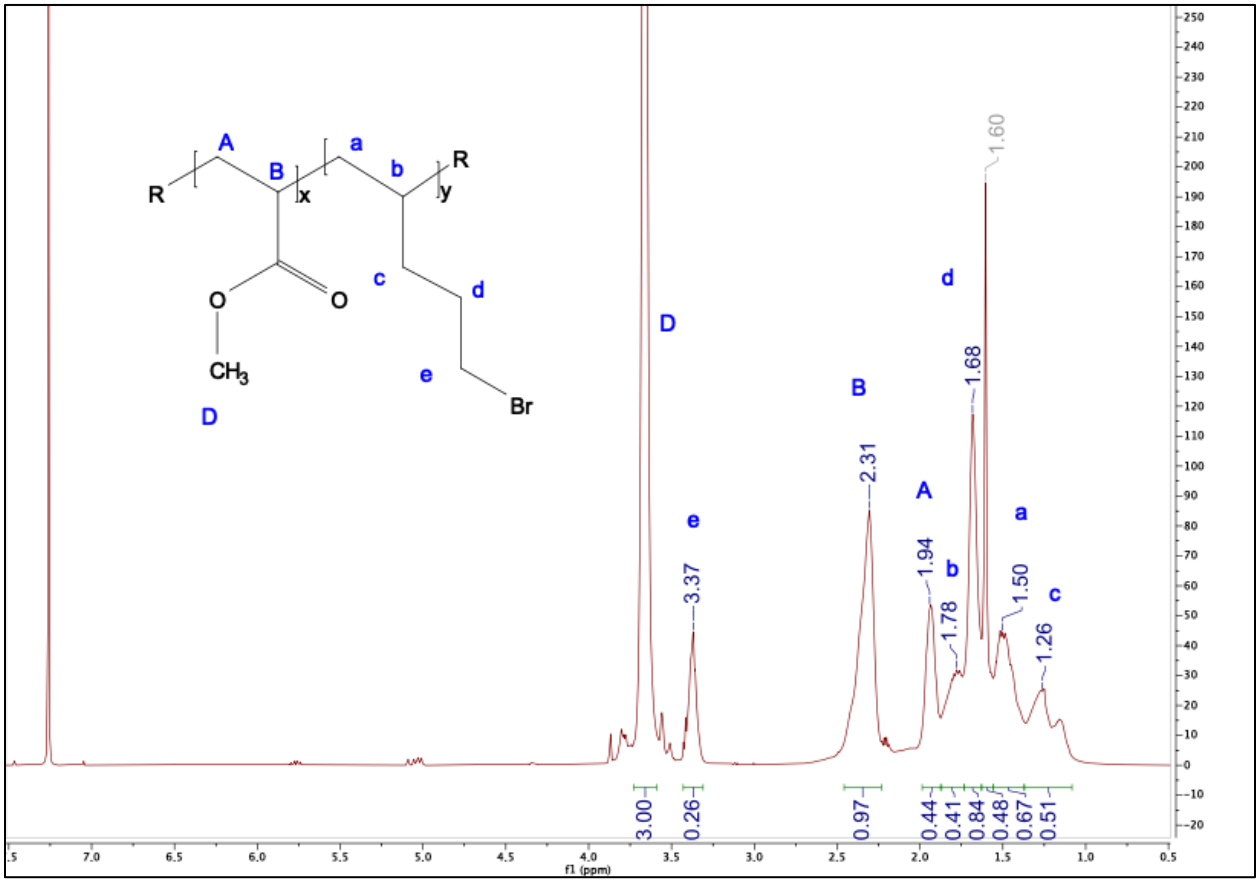

Figure 6: ^{1}H NMR spectrum of mock polymer, poly (methylacrylate-*co*-5-bromo-1-pentene)

Table 1: Summary of poly (methylacrylate-*co*-5-bromo-1-pentene) synthesis reactions

Entry	Percent Yield	Percent Bromination	NMR Spectrum Appendix Location
1	29.7%	17.0%	A1
2	38.3%	15.5%	A2
3	28.2%	13.4%	A3
4	34.6%	14.5%	A4
Average	32.7%	15.1%	

The chemical shift of peak "e" (Fig. 6) is significant because all chemical modifications throughout this work occur at the terminus of the alkane side chain that originally carried the bromine group. Subsequent polymer-analogous conversions will cause the chemical environment of the methylene group directly adjacent to the side chain terminus (peak e, Fig. 6) to change at each step of the synthesis. Therefore, the main method of determining the success of each synthesis step was by analyzing the presence and position of the peak corresponding to that particular methylene group and comparing it to the expected chemical shift. For this reason, "100% conversion" is defined as the complete disappearance of the original peak (peak e, Fig 6, at δ=3.37 ppm in this example), and reappearance in a new position based on the new chemical environment. Because there are no other peaks in Figure 6 that correspond to the methylene group "e", the number of side chains in the mock polymer containing the desired terminal bromine can be calculated. In addition, it can be determined that only bromine – and no other terminal group – is found in this position. Once this has been established, the polymer is ready for use in the next step of the synthesis.

4.2 Bulk synthesis of PHA mock polymer, poly (methylacrylate-co-5-bromo-1-pentene) using photoinitiated radical polymerization

An effort to explore other methods of radical polymerization was made to potentially increase the efficiency and reduce the amount of reagent needed for each mock polymer synthesis. Photoinitiated radical polymerization was considered because the reaction could be done in bulk (i.e., only monomer and initiator are used, and solvent is not needed), the reaction can be performed at 25ºC, and polymerization could reach completion in 1 hr compared to 24 hr needed for the AIBN initiated polymerization discussed in the Section 4.1. The reaction for the photoinitiated radical polymerization is outlined in Scheme 2.

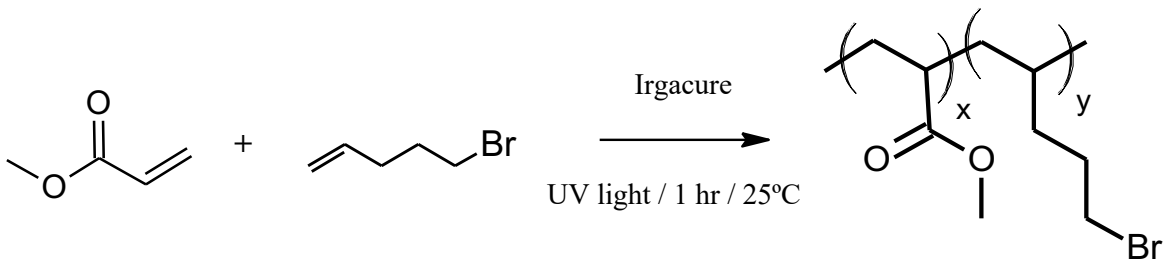

Scheme 2: Synthesis of mock polymer, poly (methylacrylate-co-5-bromo-1-pentene) by Irgacure photoinitiated free radical polymerization

The reaction mixture was set underneath a UV lamp for 1 hr, and then visually observed to determine if any polymer had formed. The expected consistency of the product is a very viscous honey-like substance, but the solution was not viscous, and still had the same consistency as the starting materials. The solution was left under the UV lamp for one more hour and observed once more. At this point, the entire solution had evaporated, and no

product had formed, so the photoinitiation reaction was considered to be a failure and was not investigated further.

4.3 Synthesis of poly (5-bromo-1-pentene)

Bulk synthesis of pure 5-bromo-1-pentene was attempted using AIBN initiated radical polymerization in order to increase the number of side chains containing a terminal bromine. Although the 15% bromination observed in poly (methylacrylate-*co*-5-bromo-1-pentene) is comparable to what is observed in brominated biosynthesized PHA, this experiment was done in order to create a starting material that allowed the click reactions to have the highest chance of success, and to determine if the total number of terminal bromine atoms present is beneficial for the conversion to the click product in the final step of the synthesis.

The reaction for the radical polymerization of poly (5-bromo-1-pentene) is outlined in Scheme 3. The reaction was performed in a similar manner as the synthesis of poly (methylacrylate-co-5-bromo-1-pentene) (see Section 4.1). The solvent was removed by rotary evaporation, and the remaining solution was added into stirred cold methanol to precipitate, however no product precipitated. Because of this, it was determined only the monomers and initiator were present in solution in their initial forms, and that no polymer had formed during the reaction.

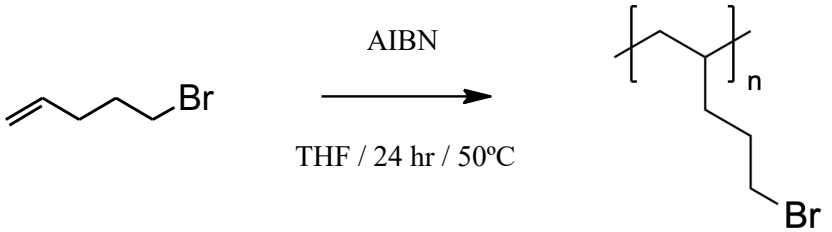

Scheme 3: Synthesis of poly (5-bromo-1-pentene) by free radical polymerization

This is possibly due to the movement of the radical within the 5-bromo-1-pentene molecule as it takes part in the polymerization reaction. While the radical is initially present at the terminal 2º carbon atom, the freedom of movement within the 5-bromo-1-pentene molecule allows the bromine group at the end of the chain to fold back on itself and interact with the carbon radical, transferring the radical to the more stable location within the CH_2-Br bond. This shift would cause the bromine radical to dissociate from the 5-bromo-1-pentene molecule, leaving the radical in the incorrect position, causing polymerization to terminate prematurely (See Scheme 4). This scenario could be theoretically favorable because the bond dissociation energy required to form a radical from an alkyl halide is much lower than the energy required to form a radical from a hydrogen on a terminal alkene, allowing the radical to exist in a more chemically stable environment that ultimately terminates the polymerization (60).

This could also act as an explanation for the lower than expected number terminal bromine groups present in the mock copolymer (15% brominated side chains) when the polymerization included a 1:1 molar ratio of methyl acrylate and 5-bromo-1-pentene monomers. However, this is not necessarily a drawback in this scenario because the number of brominated side chains in the mock copolymer is comparable to what is observed with the biosynthesized PHA.

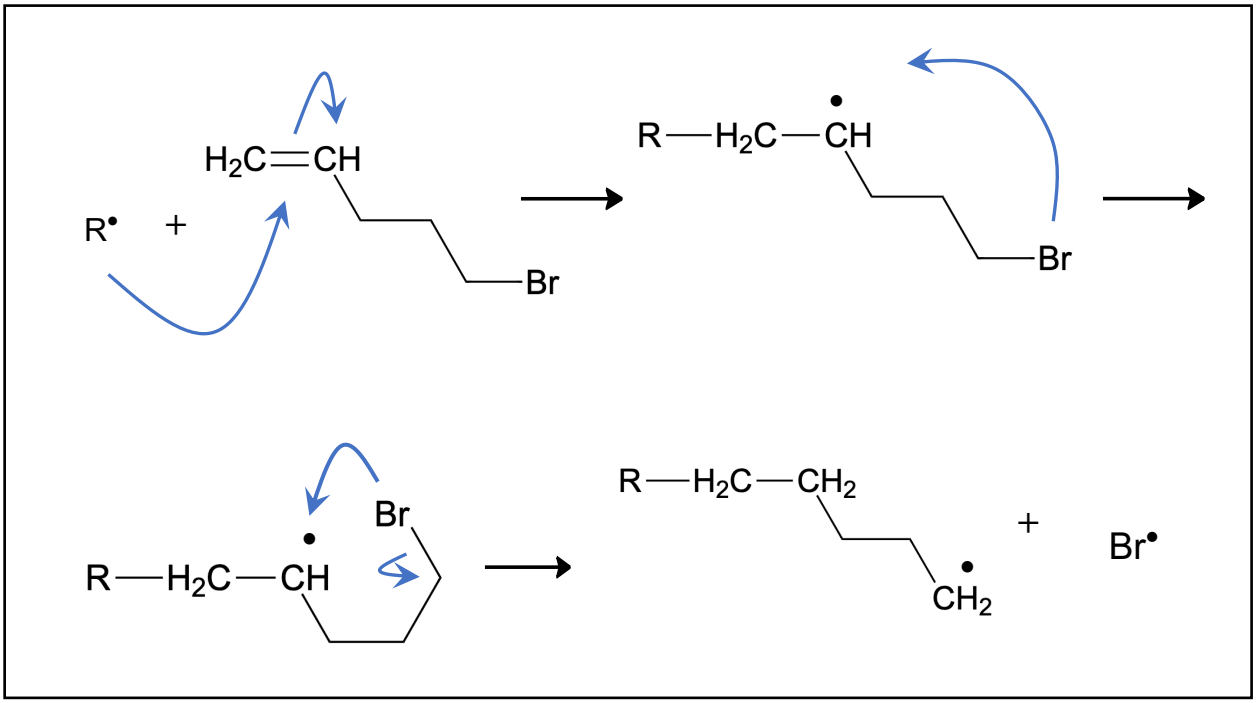

Scheme 4: Theoretical movement of radical species during the attempted polymerization of 5-bromo-1-pentene. The radical initiator is designated as " R• ". The movement of the radical electrons is designated by blue arrows.

4.4 Synthesis of poly (acrylic acid-co-5-bromo-1-pentene)

One benefit of click chemistry is that the reaction can be performed in a variety of solvents such as THF, DMF, and water. Since poly (methylacrylate-*co*-5-bromo-1-pentene) is insoluble in water, an attempt was made to synthesize a similar structurally analogous mock polymer that would be water soluble. This new mock polymer used acrylic acid and 5-bromo-1-pentene as monomer starting materials, which would allow the polymer to be soluble in water. This is an important property for the polymer to have, because the majority of PHAs are used in the biomedical field, and even if the polymer can be easily modified using click chemistry in organic solvents, the extra effort and cost associated with the removal of common organic solvents will have to be considered when scaling up to larger productions. In addition, water soluble PHAs have also been prepared (61) The reaction for the synthesis of poly (acrylic acid-co-5-bromo-1-pentene) is outlined in Scheme 5.

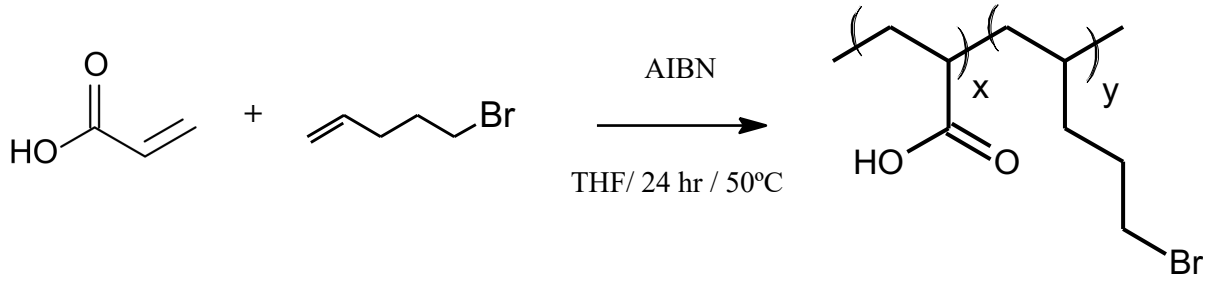

Scheme 5: Synthesis of water-soluble mock polymer, poly (acrylic acid-co-5-bromo-1-pentene) by free radical polymerization

The product was analyzed using ^{1}H NMR (Figure 7), and the percent of side chains containing a terminal bromine functional group was calculated. The final product had a percent yield of 38.4%, but the number of terminal bromine moieties was 3.5%, which is less than half of the number of terminal bromine groups typically present in poly (methylacrylate-*co*-5-bromo-1-pentene). However, poly (acrylic acid-*co*-5-bromo-1-pentene) is easily dissolved in water and methanol, which can be useful if it is possible to increase the percent of brominated side chains. Ultimately, no other substitutes for the original mock polymer poly (methylacrylate-*co*-5-bromo-1-pentene) were synthesized. Because if this, poly (methylacrylate-*co*-5-bromo-1pentene) was used as the starting material for the remainder of the click-preparation synthesis.

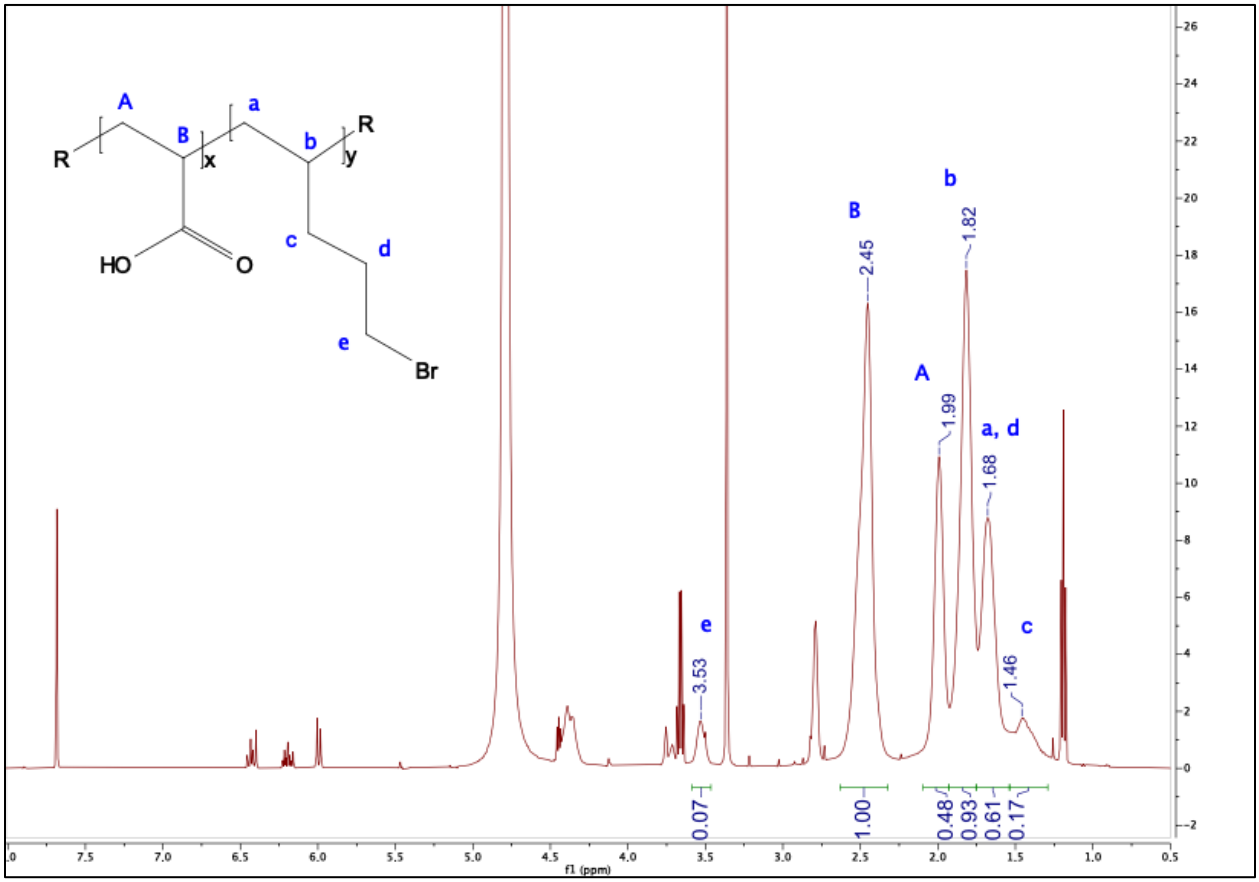

Figure 7: ^{1}H NMR spectrum of water-soluble mock polymer, poly (acrylic acid-co-5-bromo-1-pentene)

4.5 Formation of azide-terminated mock copolymer, poly (methylacrylate-co-5-azido-1-pentene) by SN2 Nucleophilic Substitution of poly (methylacrylate-co-5-bromo-1-pentene)

In order to produce the click-ready mock copolymer, the terminal bromine groups on the alkane side chain of the mock polymer were substituted with a terminal azide group. This reaction is outlined in Scheme 6.

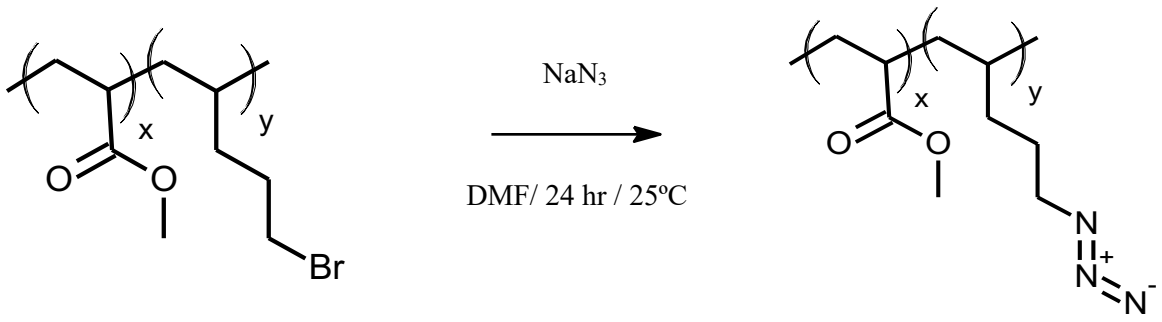

Scheme 6: Synthesis of click-ready mock polymer, poly (methylacrylate-co-5-azido-1-pentene) by S_N2 nucleophilic substitution

The average percent product yield was 63.0%, but the yields generally increased with each subsequent reaction as more effective methods of reaction preparation and product drying were implemented (Table 2). The effect of different reaction preparation and drying methods on percent yields is discussed further in section 4.8.

The most notable result of this synthesis step is the consistent complete conversion of the terminal bromine to the terminal azide functionality. The extent of conversion was determined using ^{1}H NMR spectroscopy (Figure 8), and close attention was paid again to the peak corresponding to the methylene group adjacent to the terminal azide group (peak e, Fig. 8, δ=3.25 ppm).

Initially, when a terminal bromine group was attached to the alkane side chain, this same methylene group (peak e, Fig. 6, δ=3.37 ppm) was deshielded by the electronegative bromine atom and shifted downfield. As the substitution of terminal bromine to terminal azide occurred, this peak at δ=3.37 ppm (Fig. 6) shifted upfield to δ=3.25 ppm (Fig. 8) indicating the presence of the terminal azide group, which is less deshielding than the bromine atom, and caused the adjacent methylene group (peak e) to have a smaller chemical shift (see Fig. 9). Since there is only one peak corresponding to the methylene group "e" in Figure 8, this reaction was considered to have 100.0% conversion to the terminal azide functionality and is ready to be used in subsequent click reactions once dry. This result has also been exhibited with the conversion of biosynthesized brominated PHA to click-ready azido-PHA (10).

Table 2: Summary of poly (methylacrylate-*co*-5-azido-1-pentene) synthesis reactions

Entry	Percent Yield	Percent Conversion to Azide	NMR Spectrum Appendix Location
1	46.4%	100.0%	A5
2	54.8%	100.0%	A6
3	48.3%	100.0%	A7
4	48.7%	100.0%	A8
5	49.6%	100.0%	A9
6	57.4%	100.0%	A10
7	68.6%	100.0%	A11
8	87.4%	100.0%	A12
9	81.6%	100.0%	A13
10	87.1%	100.0%	A14
Average	63.0%	100.0%	

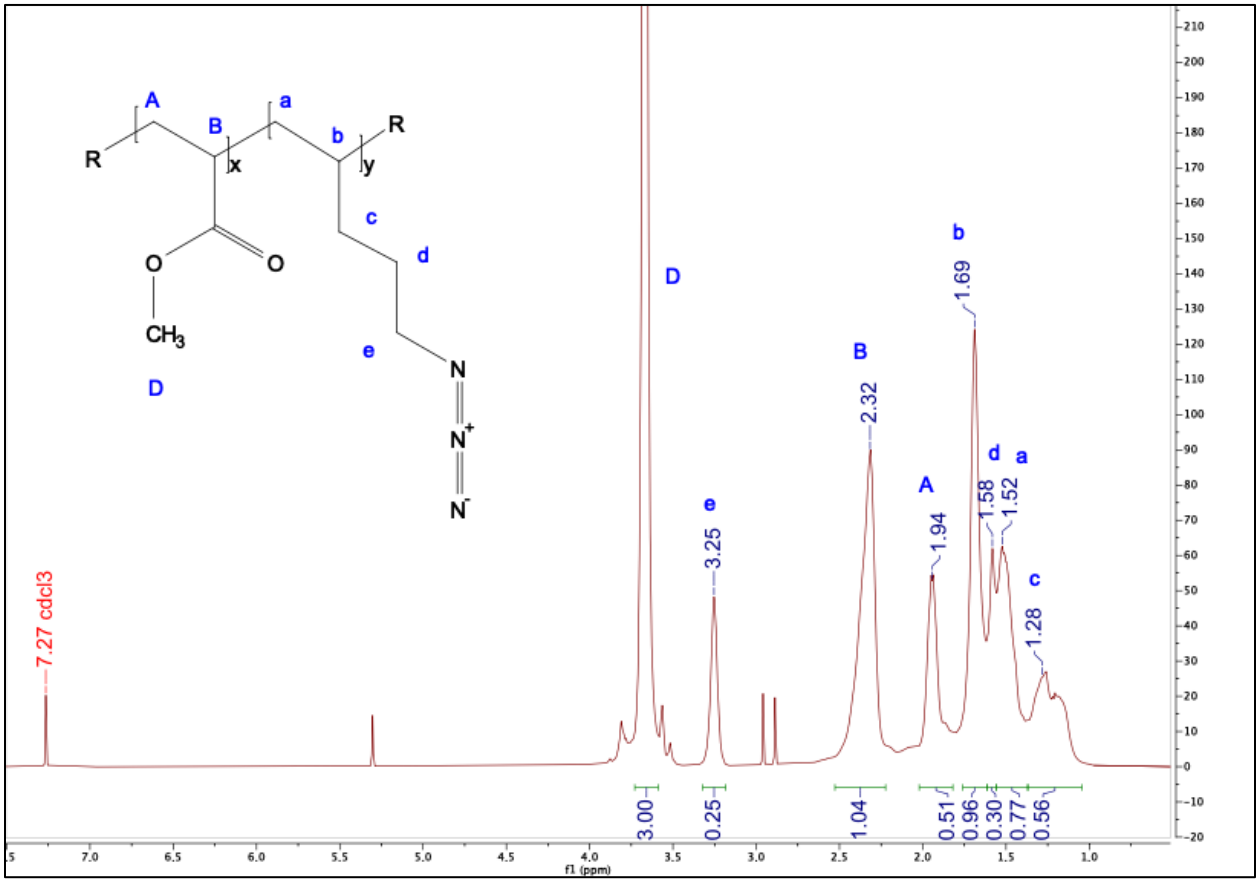

Figure 8: ^{1}H NMR spectrum of click-ready mock polymer, poly (methylacrylate-co-5-azido-1-pentene)

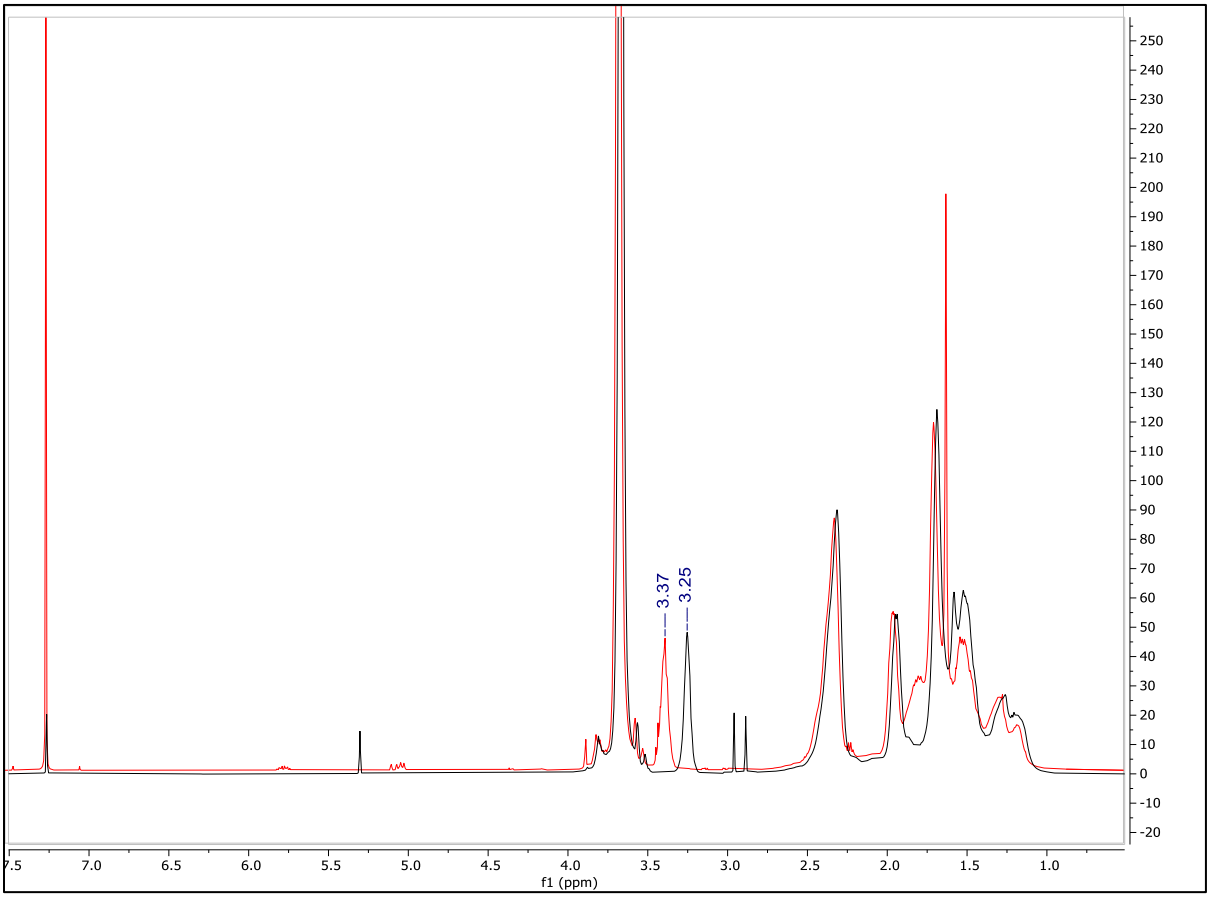

Figure 9: Overlaid ^{1}H NMR spectra of poly (methylacrylate-co-5-bromo-1-pentene) (red spectrum) and poly (methylacrylate-co-5-azido-1-pentene) (black spectrum) to show the chemical shift of the peak corresponding to the methylene group adjacent to the alkane side chain terminus

The three main barriers to successfully modifying PHAs using click chemistry are: (1) the relatively low number of side chains containing a terminal bromine group, (2) being able to substitute all terminal bromine moieties with azide moieties, and (3) successfully binding the desired functional group to all terminal azide moieties on the polymer. Although some experiments that consider increasing the percent bromination of the side chains have been discussed, the solution to overcoming this barrier is somewhat beyond the scope of this project. However, the ability to consistently convert all terminal bromine moieties to azide moieties using a simple S_N2 substitution is a valuable indicator of the usefulness of click chemistry as a PHA modification tool. This is because the success of the complete conversion of bromine to azide leaves little chance for the development of synthetic by-products, and the high percent yield indicates high reaction efficiency, both of which create a situation that contributes to overcoming the final barrier; successfully converting all azide moieties to the final click product.

4.6 Effect of Solvent, Catalyst, and Chelating Ligand on the click conversion of the azido-mock copolymer, poly (methylacrylate-co-5-azido-1-pentene)

The main goal of this project was to determine the reaction conditions (solvent, catalyst, and chelating ligand) that consistently produce 100% conversion to the desired click product regardless of the functional group that is used. Two solvents (THF and DMF), 3 catalyst systems ($CuSO_4 \bullet 5H_2O$ / sodium-*L*-ascorbate, CuBPMEN / sodium-*L*-ascorbate, and $CuBr(PPh_3)_3$), and 3 nitrogenous chelating ligands (DIPEA, PMDETA, and triethylamine) were used in these experiments and their effect on the degree of conversion to both propargyl

benzoate and propargyl acetate functional groups were assessed. The structures for the click substrates, catalysts and chelating ligands used are shown in Figure 10.

Propargyl benzoate and propargyl acetate were chosen as substrates for all click reactions because of their very different behavior in click reactions of PHAs previously observed (59). Propargyl benzoate has been shown to click successfully to PHA while propargyl acetate was shown to have a lower degree of conversion. In addition, little evidence of the successful click conversion of PHAs or PHA structural analogs with propargyl acetate is available, which means that determining the reaction conditions that facilitate 100% click conversion to the acetate functional group, a problematic click substrate, will yield beneficial new information that can be applied to other click reactions. The general reaction for the copper-catalyzed azide alkyne cycloaddition with the click-ready mock polymer is outlined in Scheme 7 and Scheme 8.

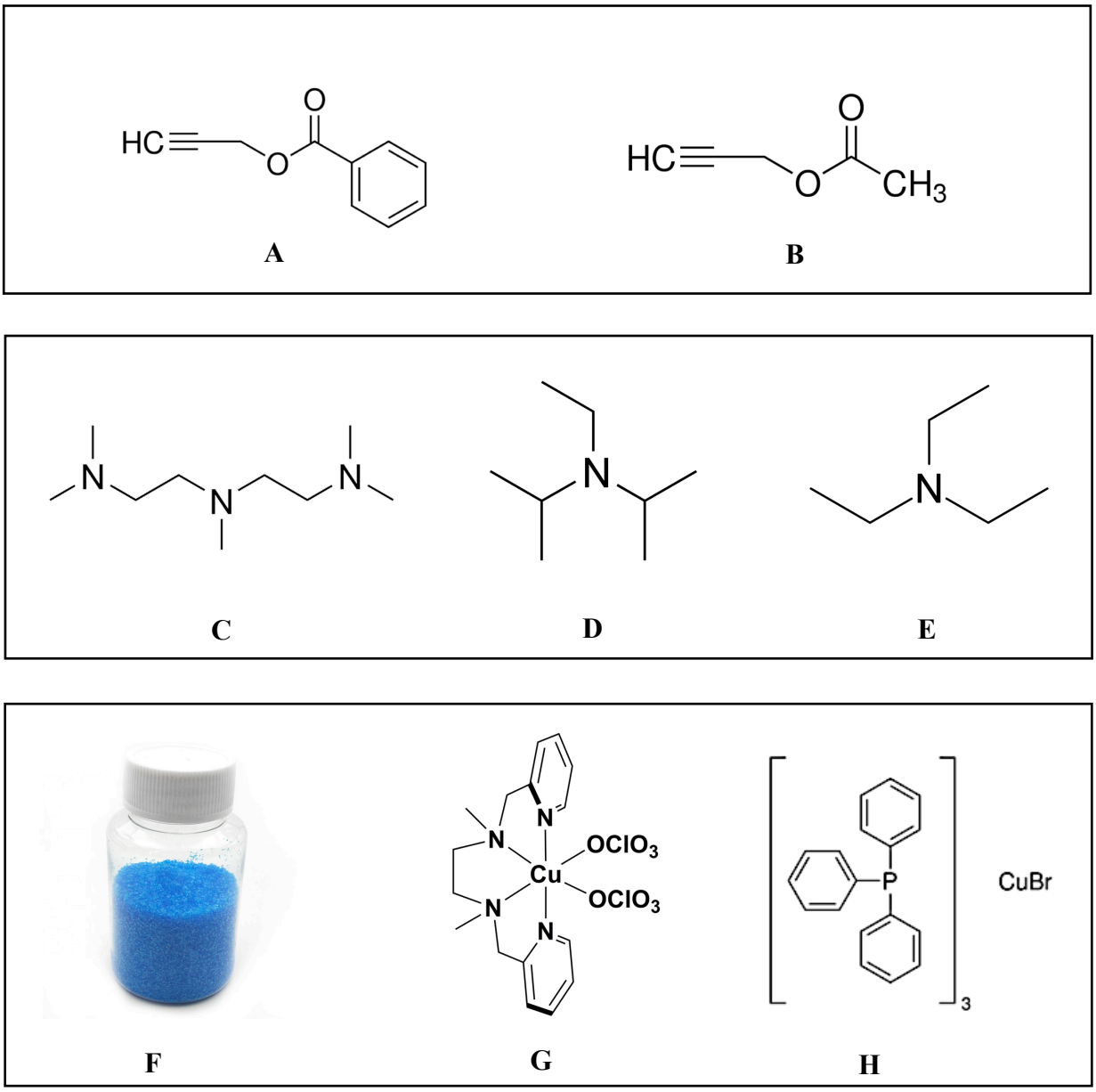

Figure 10: Structure of reagents used in CuAAC reactions including the Click Substrates: A) propargyl benzoate, and B) propargyl acetate; Chelating Nitrogenous Ligands: C) PMDETA, D) DIPEA, and E) Triethylamine; and Catalysts F) $CuSO_4 \bullet 5H_2O$, G) CuBPMEN, and H) $CuBr(PPh_3)_3$

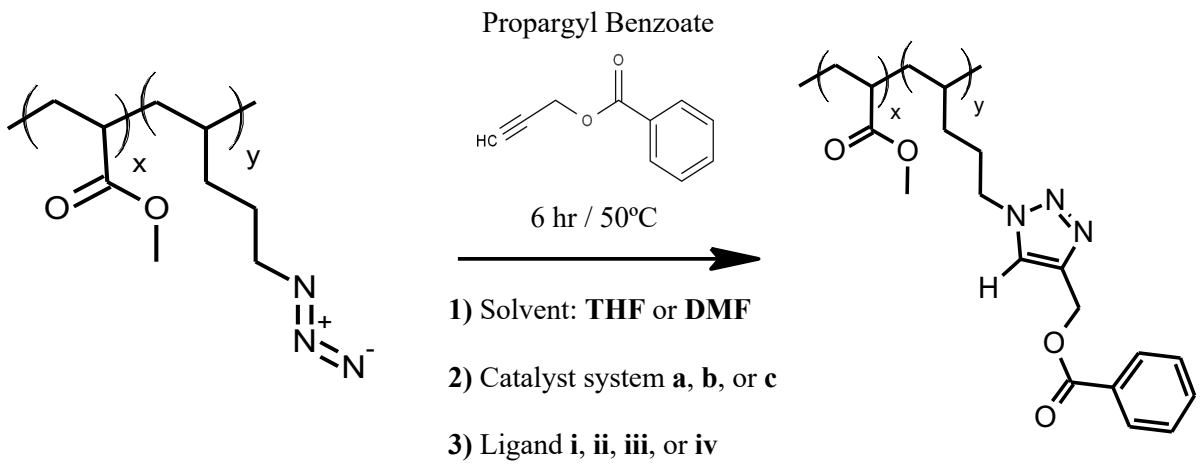

Scheme 7: CuAAC click reaction with propargyl benzoate using solvents: THF or DMF, catalyst systems: a) $CuSO_4 \bullet 5H_2O$ / Na Ascorbate, b) CuBPMEN / Na Ascorbate, or c) $CuBr(PPh_3)_3$, and Ligands: i) DIPEA, ii) PMDETA, iii) triethylamine, or iv) no ligand.

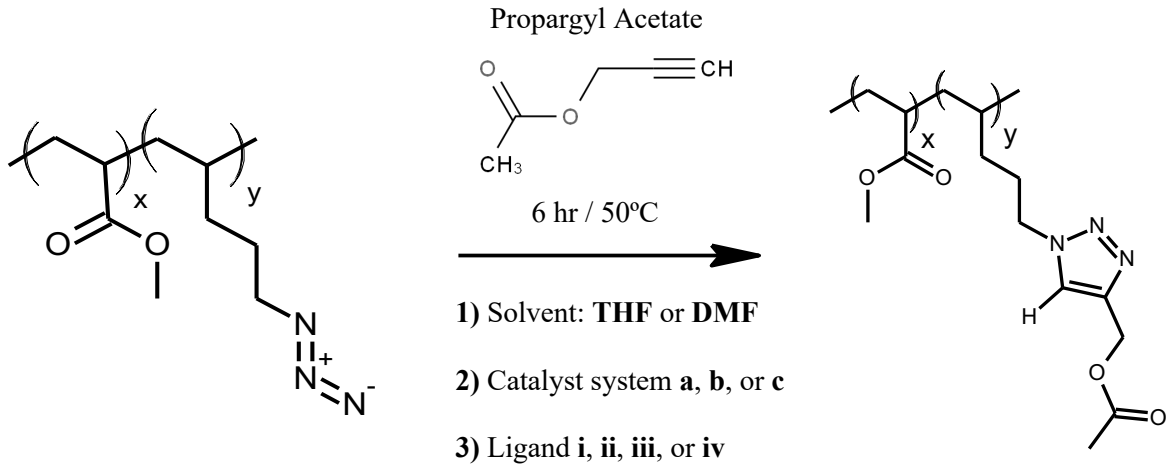

Scheme 8: CuAAC click reaction with propargyl acetate using solvents: THF or DMF, catalyst systems: a) $CuSO_4 \bullet 5H_2O$ / Na Ascorbate, b) CuBPMEN / Na Ascorbate, or c) $CuBr(PPh_3)_3$, and ligands: i) DIPEA, ii) PMDETA, iii) triethylamine, or iv) no ligand.

4.6.1 Effect of Solvent on the click conversion of the azido-mock copolymer, poly (methylacrylate-co-5-azido-1-pentene)

Initially click reactions were performed using $CuSO_4 \bullet 5H_2O$ and CuBPMEN with either DMF or THF as a solvent in order to determine the effects the solvent may have on the degree of conversion for both propargyl benzoate and propargyl acetate. The final products were analyzed using ^1H NMR spectroscopy (example spectra: Figure 11 & 12), and the percent conversion to the final click product was determined (Table 3).

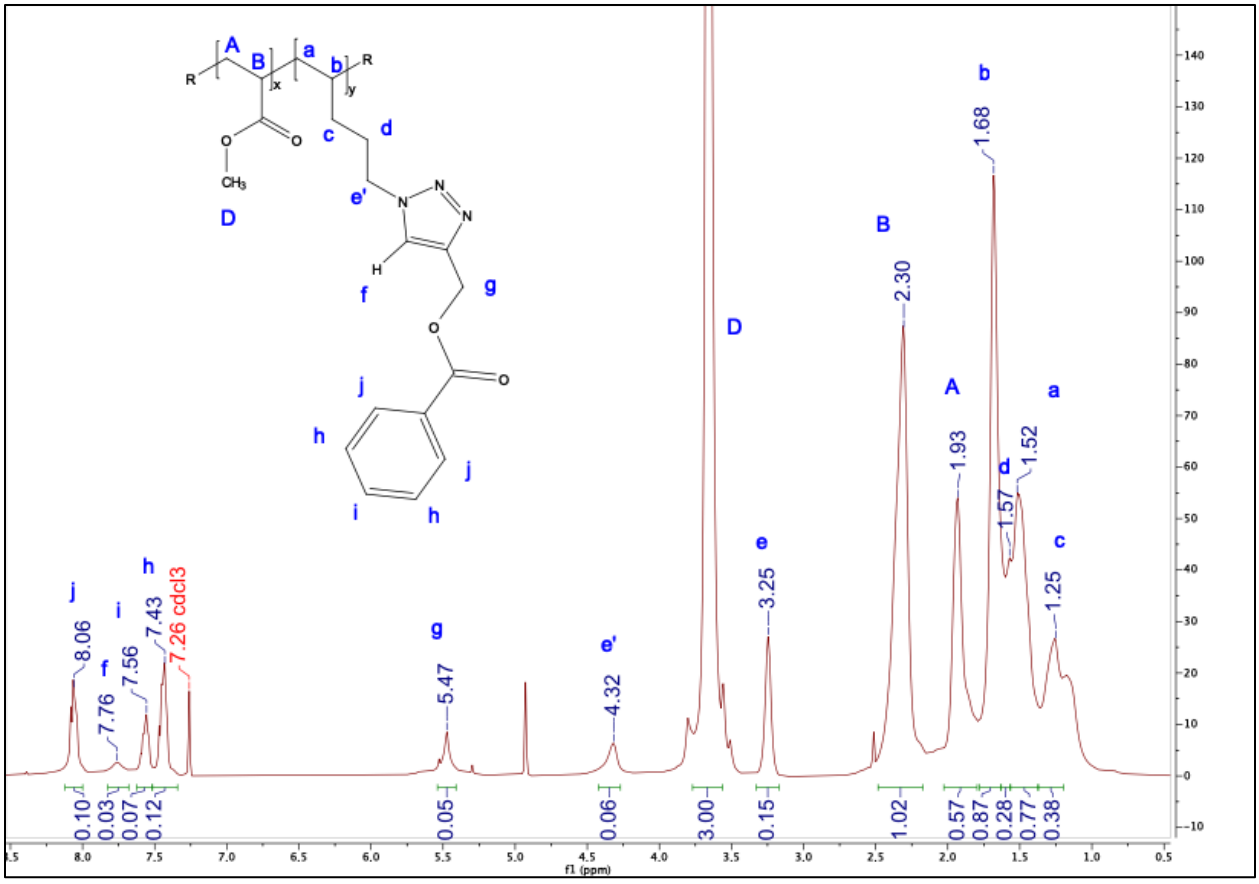

Figure 11: ^1H NMR spectrum of 1,4-disubstituted 1,2,3-triazole click product with propargyl benzoate attached. This click reaction was performed using $CuSO_4 \bullet 5H_2O$ / Na Ascorbate in THF

The presence of propargyl benzoate was confirmed by the aromatic peaks (Fig. 11, peak h at δ=7.43 ppm, peak i at δ=7.56 ppm, and peak j at δ=8.06 ppm), as well as the triazoline proton (peak f, Fig 11, δ=7.76 ppm) which signify the presence of the now-terminal benzoate group as well the formation of the 1,4-disubstituted 1,2,3-triazole ring characteristic of CuAAC reactions. The presence of the attached benzoate group is further confirmed by the appearance of the newly attached benzoate methylene group (peak g, Fig. 11, δ=5.47 ppm), which has the same integration as the alkane methylene (peak e', Fig. 11, δ=4.32 ppm).

The extent of conversion to the final click product was determined again by monitoring the presence and chemical shift of the protons on the methylene group adjacent to the alkane side chain terminus (Fig. 11, peak e, δ=3.25 ppm and peak e', δ=4.32 ppm). Figure 11 shows two peaks that represent the same methylene group, because the methylene group is present in two distinct chemical environments within the polymer. This means that some of the terminal azide from the mock polymer starting material was successfully converted to propargyl benzoate (peak e', Fig 11, δ=4.32 ppm), while some still remains in the original azide-terminated form (peak e, Fig. 11, δ=3.25 ppm, compare peak e in Figs. 8 & 11 at δ=3.25 ppm). Because some, but not all, of the side chains containing a click-ready terminal azide were converted to propargyl benzoate, the conversion is not 100% successful. The percent conversion is then determined by calculating the integration of peak e' as a percentage of the sum of the integrations of both peak e and peak e' (Fig. 11). These results are found in Table 3.

Subsequently, reactions with propargyl acetate (Scheme 8) in either THF or DMF with $CuSO_4 \bullet 5H_2O$ or CuBPMEN were performed. The ^1H NMR spectra were analyzed in a

similar way as with propargyl benzoate reactions, and the degree of conversion to the acetate-attached click product was determined. An example spectrum for the CuAAC reaction with propargyl acetate and $CuSO_4 \bullet 5H_2O$ is shown in Figure 12.

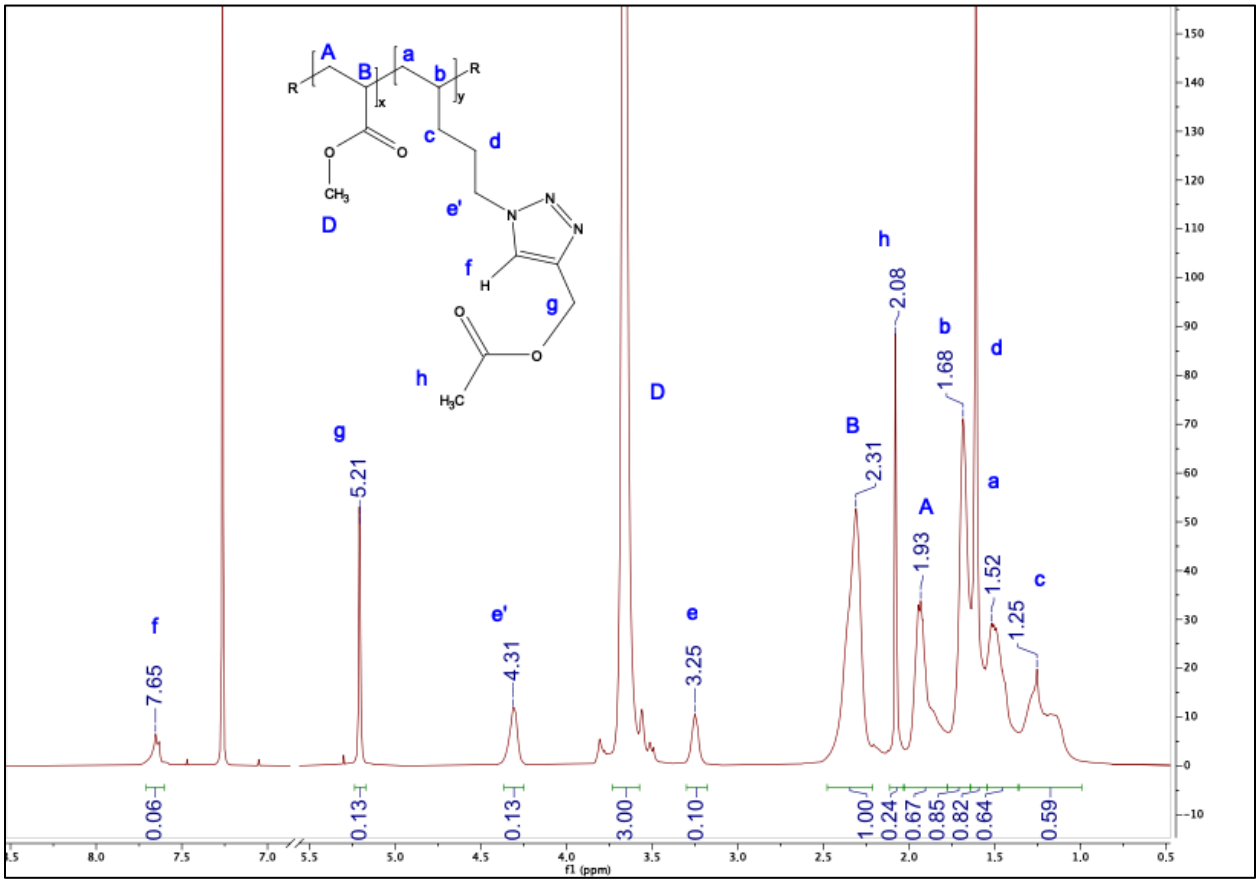

Figure 12: ^{1}H NMR spectrum of 1,4-disubstituted 1,2,3-triazole click product with propargyl acetate attached. This click reaction was performed using $CuSO_4 \bullet 5H_2O$ / Na Ascorbate in THF

The presence of the acetate functional group is confirmed by the appearance of the terminal acetate methyl group (peak h, Fig. 12, δ=2.08 ppm), the methylene group of the acetate attached to the triazole ring (peak g, Fig. 12, δ=5.21 ppm), and the single triazoline proton (peak f, Fig. 12, δ=7.65 ppm) which shows the formation of the characteristic triazole

ring. The extent of conversion to the final click product was determined by monitoring the presence and chemical shift of the protons on the methylene group adjacent to the alkane side chain terminus (Fig. 12, peak e, δ=3.25 ppm and peak e', δ=4.31 ppm; compare Figs. 11 and 12). As mentioned previously, the extent of conversion to the click product is determined using the integrations of these two peaks, (peak e and peak e', Fig. 12). Since the peak that corresponds to the presence of terminal azide (peak e, Fig. 12, δ=3.25 ppm) is present in the spectrum, it was concluded that only a portion of the click-ready terminal azide groups on the polymer were converted to propargyl acetate, and some unreacted terminal azide still remained.

The effect of solvent on the click conversion of propargyl acetate and propargyl benzoate was evaluated by performing click reactions using one of two Cu(II) catalysts ($CuSO_4 \bullet 5H_2O$ or CuBPMEN), and one of two solvents (THF or DMF). Reactions were performed at 50ºC for 6 hours and the degree of conversion to the final click product was determined. The average degree of conversion for each reaction is displayed in Figure 13.

Firstly, it is worth noting that neither propargyl benzoate or propargyl acetate consistently exhibited 100% conversion in either solvent or with either catalyst. Notably, 100% conversion was reached at least once when propargyl benzoate was clicked with CuBPMEN as a catalyst. The degree of conversion was generally the same when clicking propargyl benzoate as it was with propargyl acetate when $CuSO_4 \bullet 5H_2O$ was used as a catalyst, which does not necessarily coincide with the expected trend (10). However, the degree of conversion to propargyl benzoate was substantially higher than propargyl acetate when using CuBPMEN. In addition, reactions performed with $CuSO_4 \bullet 5H_2O$ and propargyl

benzoate had a comparable degree of conversion compared to reactions performed with CuBPMEN and propargyl benzoate, regardless of the solvent used.

The overall product yield for the click reactions was somewhat random (Table 3), but the majority of the reactions performed did not exhibit the high yields typically expected from CuAAC reactions (9). Determining the cause of this issue is discussed further in Section 4.8. In general, CuAAC reactions performed in DMF had a higher percent conversion to the click product compared to reactions performed in THF. For this reason, all subsequent CuAAC reactions were performed in DMF in order to give the best chance to achieve a higher degree of conversion.

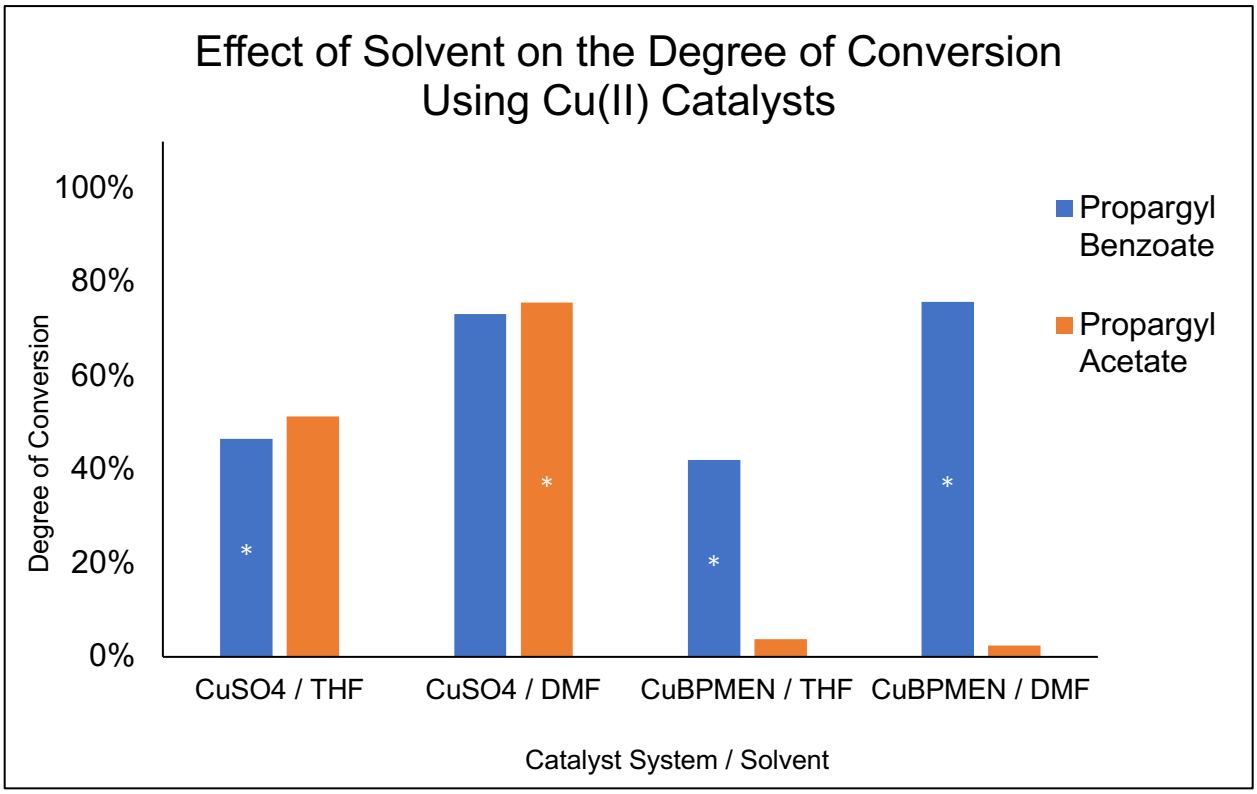

Figure 13: Average degree of conversion of poly (methylacrylate-co-5-azido-1-pentene) to the desired 1,4-disubstituted 1,2,3-triazole product with either propargyl acetate or propargyl benzoate attached using two different solvents (THF or DMF) and two different catalysts ($CuSO_4 \bullet 5H_2O$ or CuBPMEN). Reactions were performed either in duplicate or in triplicate. Triplicate reactions denoted by "*".

Table 3: Summary of CuAAC synthesis reactions to determine effects of solvent on the extent of conversion to the desired click product. All reactions were performed for 6 hr.

Entry	Click Substrate	Catalyst System	Solvent	Yield (%)	Degree of Conversion (%)	NMR Spectrum Appendix Location
1	Benzoate	$CuSO_4$ / Sodium Ascorbate	THF	78.80%	91.67%	A15
2	Benzoate	$CuSO_4$ / Sodium Ascorbate	THF	60.15%	28.57%	A16
3	Benzoate	$CuSO_4$ / Sodium Ascorbate	THF	70.72%	19.23%	A17
4	Benzoate	$CuSO_4$ / Sodium Ascorbate	DMF	24.70%	78.27%	A18
5	Benzoate	$CuSO_4$ / Sodium Ascorbate	DMF	46.19%	68.18%	A19
6	Benzoate	CuBPMEN / Sodium Ascorbate	THF	36.01%	8.33%	A20
7	Benzoate	CuBPMEN / Sodium Ascorbate	THF	100.00%	100.00%	A21
8	Benzoate	CuBPMEN / Sodium Ascorbate	THF	22.09%	17.86%	A22
9	Benzoate	CuBPMEN / Sodium Ascorbate	DMF	14.43%	27.27%	A23
10	Benzoate	CuBPMEN / Sodium Ascorbate	DMF	52.59%	100.00%	A24
11	Benzoate	CuBPMEN / Sodium Ascorbate	DMF	53.42%	100.00%	A25
12	Acetate	$CuSO_4$ / Sodium Ascorbate	THF	29.83%	46.15%	A26
13	Acetate	$CuSO_4$ / Sodium Ascorbate	THF	33.75%	56.52%	A27
14	Acetate	$CuSO_4$ / Sodium Ascorbate	DMF	22.30%	95.65%	A28

15	Acetate	$CuSO_4$ / Sodium Ascorbate	DMF	-	36.36%	A29
16	Acetate	$CuSO_4$ / Sodium Ascorbate	DMF	96.62%	94.74%	A30
17	Acetate	CuBPMEN / Sodium Ascorbate	THF	13.42%	3.85%	A31
18	Acetate	CuBPMEN / Sodium Ascorbate	THF	96.09%	3.83%	A32
19	Acetate	CuBPMEN / Sodium Ascorbate	DMF	34.49%	3.85%	A33
20	Acetate	CuBPMEN / Sodium Ascorbate	DMF	38.09%	1.00%	A34

4.6.2 Effect of Catalyst on the click conversion of the azido-mock copolymer, poly (methylacrylate-co-5-azido-1-pentene)

Click reactions rely on a Cu(I) oxidation state to for catalysis, but Cu(I) species often oxidize readily to Cu(II) when exposed to air, and can be difficult to work with because they require specific reaction conditions, such as being used under inert gas, in order to effectively stabilize the metal center in the correct oxidation state. This scenario fails two criteria typically associated with click reactions: that the reactions and reaction setups should be simple, and that the reactants should be unaffected by the presence of oxygen and water. This has led to the implementation of $CuSO_4 \bullet 5H_2O$, a Cu(II) species, and sodium-*L*-ascorbate, a common reducing agent as the typical catalyst system for CuAAC reactions, because these reagents are cost effective, readily available, more resilient to environmental factors, and generally produce the desired results.

However, as discussed in section 4.6.2, Cu(II) species are not capable of consistently producing 100% conversion of the PHA analogous mock polymer to the desired click product regardless of solvent or click substrate used. Therefore, introducing different catalysts may increase the degree of conversion. In order to determine this, the click reactions performed in DMF using $CuSO_4 \bullet 5H_2O$ and CuBPMEN were compared to reactions performed with $CuBr(PPh_3)_3$ using both click substrates.

$CuBr(PPh_3)_3$ is a Cu(I) species that is stabilized by three triphenylphosphine groups that protect the metal center from oxidation (See Fig. 10H). This allows the Cu(I) metal complex to be relatively stable in air and does not require the addition of sodium ascorbate as a reducing agent. The reactions using $CuBr(PPh_3)_3$ were performed under the same conditions as previous reactions (6 hr at 50ºC), and the final product was analyzed using ^1H

NMR spectroscopy. An example spectrum of the click reaction using $CuBr(PPh_3)_3$ is shown in Figure 14.

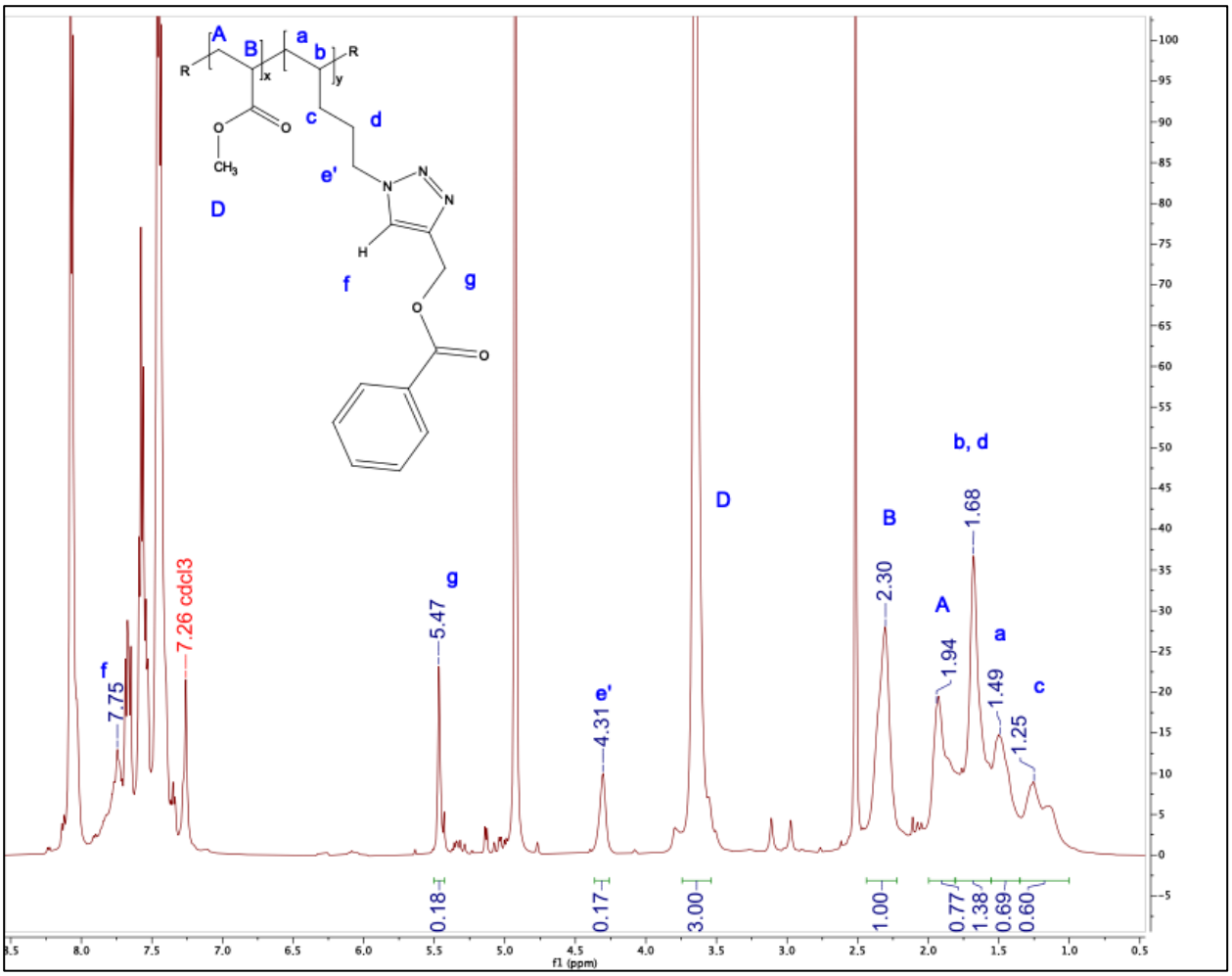

Figure 14: ^1H NMR spectrum of 1,4-disubstituted 1,2,3-triazole click product with propargyl benzoate attached. This click reaction was performed using $CuBr(PPh_3)_3$ in DMF

Figure 14 shows the expected peaks that correspond to the presence of the triazole ring (peak e' at 4.31 ppm, peak f at 7.75 ppm, and peak g at 5.47 ppm), which confirms that the reaction did occur as expected. However, the aromatic peaks typically associated with

triphenylphosphine occur at a similar chemical shift as the aromatic peaks expected from the newly clicked benzoate functional group, causing an overlap, and making it impossible to definitively identify the benzoate peaks. Because of this, the presence of the clicked benzoate can only be confirmed by the triazole peaks mentioned previously (Fig. 14, peak e' at δ4.31 ppm, and peak g at δ=5.47 ppm). The presence of reactants left over from the reaction is due to washing methods that are not completely effective at removing all excess reagents. Typical washes were done in methanol, 1-propanol, hexanes, and water, but $CuBr(PPh_3)_3$ is either insoluble or only partially soluble in these solvents and would not wash off the product easily (62). However, $CuBr(PPh_3)_3$ is more soluble in other organic solvents such as ethanol, 2-propanol, benzene, and toluene (62). Washing with either of these solvents may improve the purity of the final product and make the confirmation of the clicked benzoate peaks easier to achieve.

In addition, the click product referred to in Figure 14 shows only one peak (peak e') that corresponds to the methylene group adjacent to the alkane side chain terminus. For this reason, it was concluded that all methylene groups in that position had the same chemical environment, and that all available terminal azide moieties were converted to the desired click product (compare Figures 11 and 14). One hundred percent conversion was only consistently observed when using propargyl benzoate and $CuBr(PPh_3)_3$, and the average degree of conversion with propargyl acetate and $CuBr(PPh_3)_3$ was 81.82% (Figure 15). A summary of the data in this study is found in Table 4.

The degree of conversion consistently reaches 100% when using $CuBr(PPh_3)_3$ and propargyl benzoate, but this consistency is not exhibited when using $CuBr(PPh_3)_3$ and propargyl acetate, which has an average degree of conversion of 81.82%, only a 6.24%

increase from the standard catalyst, $CuSO_4 \bullet 5H_2O$. Reactions performed in CuBPMEN had a comparable degree of conversion compared to $CuSO_4 \bullet 5H_2O$, but a significantly higher degree of conversion was exhibited with propargyl benzoate (75.76 % conversion) versus propargyl acetate (2.43 % conversion). Therefore, it was concluded that performing click reactions with a catalyst that is initially held stable in the Cu(I) state improves the degree of conversion of the click reaction.

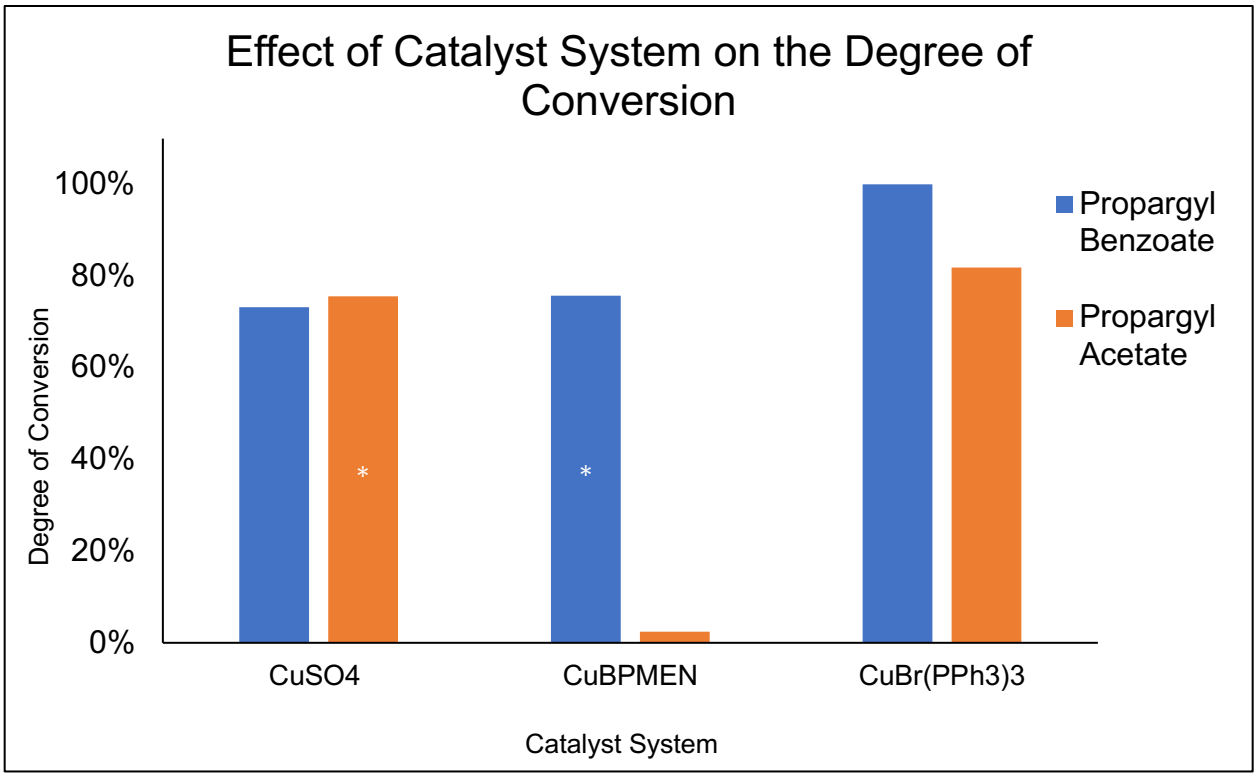

Figure 15: Average degree of conversion of poly (methylacrylate-co-5-azido-1-pentene) to the desired 1,4-disubstituted 1,2,3-triazole product in DMF with either propargyl acetate or propargyl benzoate attached using three different catalysts ($CuSO_4 \bullet 5H_2O$, CuBPMEN, or $CuBr(PPh_3)_3$). Reactions were performed either in duplicate or in triplicate. Triplicate reactions denoted by "*".

Table 4: Summary of CuAAC synthesis reactions to determine effects of catalyst system on the degree of conversion to the desired click product

Entry	Click Substrate	Catalyst System	Yield (%)	Degree of Conversion (%)	NMR Spectrum Appendix Location
1	Benzoate	$CuSO_4$ / Sodium Ascorbate	24.70%	78.27%	A18
2	Benzoate	$CuSO_4$ / Sodium Ascorbate	46.19%	68.18%	A19
3	Benzoate	CuBPMEN / Sodium Ascorbate	14.43%	27.27%	A23
4	Benzoate	CuBPMEN / Sodium Ascorbate	52.59%	100.00%	A24
5	Benzoate	CuBPMEN / Sodium Ascorbate	53.42%	100.00%	A25
6	Acetate	$CuSO_4$ / Sodium Ascorbate	22.30%	95.65%	A28
7	Acetate	$CuSO_4$ / Sodium Ascorbate	-	36.36%	A29
8	Acetate	$CuSO_4$ / Sodium Ascorbate	96.62%	94.74%	A30
9	Acetate	CuBPMEN / Sodium Ascorbate	34.49%	3.85%	A33
10	Acetate	CuBPMEN / Sodium Ascorbate	38.09%	1.00%	A34
11	Benzoate	$CuBr(PPh_3)_3$	-	100.00%	A35
12	Benzoate	$CuBr(PPh_3)_3$	97.43%	100.00%	A36
13	Acetate	$CuBr(PPh_3)_3$	85.30%	63.63%	A37
14	Acetate	$CuBr(PPh_3)_3$	92.94%	100.00%	A38

4.6.3 Effect of Chelating Ligands on the click conversion of the azido-mock copolymer, poly (methylacrylate-co-5-azido-1-pentene)

Fokin and Finn suggest that the introduction of organic bases that act as chelating ligands will stabilize the Cu(I) species during CuAAC reactions (55). It was hypothesized that the stabilization of the Cu(I) species in click reactions could also increase the degree of conversion to the desired click product for PHA analogous conversions. The effect of three different chelating nitrogenous ligands (DIPEA, PMDETA, and triethylamine (see Figure 10 c-e)) on the degree of conversion of the PHA analogous mock polymer were evaluated. Reactions were performed with either propargyl acetate or propargyl benzoate in DMF. Figure 16 shows the degree of conversion to propargyl benzoate exhibited for each of the 3 chelating ligands compared to the degree of conversion observed when no ligand is present in the reaction.

The most notable result exhibited in Figure 16 was the consistent complete conversion exhibited by all reactions performed with $CuBr(PPh_3)_3$ as a catalyst, regardless of the ligand or click substrate that was used. In addition, the presence of any of the three ligands increased the degree of conversion for propargyl benzoate for each of the three catalysts. Some conditions displayed small increases (5.34% increase for $CuSO_4 \bullet 5H_2O$ with PMDETA), and other conditions produced much larger increases (36.36% increase for CuBPMEN with triethylamine) compared to the control reactions performed with no ligand present.

Although the reason for the differing ability of these ligands cannot be determined solely from these experiments, the relatively low degree of conversion observed when PMDETA was present in $CuSO_4 \bullet 5H_2O$ click reactions is significant, especially when both

DIPEA and triethylamine produced an average degree of conversion of 100%. The same is true for DIPEA present in reactions performed with CuBPMEN, which had a relatively low degree of conversion compared to PMDETA and triethylamine, both of which yielded at or near 100% conversion to propargyl benzoate.

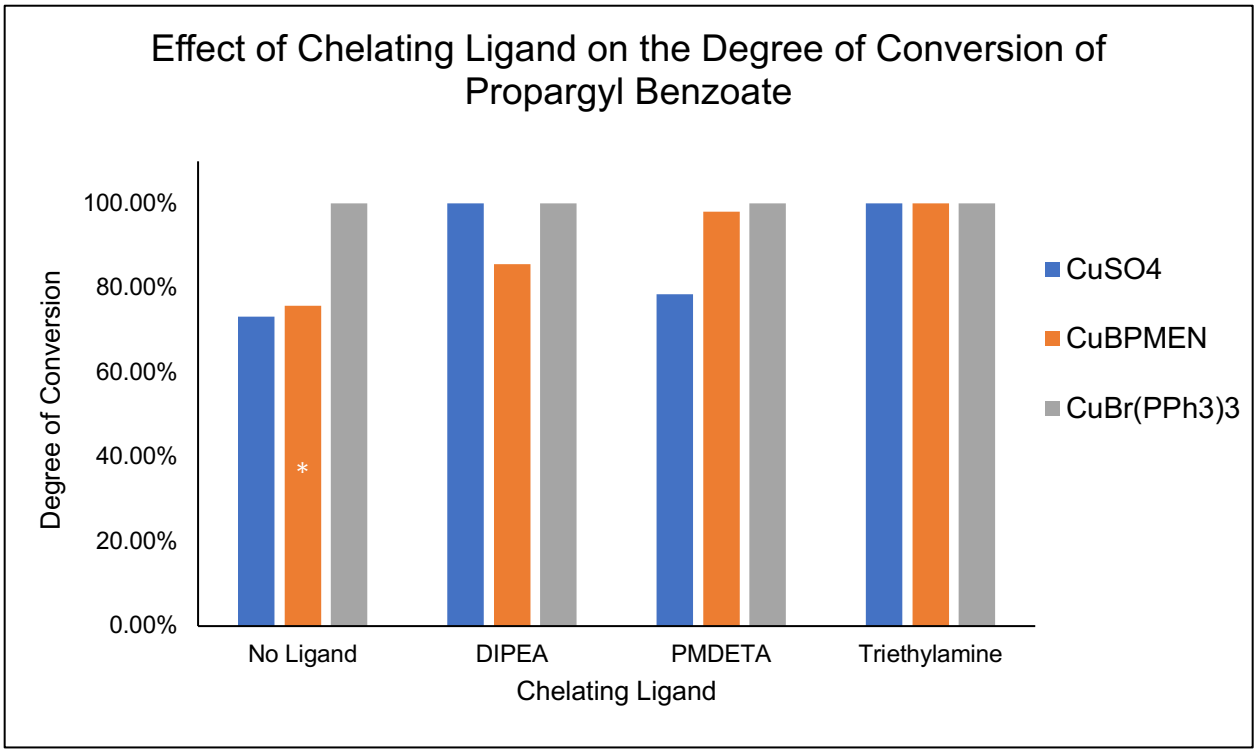

Figure 16: Average degree of conversion of poly (methylacrylate-co-5-azido-1-pentene) to the 1,4-disubstituted 1,2,3-triazole product with propargyl benzoate attached, using one of three different chelating ligands (DIPEA, PMDETA, or triethylamine) and one of three different catalysts ($CuSO_4 \bullet 5H_2O$, CuBPMEN, and $CuBr(PPh_3)_3$) per reaction. All reactions were performed in DMF. Reactions were performed either in duplicate or in triplicate. Triplicate reactions denoted by "*".

The trend of generally positive effects exhibited when a ligand is present in the reaction is not observed when considering click reactions with propargyl acetate as a substrate. Figure 17 shows the degree of conversion to propargyl acetate exhibited for each of the 3 chelating ligands compared to the conversion observed when no ligand is present in the reaction. Again, 100% conversion is observed when $CuBr(PPh_3)_3$ is used in the presence of either of the three ligands, which is the most important result of this work. The significance of reproducible complete conversion to propargyl acetate suggests that the use of a catalyst initially present in the Cu(I) oxidation state such as $CuBr(PPh_3)_3$ that is further stabilized by a chelating ligand such as DIPEA, PMDETA, or triethylamine is necessary. Obviously, 100% conversion to propargyl benzoate was achieved under several conditions (Figure 16), but the conversion of the most stubborn click substrates like propargyl acetate require the presence of a catalyst like $CuBr(PPh_3)$. A summary of the data produced for this study is found in Table 5.

Some significant improvement to the degree of conversion was exhibited with $CuSO_4 \bullet 5H_2O$ and CuBPMEN in the presence of DIPEA and triethylamine, but conversions with these Cu(II) catalysts and PMDETA showed much less of an increase in the case of CuBPMEN, and showed an overall negative effect to the degree of conversion in the case of $CuSO_4 \bullet 5H_2O$.

Ultimately, the consistent 100% conversion to both propargyl acetate and propargyl benzoate when $CuBr(PPh_3)_3$ is used as a catalyst in the presence of a any of the three ligands used in this work opens the doors widely for exploration into the efficacy of these reaction conditions in other CuAAC reactions.

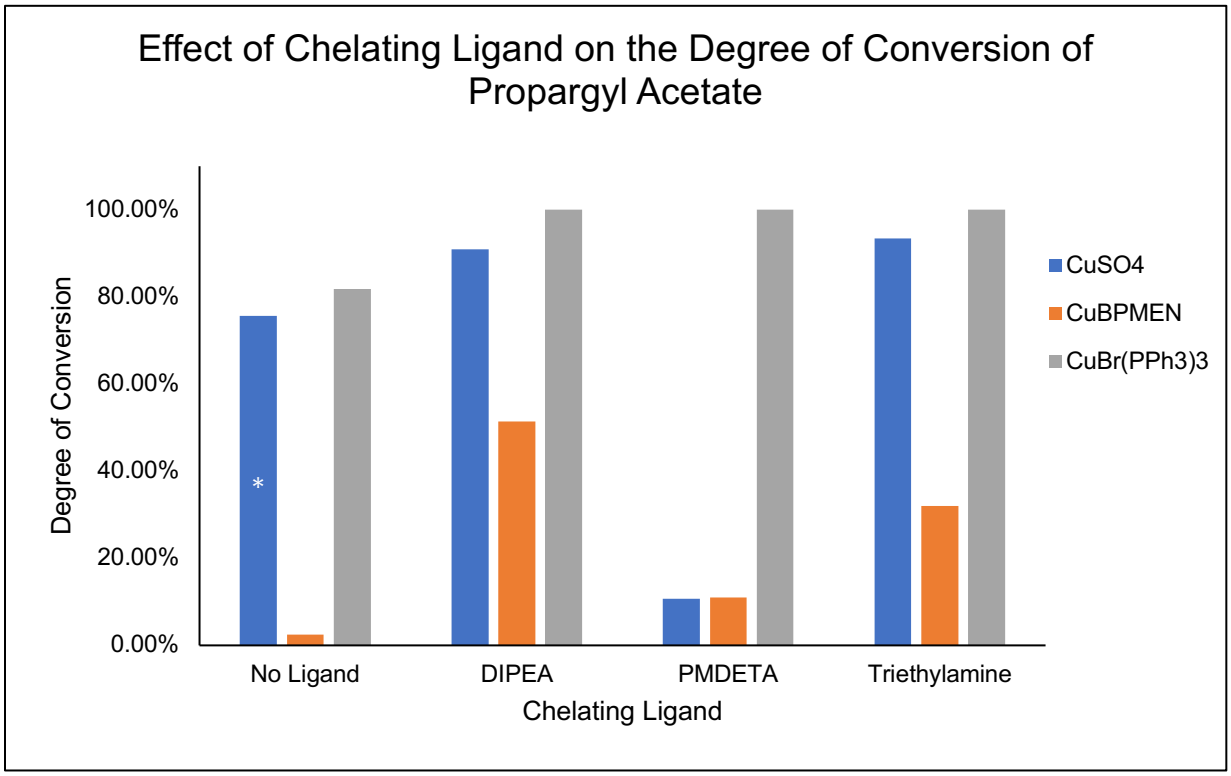

Figure 17: Average degree of conversion of poly (methylacrylate-co-5-azido-1-pentene) to the 1,4-disubstituted 1,2,3-triazole product with propargyl acetate attached, using one of three different chelating ligands (DIPEA, PMDETA, or triethylamine) and one of three different catalysts ($CuSO_4 \bullet 5H_2O$, CuBPMEN, and $CuBr(PPh_3)_3$) per reaction. All reactions were performed in DMF. Reactions were performed either in duplicate or in triplicate. Triplicate reactions denoted by "*".

Table 5: Summary of CuAAC synthesis reactions to determine effects of chelating ligands on the degree of conversion to the desired click product

Entry	Click Substrate	Catalyst System	Ligand	Yield (%)	Degree of Conversion (%)	NMR Spectrum Appendix Location
1	Benzoate	$CuSO_4$ / Sodium Ascorbate	No Ligand	24.70%	78.27%	A18
2	Benzoate	$CuSO_4$ / Sodium Ascorbate	No Ligand	46.19%	68.18%	A19
3	Benzoate	$CuSO_4$ / Sodium Ascorbate	DIPEA	100.00%	100.00%	A39
4	Benzoate	$CuSO_4$ / Sodium Ascorbate	DIPEA	100.00%	100.00%	A40
5	Benzoate	$CuSO_4$ / Sodium Ascorbate	PMDETA	71.08%	57.14%	A41
6	Benzoate	$CuSO_4$ / Sodium Ascorbate	PMDETA	100.00%	100.00%	A42
7	Benzoate	$CuSO_4$ / Sodium Ascorbate	Triethylamine	96.75%	100.00%	A43
8	Benzoate	$CuSO_4$ / Sodium Ascorbate	Triethylamine	100.00%	100.00%	A44
9	Benzoate	CuBPMEN / Sodium Ascorbate	No Ligand	14.43%	27.27%	A23
10	Benzoate	CuBPMEN / Sodium Ascorbate	No Ligand	52.59%	100.00%	A24
11	Benzoate	CuBPMEN / Sodium Ascorbate	No Ligand	53.42%	100.00%	A25
12	Benzoate	CuBPMEN / Sodium Ascorbate	DIPEA	52.72%	71.43%	A45
13	Benzoate	CuBPMEN / Sodium Ascorbate	DIPEA	100.00%	100.00%	A46
14	Benzoate	CuBPMEN / Sodium Ascorbate	PMDETA	94.34%	100.00%	A47

15	Benzoate	CuBPMEN / Sodium Ascorbate	PMDETA	78.79%	96.29%	A48
16	Benzoate	CuBPMEN / Sodium Ascorbate	Triethylamine	84.76%	100.00%	A49
17	Benzoate	CuBPMEN / Sodium Ascorbate	Triethylamine	78.95%	100.00%	A50
18	Benzoate	$CuBr(PPh_3)_3$	No Ligand	-	100.00%	A35
19	Benzoate	$CuBr(PPh_3)_3$	No Ligand	97.43%	100.00%	A36
20	Benzoate	$CuBr(PPh_3)_3$	DIPEA	20.34%	100.00%	A51
21	Benzoate	$CuBr(PPh_3)_3$	DIPEA	26.76%	100.00%	A52
22	Benzoate	$CuBr(PPh_3)_3$	PMDETA	52.90%	100.00%	A53
23	Benzoate	$CuBr(PPh_3)_3$	PMDETA	23.33%	100.00%	A54
24	Benzoate	$CuBr(PPh_3)_3$	Triethylamine	73.66%	100.00%	A55
25	Benzoate	$CuBr(PPh_3)_3$	Triethylamine	52.32%	100.00%	A56
26	Acetate	$CuSO_4$ / Sodium Ascorbate	No Ligand	22.30%	95.65%	A28
27	Acetate	$CuSO_4$ / Sodium Ascorbate	No Ligand	-	36.36%	A29
28	Acetate	$CuSO_4$ / Sodium Ascorbate	No Ligand	96.62%	94.74%	A30
29	Acetate	$CuSO_4$ / Sodium Ascorbate	DIPEA	12.27%	81.82%	A57
30	Acetate	$CuSO_4$ / Sodium Ascorbate	DIPEA	91.50%	100.00%	A58
31	Acetate	$CuSO_4$ / Sodium Ascorbate	PMDETA	40.86%	13.79%	A59

32	Acetate	$CuSO_4$ / Sodium Ascorbate	PMDETA	87.11%	7.69%	A60
33	Acetate	$CuSO_4$ / Sodium Ascorbate	Triethylamine	91.50%	100.00%	A61
34	Acetate	$CuSO_4$ / Sodium Ascorbate	Triethylamine	95.55%	86.96%	A62
35	Acetate	CuBPMEN / Sodium Ascorbate	No Ligand	34.49%	3.85%	A33
36	Acetate	CuBPMEN / Sodium Ascorbate	No Ligand	38.09%	1.00%	A34
37	Acetate	CuBPMEN / Sodium Ascorbate	DIPEA	66.09%	41.67%	A63
38	Acetate	CuBPMEN / Sodium Ascorbate	DIPEA	29.70%	61.11%	A64
39	Acetate	CuBPMEN / Sodium Ascorbate	PMDETA	17.56%	7.14%	A65
40	Acetate	CuBPMEN / Sodium Ascorbate	PMDETA	38.75%	14.81%	A66
41	Acetate	CuBPMEN / Sodium Ascorbate	Triethylamine	92.99%	29.41%	A67
42	Acetate	CuBPMEN / Sodium Ascorbate	Triethylamine	37.87%	34.62%	A68
43	Acetate	$CuBr(PPh_3)_3$	No Ligand	85.30%	63.63%	A37
44	Acetate	$CuBr(PPh_3)_3$	No Ligand	92.94%	100.00%	A38
45	Acetate	$CuBr(PPh_3)_3$	DIPEA	10.47%	100.00%	A69
46	Acetate	$CuBr(PPh_3)_3$	DIPEA	-	100.00%	A70
47	Acetate	$CuBr(PPh_3)_3$	PMDETA	47.42%	100.00%	A71
48	Acetate	$CuBr(PPh_3)_3$	PMDETA	95.42%	100.00%	A72

49	Acetate	$CuBr(PPh_3)_3$	Triethylamine	83.10%	100.00%	A73
50	Acetate	$CuBr(PPh_3)_3$	Triethylamine	89.70%	100.00%	A74

4.7 CuAAC of azido-copolymer, poly (methylacrylate-co-5-azido-1-pentene), using CuSO4•5H2O and CuBr(PPh3)3 at different reaction times

In order to determine the most efficient reaction time, several conditions were assessed. Typically, CuAAC reactions with PHAs were performed for 3 hours, but a longer reaction time was considered in order to allow as much time as necessary for the reaction to reach completion (10, 59, 63). Four different reaction times were used and the degree of conversion for each is shown in Figure 18. All reactions were performed with $CuSO_4•5H_2O$ in THF using propargyl benzoate as the click substrate with at least one reaction performed for each time point.

The first thing to consider is that longer reaction times produced lower degrees of conversion, however, degree of conversion for 3 and 6 hr reactions are comparable to one another and are about two times the degree of conversion for the 14 and 22 hr reactions. Overall, these results do not necessarily indicate that a longer reaction time will yield a larger or smaller degree of conversion, because degree of conversion is usually lower in THF compared to DMF, and that only two of the four conditions were performed in duplicate (See Table 6). Instead, these results were used as a preliminary guide for future reactions where a 6 hr reaction was considered to be as long as the reaction could potentially be performed before the degree of conversion began to be negatively affected.

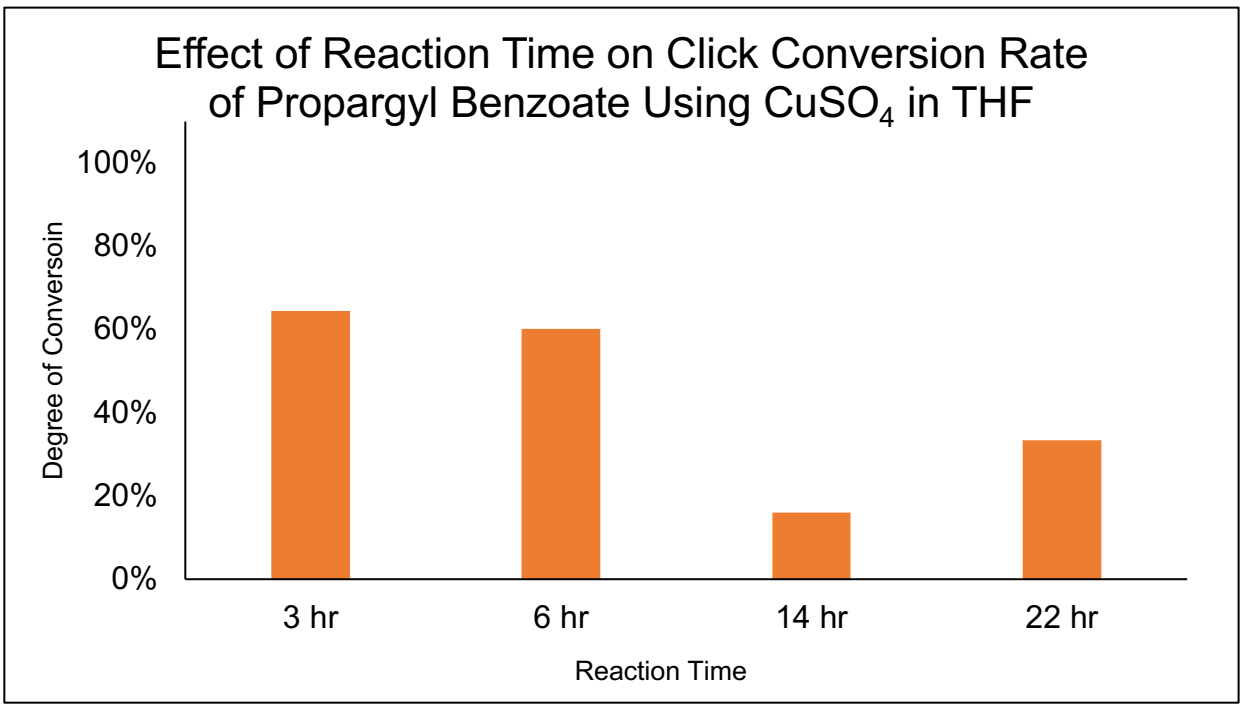

Figure 18: Average degree of conversion of poly (methylacrylate-co-5-azido-1-pentene) to the 1,4-disubstituted 1,2,3-triazole product with propargyl benzoate attached. Reactions were performed in THF using either $CuSO_4 \bullet 5H_2O$ with either 3, 6, 14, or 22 hr reaction times. Reactions were performed in duplicate for only the 3 and 6 hr reactions.

Further suggestion for using a 6 hr reaction time was established when using $CuBr(PPh_3)_3$ as a catalyst. One hundred percent conversion for both propargyl benzoate and propargyl acetate was consistently observed when using $CuBr(PPh_3)_3$ in DMF in the presence of a chelating ligand when a 6 hr reaction was performed (See Section 4.6.3). However, a reaction performed with $CuBr(PPh_3)_3$, propargyl acetate and DIPEA in DMF for 3 hr produced a 91.3% conversion to the final click product. This result was significant because 100% conversion to propargyl acetate was consistently reached in 6 hr reactions when using

$CuBr(PPh_3)_3$ in the presence of any of the 3 chelating ligands used throughout this work. For this reason, 6 hr reactions were considered to be approximately the shortest a click reaction could be performed with the PHA mock polymer that still yielded 100% conversion. Ultimately, more experimentation is needed to confirm the most efficient reaction time, and to determine if a longer reaction times positively or negatively affect the degree of conversion of the PHA analogous click reactions.

Table 6: Summary of CuAAC synthesis reactions to assess the effects of reaction time on the degree of conversion to the desired click product

Entry	Click Substrate	Catalyst System	Solvent	Time (hr)	Yield (%)	Degree of Conversion (%)	NMR Spectrum Appendix Location
1	Benzoate	$CuSO_4$ / Sodium Ascorbate	THF	3	5.02%	80.95%	A75
2	Benzoate	CuSO4 / Sodium Ascorbate	THF	3	31.90%	48.00%	A76
3	Benzoate	CuSO4 / Sodium Ascorbate	THF	22	21.94%	33.33%	A77
4	Benzoate	CuSO4 / Sodium Ascorbate	THF	14	-	16.00%	A78
5	Acetate	$CuBr(PPh_3)_3$ / DIPEA	DMF	3	38.34%	91.30%	A79

4.8 Determination of cause of low yields in CuAAC reactions

Several factors throughout the synthesis of the click-ready azido mock copolymer were indicated as potential causes of relatively low yields of the final click product. Initially, when preparing the click reactions, the azido copolymer starting material was first dissolved manually in a small beaker using a spatula, then the solution was transferred to the reaction vessel. The benefit of this procedure was mainly decreasing the time required to dissolve the polymer, which can take roughly 10 minutes for 100.0 mg to completely dissolve in 15 mL of solvent. In addition, the polymer is quite sticky and difficult to manipulate, causing it to adhere to the spatula used to collect it. The wide mouth of the beaker allowed ease of manual stirring, which facilitated faster polymer dissolution.

However, polymer can be left behind in the beaker when transferring the solution to the reaction vessel. In order to ensure that all starting material dissolved in solution was included in the reaction, the polymer was dissolved by placing the spatula with the collected polymer and solvent in the round bottom flask reaction vessel and placing this setup on a stir plate. The solution was stirred gently until all polymer was removed from the spatula and dissolved into solution. The spatula was removed, and the rest of the reaction was prepared as done normally.

Another cause of low yields in click reactions was due to using azido mock copolymer starting material that was not completely dry of the solvents used (mainly DCM, DMF, or THF depending on the conditions used). At first, all polymers were allowed to dry in a fume hood for several days. Due to the sticky, soft, and viscous nature of the polymer, solvent would easily become trapped within it as it dried, and the air flow in the fume hood was not strong enough to dry the polymer completely. For this reason, residual solvent

would be present in the polymer products throughout all stages of the synthesis. When these polymers were used in subsequent reactions, they included some residual solvent, and ultimately led to lower amounts of polymer starting material. Because the starting material included polymer and residual solvent, instead of only pure polymer, the initial mass of polymer was unintentionally lower than the mass included in the click reaction.

This problem was addressed by drying all polymer starting materials and products in a 60ºC oven for several days until the mass of the polymer no longer fluctuated. Once dry, the polymer became stiffer, and more of a moldable dough-like semi-solid as opposed to the sticky jam-like partially dry polymer. After drying in the oven, there was still some residual solvent present, but the polymer was much drier than the polymers that were dried only in the fume hood.

The final cause of low yields was the precipitant used during the purification step of click reactions. Typically, the product was washed first with hexanes and then with distilled water to remove any remaining alkyne reagent and sodium ascorbate, and catalyst. The polymer was then dissolved in minimal DCM and precipitated into cold methanol. Methanol was used because it is miscible with DMF and facilitates the removal of any residual DMF remaining after rotary evaporation. However, click polymers do not precipitate readily in methanol, so a large amount of product remains dissolved in suspension and is eventually decanted. Incomplete precipitation is often indicated by a cloudy or yellowed solution. More effective precipitation is observed when using 1-propanol as a precipitant. Propanol is miscible with DMF and DCM and is a strong non-solvent for the click polymer products. The implementation of each of these procedures greatly improved the yields for click reactions and generated products that contain much less residual solvent. An outline of the

difference in procedures is shown in Figure 19, and a comparison of yields using the initial and updated methods for reaction preparation, purification, and drying is shown in Figure 20.

The expectation for yields for these reactions is close to 100%, but it is still obviously not always what is observed. This is most likely due to the presence of some residual solvent (DCM, DMF, or THF) in the polymer starting materials that is not possible to remove by simple evaporation methods. The presence of this residual solvent causes the polymer to have a malleable dough-like semi-solid nature, instead of a dry powder or crystalline nature. Because of this, the mass of polymer starting material used in click reactions will always be slightly less than the mass that is recorded and thought to be included in the reaction. More work will need to be done to have a more accurate understanding of the typical yields for these click reactions.

Initial Procedures	**Updated Procedures**
1) Polymer dissolved in small beaker, and solution poured into reaction vessel once dissolved	1) Polymer dissolved in reaction vessel
2) Azido-mock copolymer starting material was dried in a fume hood for several days	2) Azido-mock copolymer click starting material was dried in a 60ºC oven for several days
2) Click product was precipitated into cold methanol	2) Click product was precipitated into cold 1-propanol

Figure 19: Outline of different procedures used to increase the yields observed with click reactions

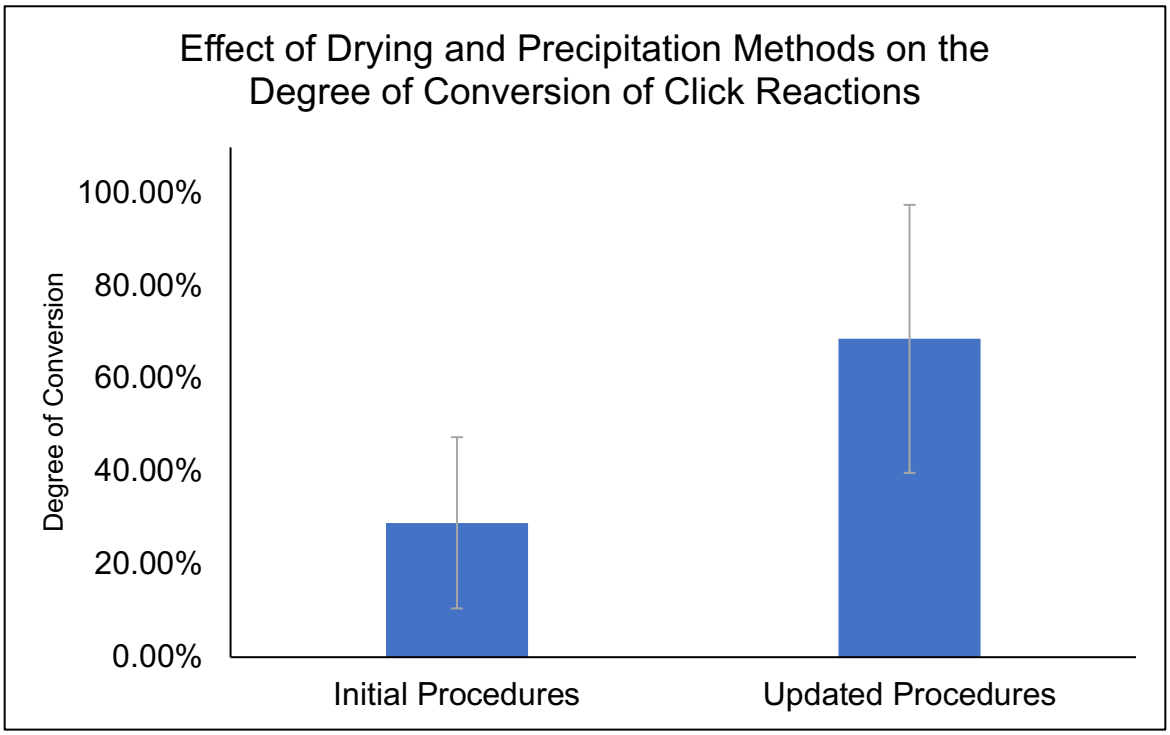

Figure 20: Average degree of conversion of poly (methylacrylate-co-5-azido-1-pentene) to the desired click product before and after procedural changes were implemented in order to increase the percent yield of click reactions. The average yield for the "Initial Procedures" category was calculated using the yields for all reactions performed before and the implementation. The average yield for the "Updated Procedures" category was calculated using the yields for all reactions performed after the implementation of new procedures.

5. Conclusions

The goal of this work was to determine the conditions required in CuAAC reactions with a PHA structural analog that consistently produce 100% conversion of all click-ready sites to the desired functional group. The efficacy of several catalysts ($CuSO_4 \bullet 5H_2O$, CuBPMEN, and $CuBr(PPh_3)_3$), solvents (THF and DMF), and chelating ligands (Triethylamine, DIPEA, and PMDETA) was investigated. Propargyl acetate and propargyl benzoate were chosen as click substrates in this work due to their differing behavior in click reactions.

Initially, the structurally analogous PHA mock copolymer was prepared by radical polymerization of methyl acrylate and 5-bromo-1-pentene to produce poly (methylacrylate-*co*-5-bromo-1-pentene). Several batches of this polymer were produced with an average yield of 32.7%, and an average of 15.1% of side chains containing a terminal bromine group. This mock copolymer was then used as the starting material for the remainder of the synthesis. Other possible structurally analogous polymers were investigated, including the water-soluble poly (acrylic acid-*co*-5-bromo-1-pentene), and the highly brominated poly (5-bromo-1-pentene), but the syntheses of these polymers presented additional problems, and were not explored further.

In order to prepare the mock copolymer for use in click reactions, all terminal bromine groups present in poly (methylacrylate-*co*-5-bromo-1-pentene) were substituted with an azide functionality through an S_N2 nucleophilic substitution. These conversions had an average yield of 63.0%, and consistently exhibited 100% conversion to the azide group.

Once the terminal azide groups are present on the mock polymer side chains, click reactions could be performed with propargyl acetate and propargyl benzoate. The initial

conditions for click reactions included THF as a solvent. However, click reactions performed in THF yielded conversions that were on average 11.7% lower than the degree of conversion exhibited in click reactions performed in DMF for both propargyl acetate and propargyl benzoate.

The effect of each of the three catalysts on the degree of conversion was also assessed. In general, reactions performed with $Cu(Br(PPh_3)_3$ had higher conversion to both propargyl acetate (81.82% conversion) and propargyl benzoate (100.00% conversion) compared to reactions performed with CuBPMEN and $CuSO_4 \bullet 5H_2O$. While 100% conversion to propargyl benzoate was achieved using $CuBr(PPh_3)_3$, none of the conditions investigated so far were capable of producing 100% conversion to propargyl acetate.

Some nitrogenous organic bases that act as chelating ligands were introduced due to their ability to stabilize the Cu(I) species during click reactions. The degree of conversion was generally increased when either DIPEA, PMDETA, or triethylamine were included in reactions performed with propargyl benzoate, and 100% conversion was consistently achieved with reactions that used any of the three ligands and had $CuBr(PPh_3)_3$ as a catalyst. Propargyl acetate was also completely clicked to the mock polymer under the same conditions, using $CuBr(PPh_3)_3$ and any of the chelating ligands. $CuSO_4 \bullet 5H_2O$ and CuBPMEN did achieve 100% conversion to propargyl benzoate when in the presence of some of the ligands, but the conversions were not as consistent as $CuBr(PPh_3)_3$. 100% conversion to propargyl acetate with $CuSO_4 \bullet 5H_2O$ occurred only twice out of nine reactions performed, and no reactions with CuBPMEN and a chelating ligand reached 100% conversion to propargyl acetate. The most successful reaction conditions observed

throughout this work are click reactions performed with $CuBr(PPh_3)_3$ in the presence of either DIPEA, PMDETA, or triethylamine.

The most significant work to be done in the future would be to perform the same experiments outlined here with biosynthesized PHA. Click reactions similar to those performed throughout this work have been performed with biosynthesized PHAs with somewhat comparable results (10, 59), with an average of 34% conversion to propargyl acetate, and an average of 100% conversion to propargyl benzoate when using $CuSO_4 \bullet 5H_2O$. However, the effect of chelating ligands and different copper catalysts has not been fully assessed when considering biosynthesized PHAs. Further, purifying the final product and removing excess catalyst and ligands is an aspect of this synthesis that needs to be addressed in order to allow the chemical modification of these PHAs to be more easily processed and used in applications such as the medical field.

In addition, the addressing the issue of product yields mentioned in Section 4.8 is necessary and can be remedied possibly by further purifying the products of each synthesis step to ensure the starting material for the subsequent step is as pure as possible. This could have a positive impact on both the overall yield of the synthesis but could potentially benefit the degree of conversion exhibited in the click reactions due to less by-product and contaminants present in the reaction. As these steps are accomplished, the next endeavor would be to evaluate even more Cu(I) catalysts to determine if the Cu(I) species itself is the reason for high degrees of conversion, or if the highly stabilizing triphenylphosphine groups are the component with the greatest positive impact.

Appendix: NMR Spectra

All ^{1}H NMR experiments were performed in deuterated chloroform ($CDCl_3$) using a 500 MHz Varian INOVA Spectrometer with 32 scans and a relaxation delay of 1 second. All spectra were analyzed using MestReNova 14.0 software.

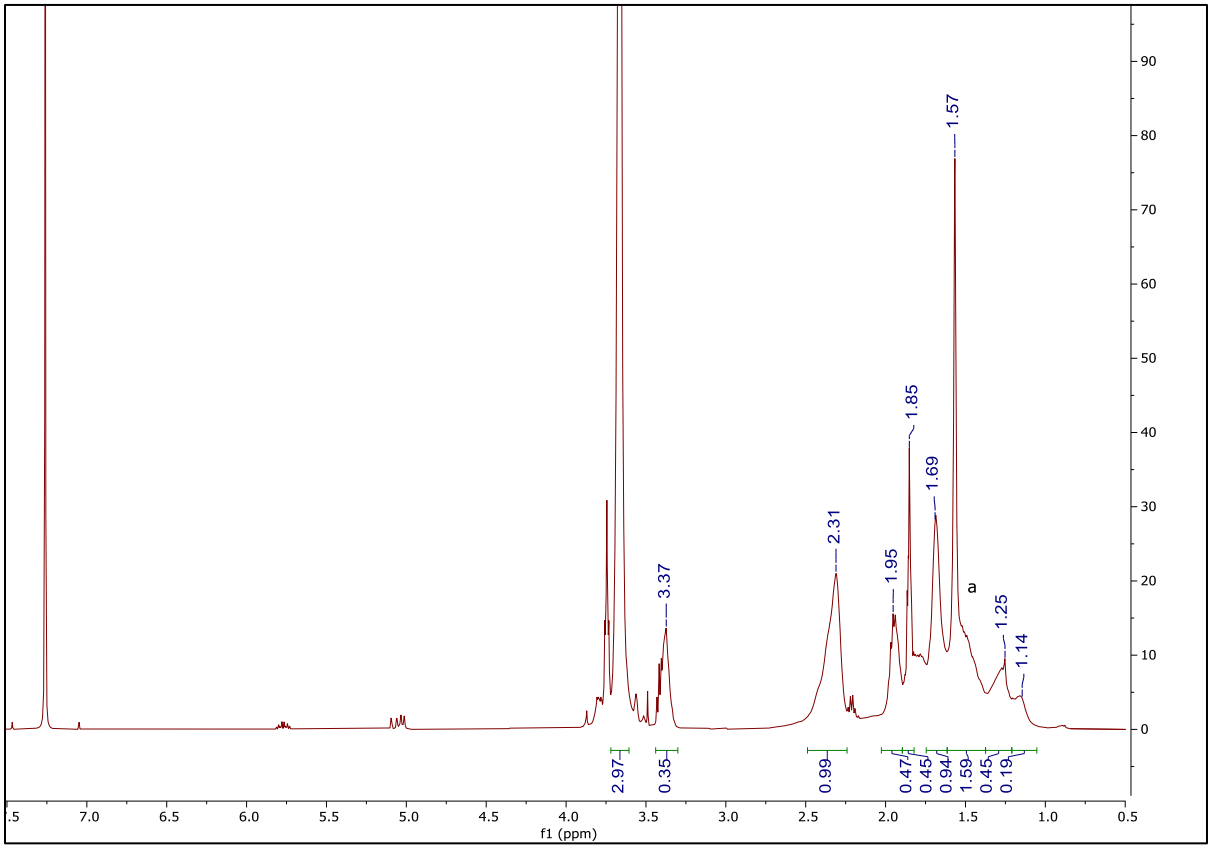

Figure A1: ^{1}H NMR spectrum of poly (methylacrylate-*co*-bromo-1-pentene) (Table 1, Entry 1)

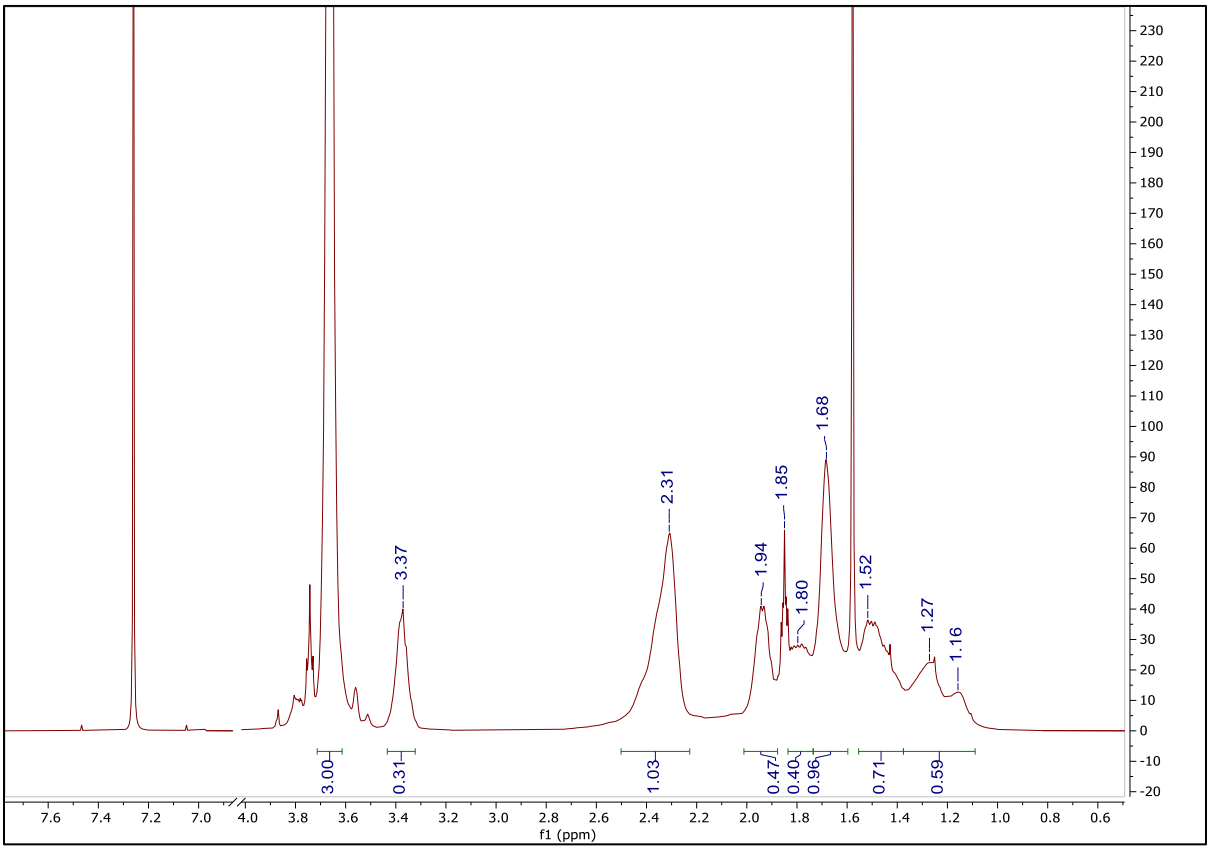

Figure A2: ^{1}H NMR spectrum of poly (methylacrylate-*co*-bromo-1-pentene) (Table 1, Entry 2)

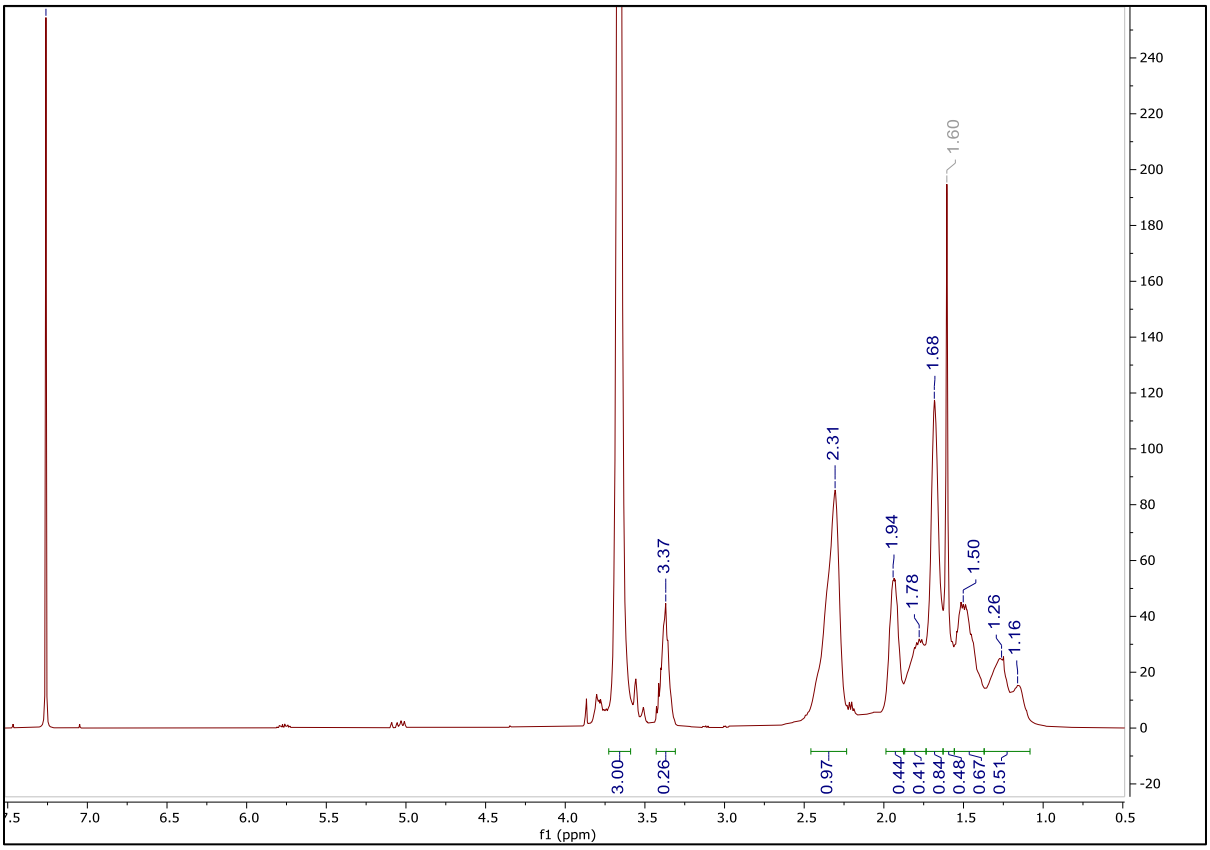

Figure A3: ^{1}H NMR spectrum of poly (methylacrylate-*co*-bromo-1-pentene) (Table 1, Entry 3)

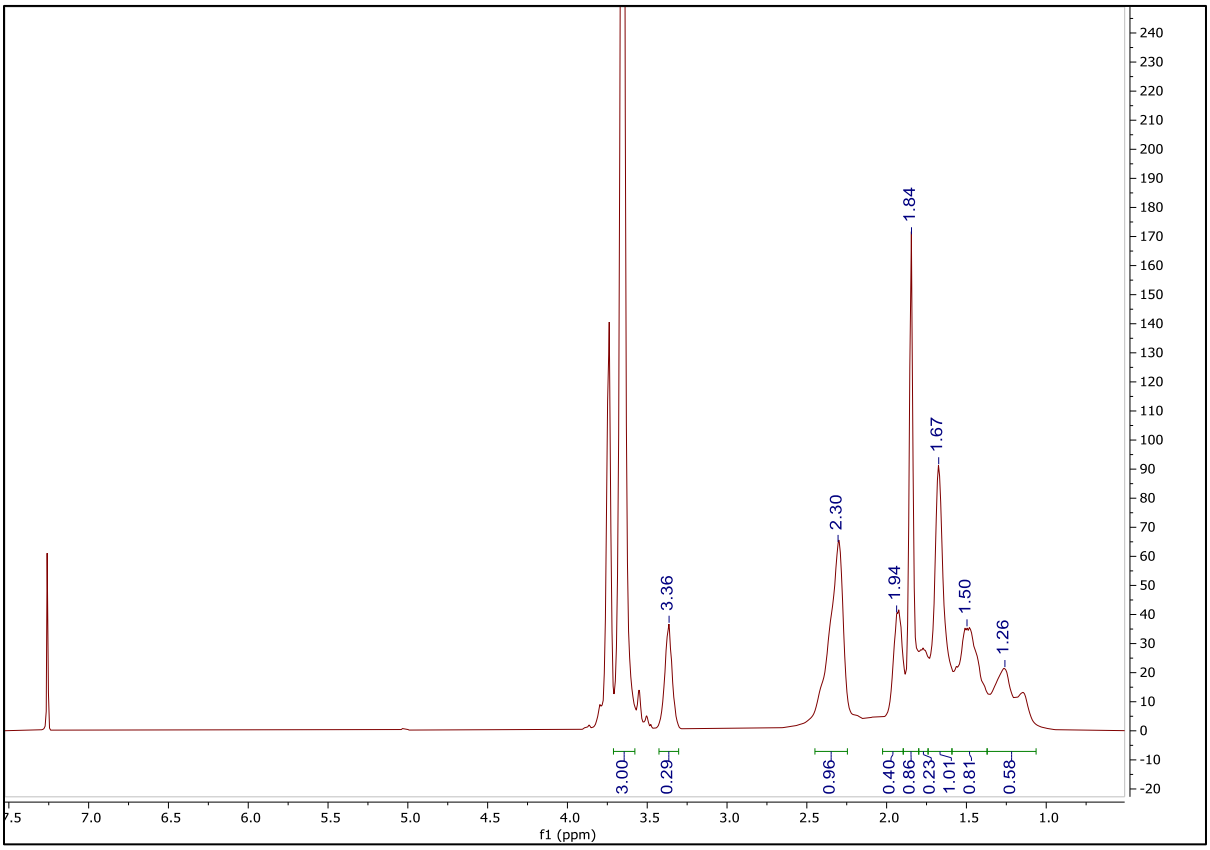

Figure A4: ^{1}H NMR spectrum of poly (methylacrylate-*co*-bromo-1-pentene) (Table 1, Entry 4)

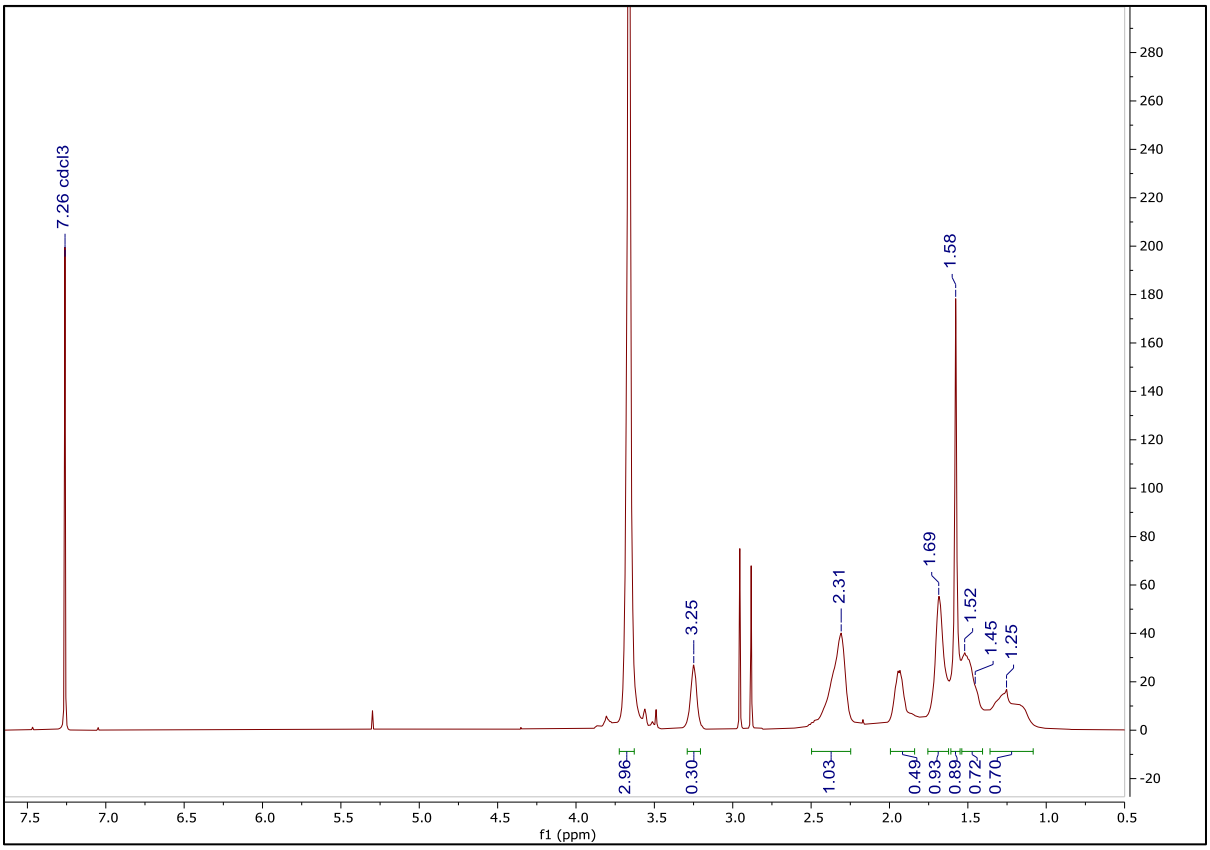

Figure A5: ^{1}H NMR spectrum of poly (methylacrylate-*co*-azido-1-pentene) (Table 2, Entry 1)

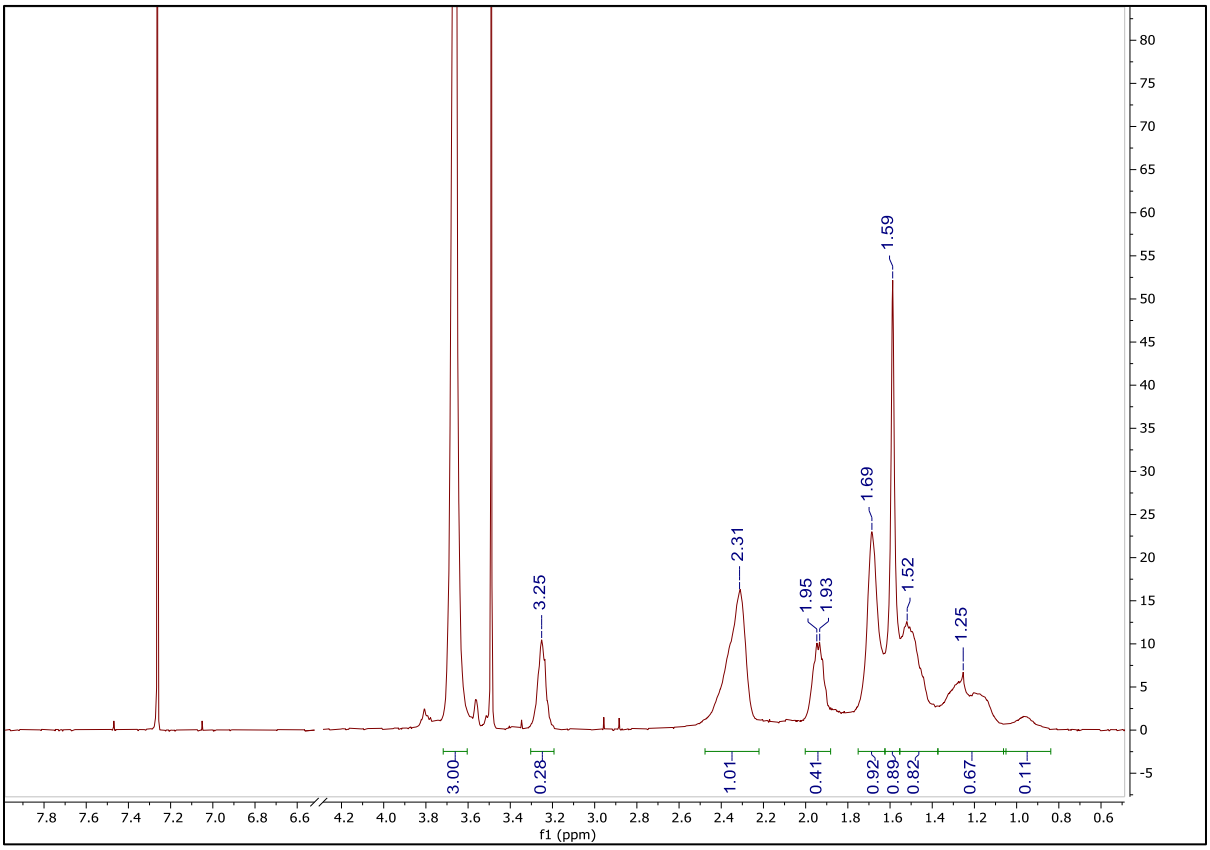

Figure A6: ^{1}H NMR spectrum of poly (methylacrylate-*co*-azido-1-pentene) (Table 2, Entry 2)

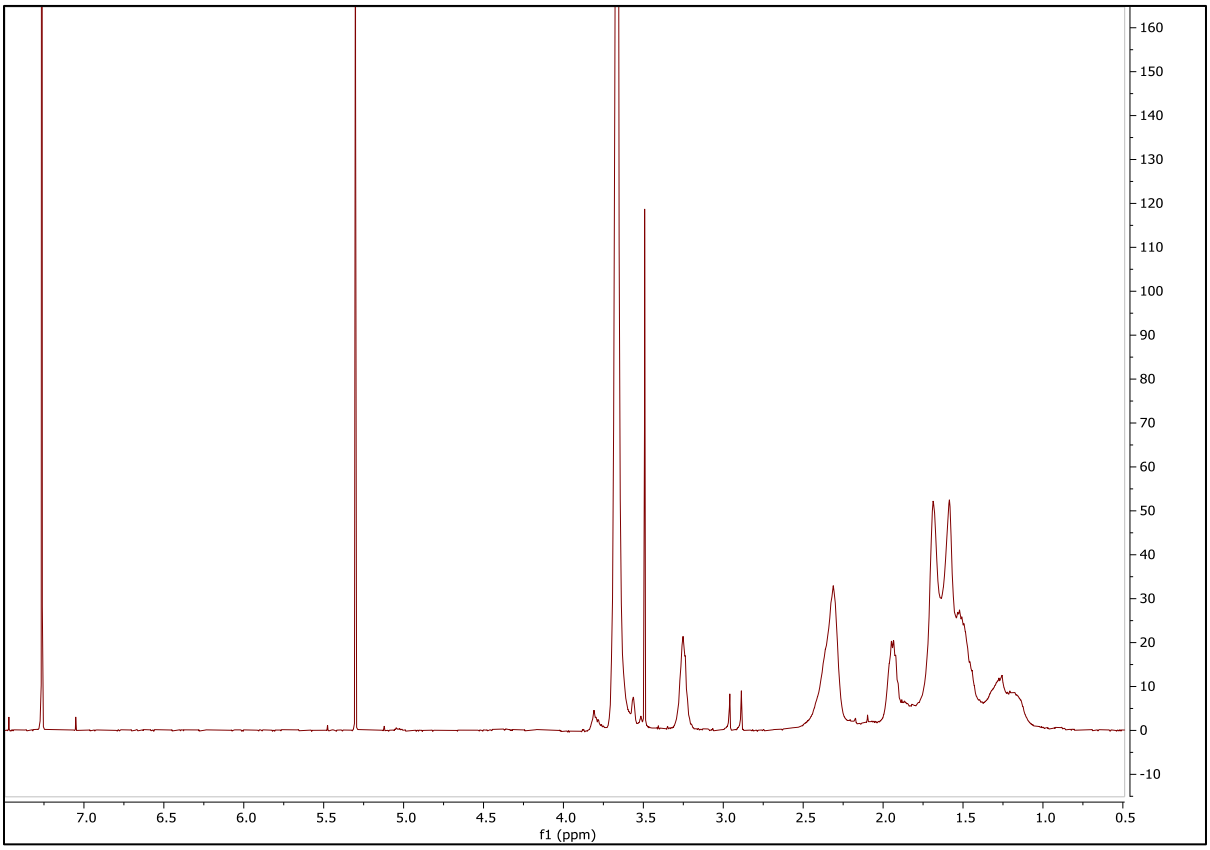

Figure A7: ^{1}H NMR spectrum of poly (methylacrylate-*co*-azido-1-pentene) (Table 2, Entry 3)

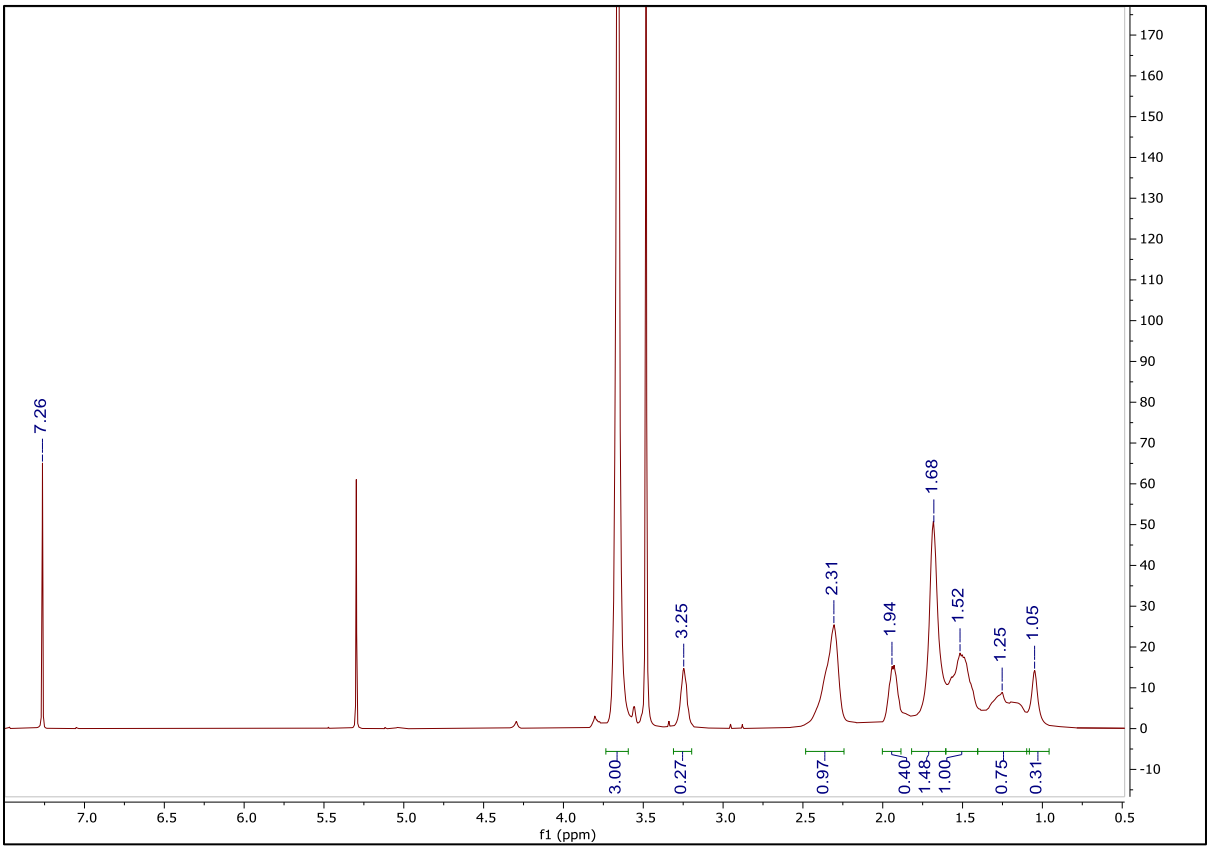

Figure A8: ^{1}H NMR spectrum of poly (methylacrylate-*co*-azido-1-pentene) (Table 2, Entry 4)

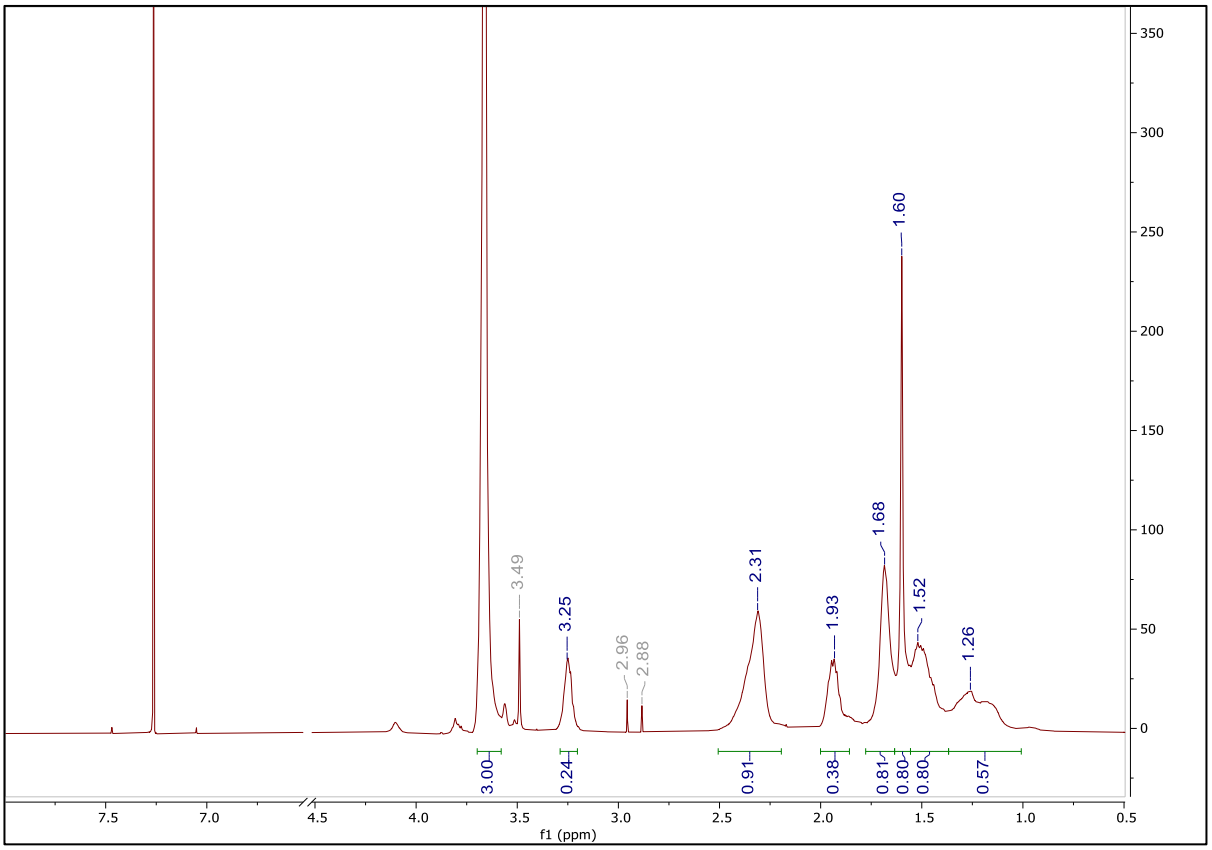

Figure A9: ^{1}H NMR spectrum of poly (methylacrylate-*co*-azido-1-pentene) (Table 2, Entry 5)

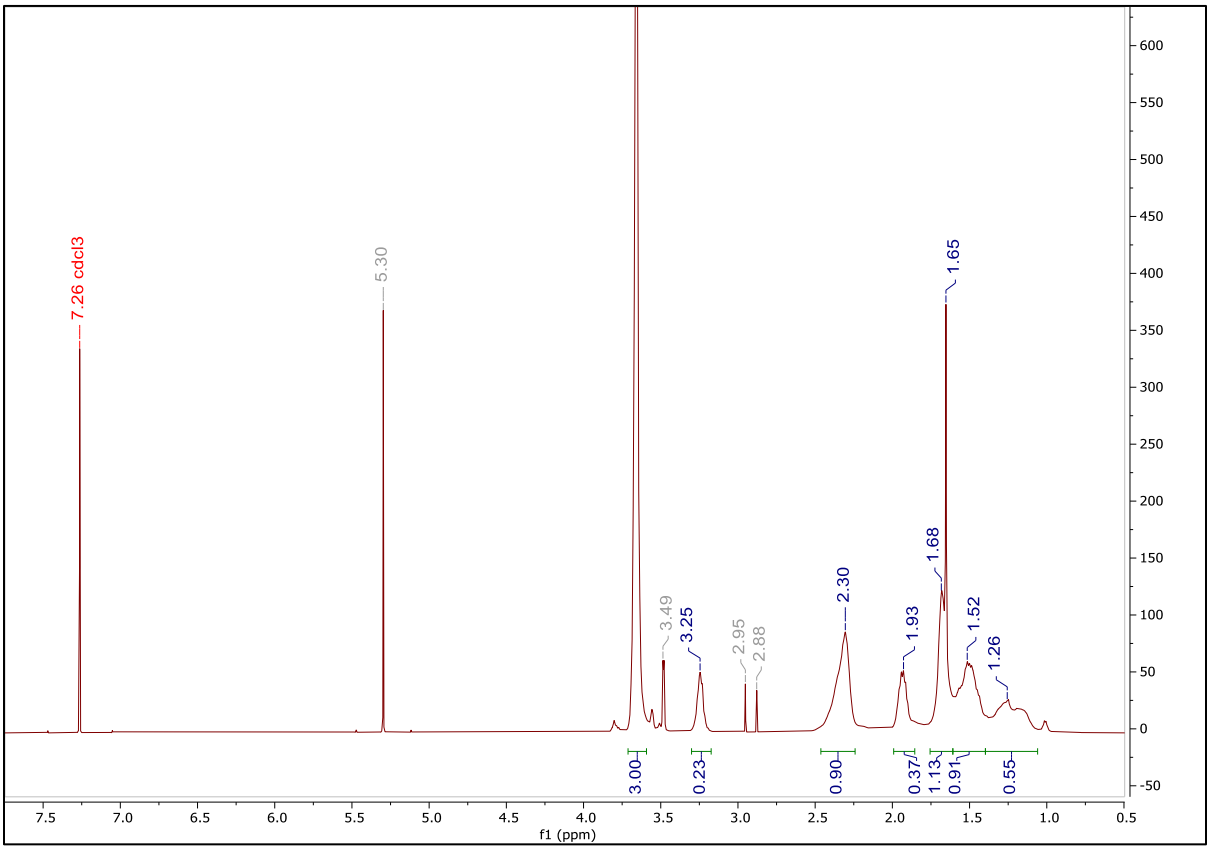

Figure A10: ^{1}H NMR spectrum of poly (methylacrylate-*co*-azido-1-pentene) (Table 2, Entry 6)

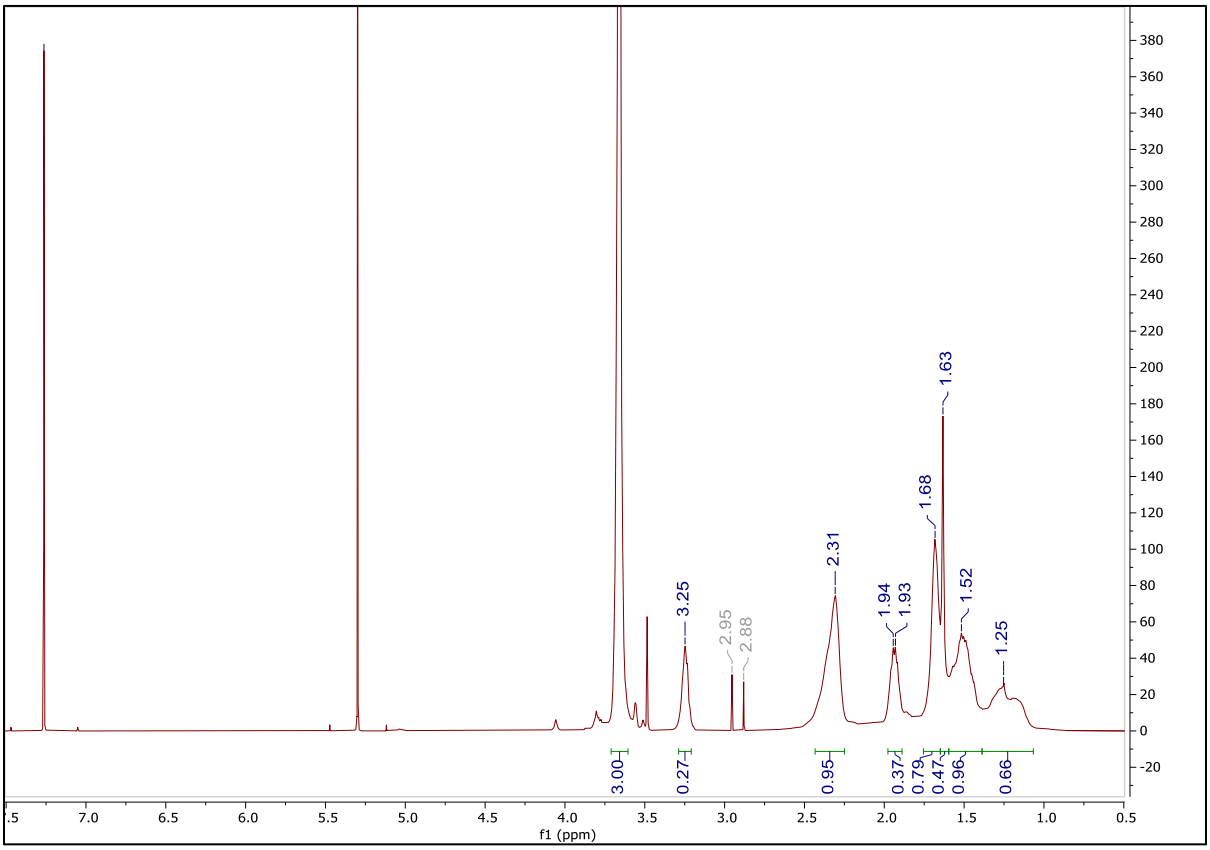

Figure A11: ^{1}H NMR spectrum of poly (methylacrylate-*co*-azido-1-pentene) (Table 2, Entry 7)

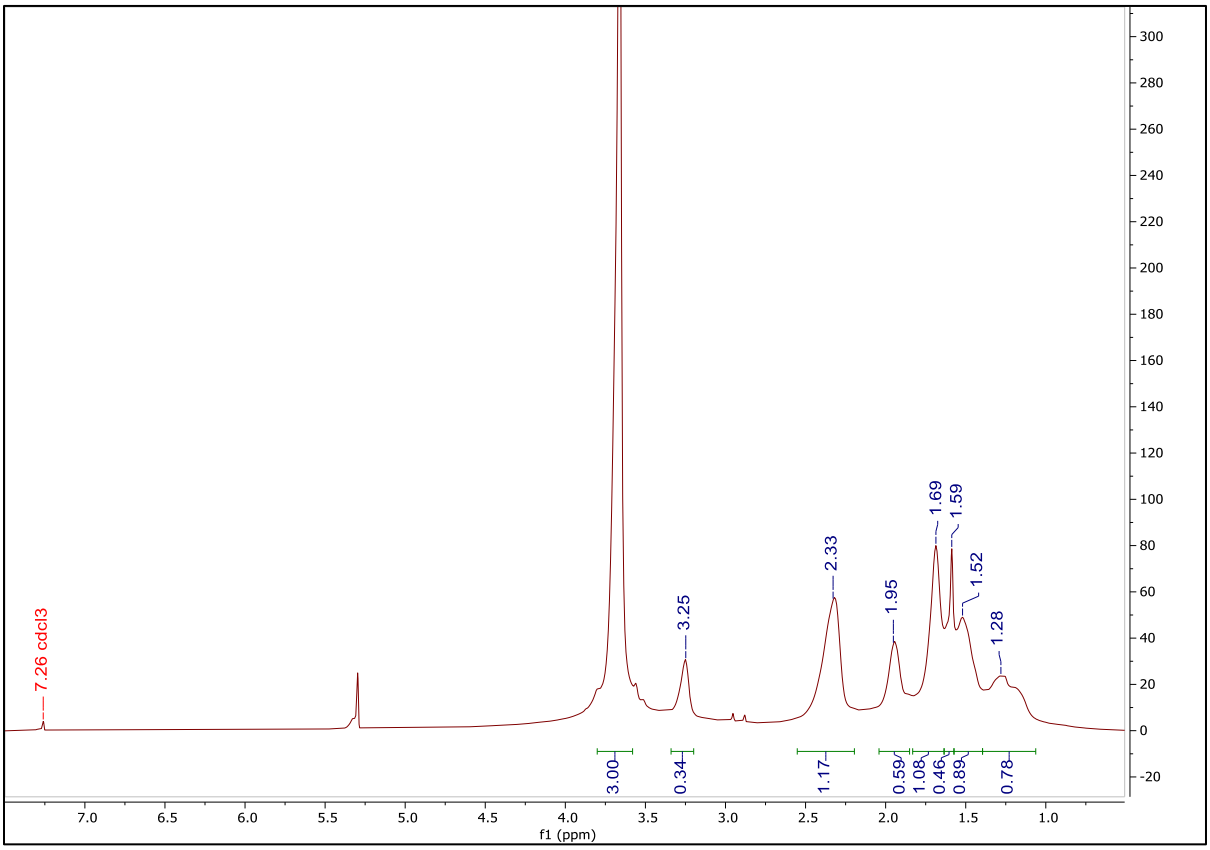

Figure A12: ^{1}H NMR spectrum of poly (methylacrylate-*co*-azido-1-pentene) (Table 2, Entry 8)

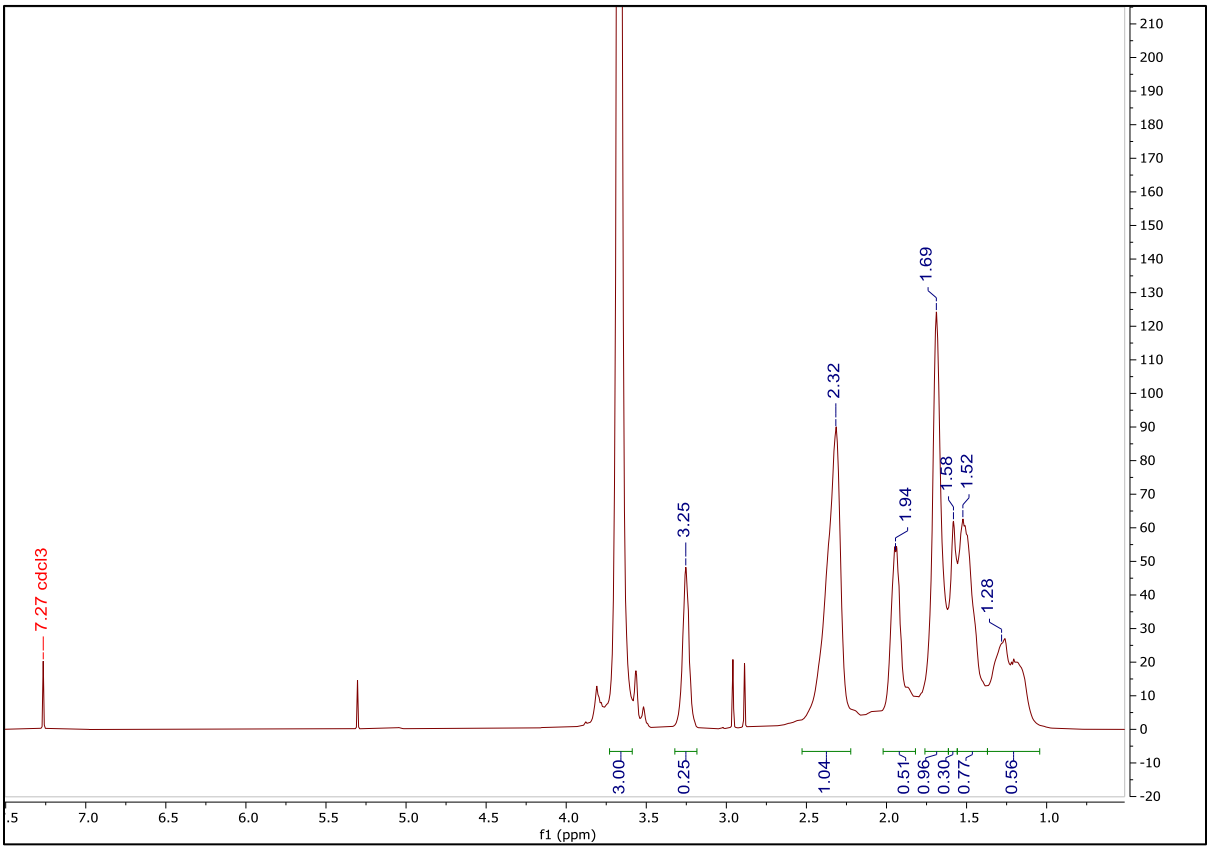

Figure A13: ^{1}H NMR spectrum of poly (methylacrylate-*co*-azido-1-pentene) (Table 2, Entry 9)

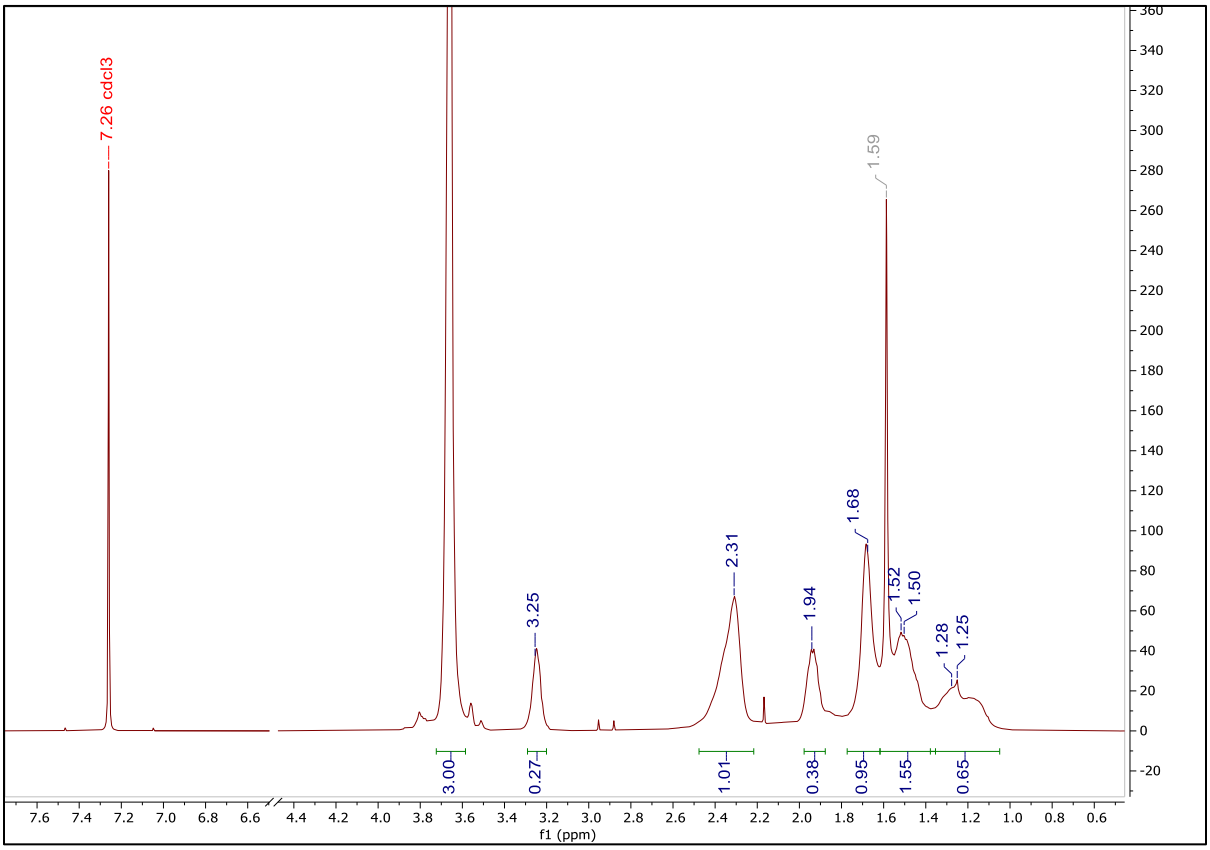

Figure A14: ^{1}H NMR spectrum of poly (methylacrylate-*co*-azido-1-pentene) (Table 2, Entry 10)

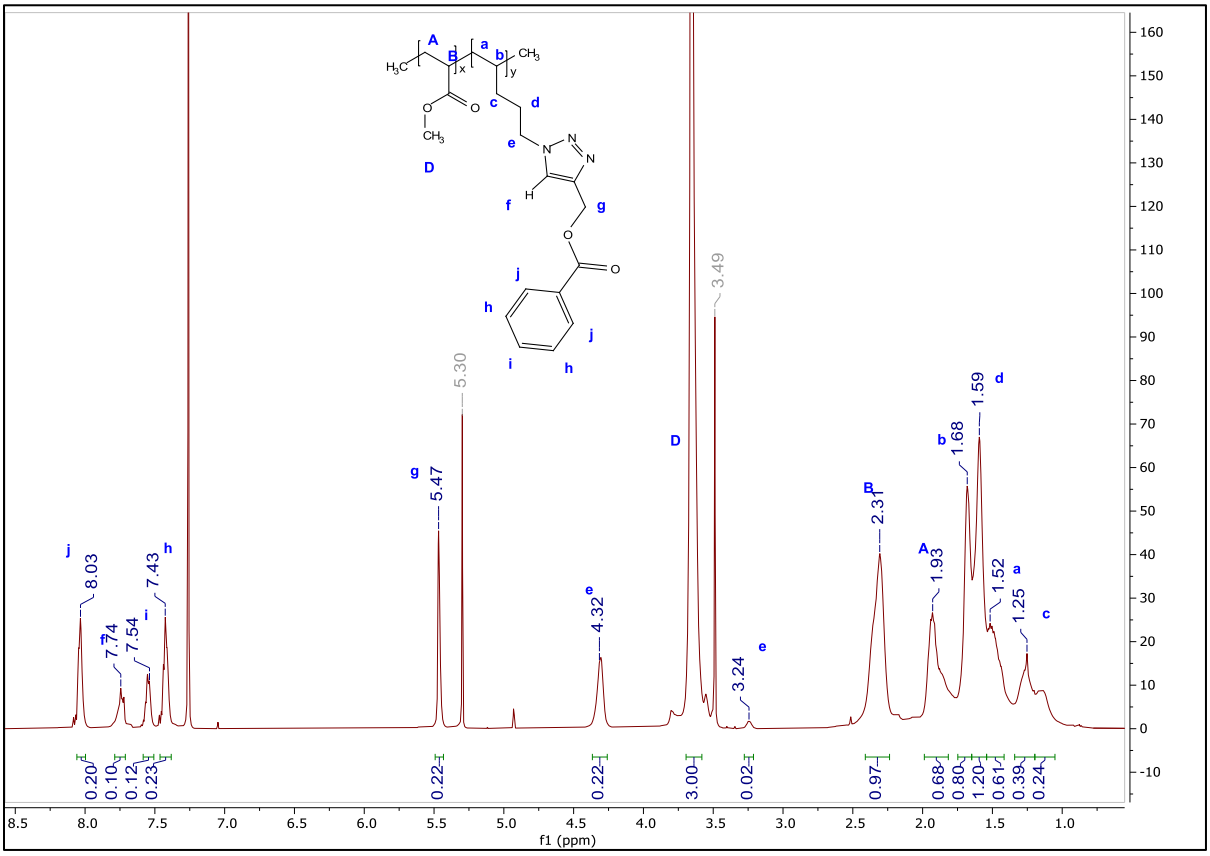

Figure A15: ^{1}H NMR spectrum of 1,4-disubstituted 1,2,3-triazole click product with propargyl benzoate attached (Table 3, Entry 1)

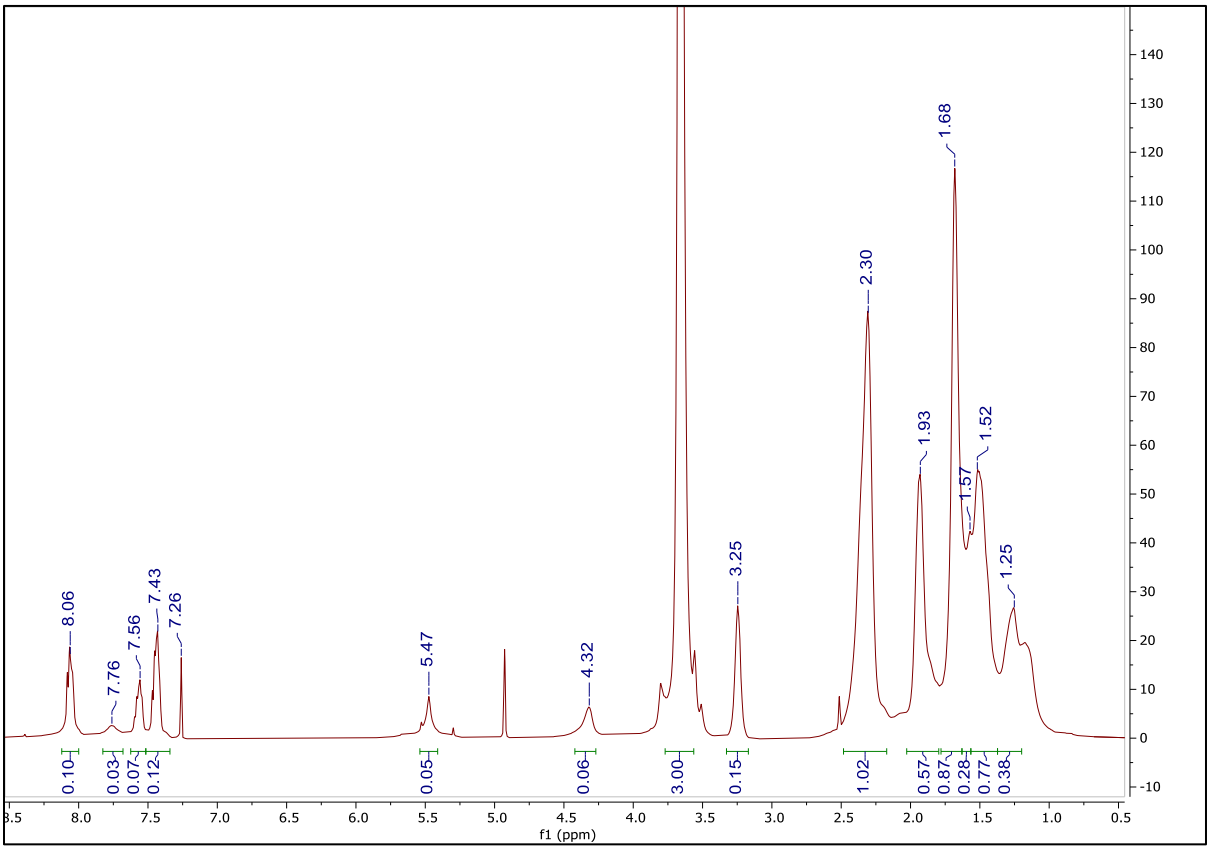

Figure A16: ^{1}H NMR spectrum of 1,4-disubstituted 1,2,3-triazole click product with propargyl benzoate attached (Table 3, Entry 2)

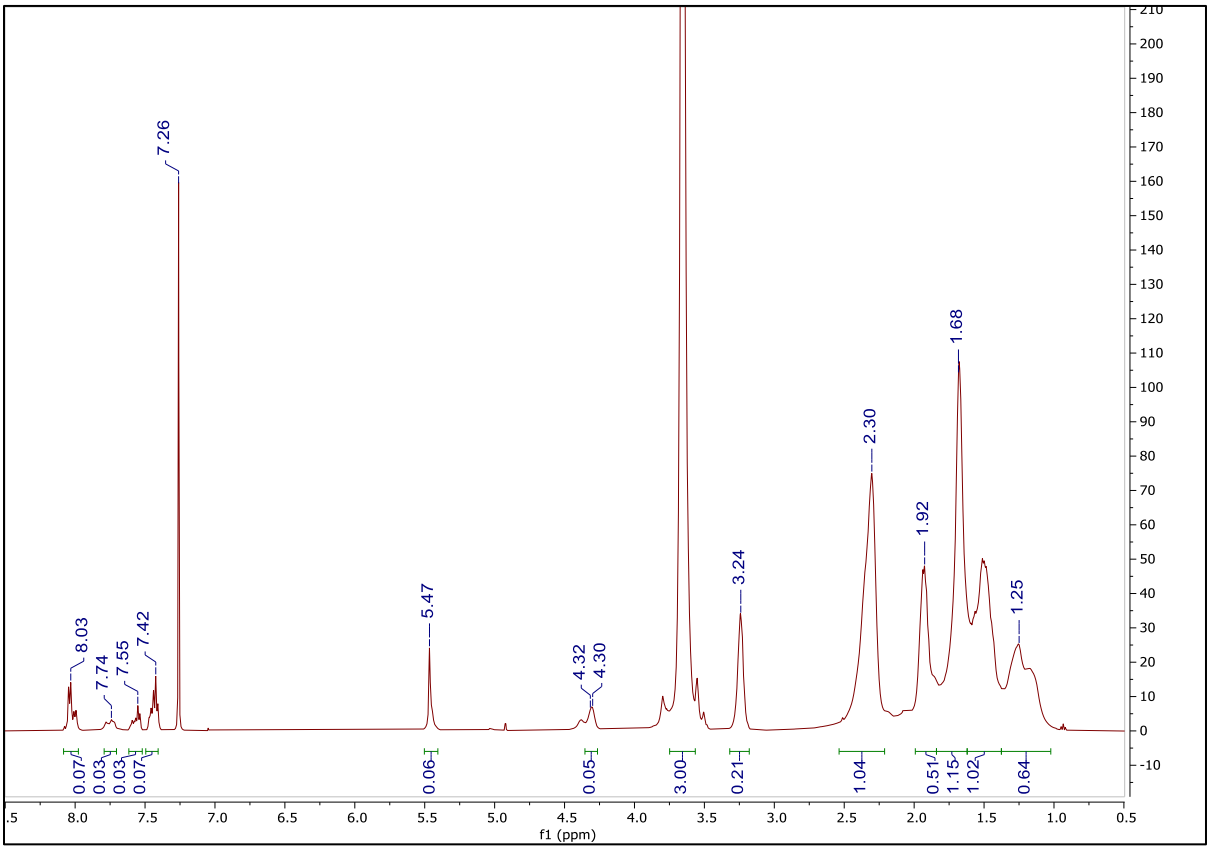

Figure A17: ^{1}H NMR spectrum of 1,4-disubstituted 1,2,3-triazole click product with propargyl benzoate attached (Table 3, Entry 3)

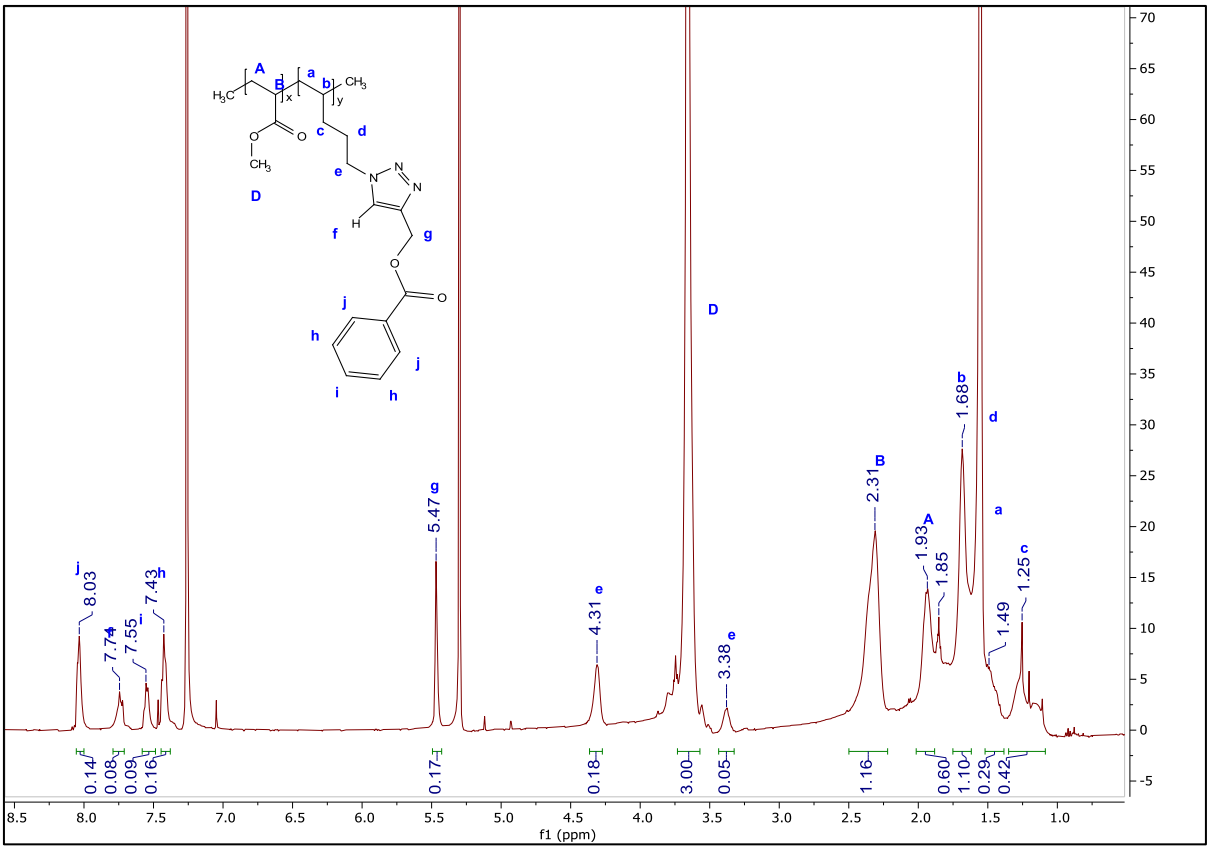

Figure A18: ^{1}H NMR spectrum of 1,4-disubstituted 1,2,3-triazole click product with propargyl benzoate attached (Table 3, Entry 4 / Table 4, Entry 1 / Table 5, Entry 1)

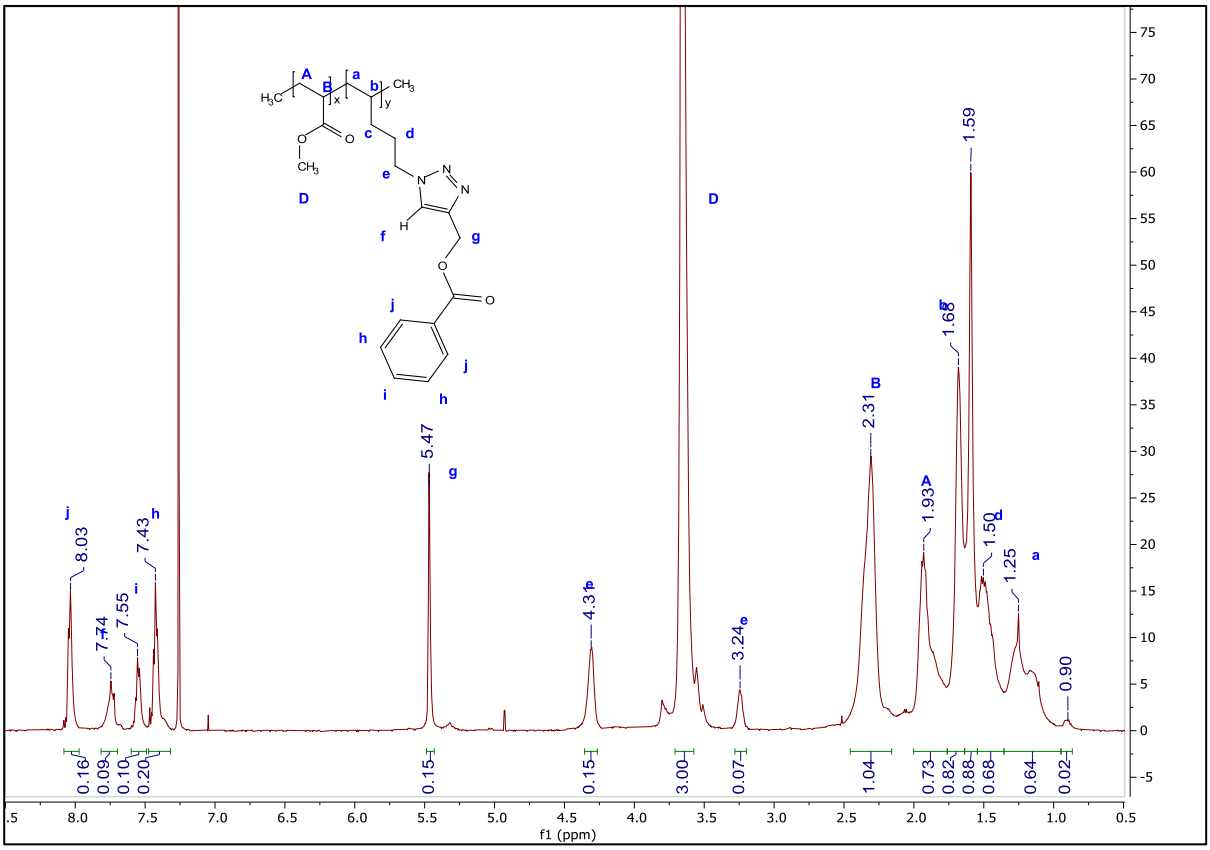

Figure A19: ^{1}H NMR spectrum of 1,4-disubstituted 1,2,3-triazole click product with propargyl benzoate attached (Table 3, Entry 5 / Table 4, Entry 2 / Table 5, Entry 2)

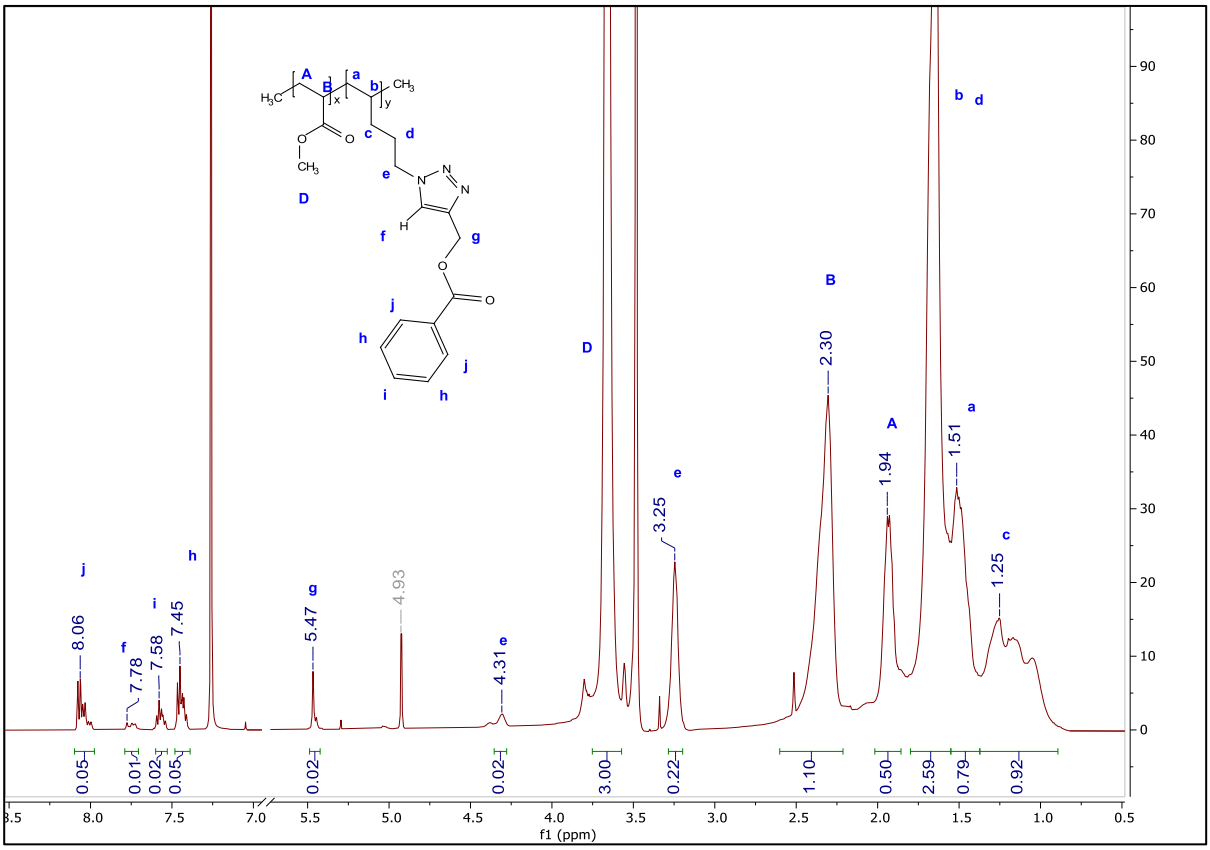

Figure A20: ^{1}H NMR spectrum of 1,4-disubstituted 1,2,3-triazole click product with propargyl benzoate attached (Table 3, Entry 6)

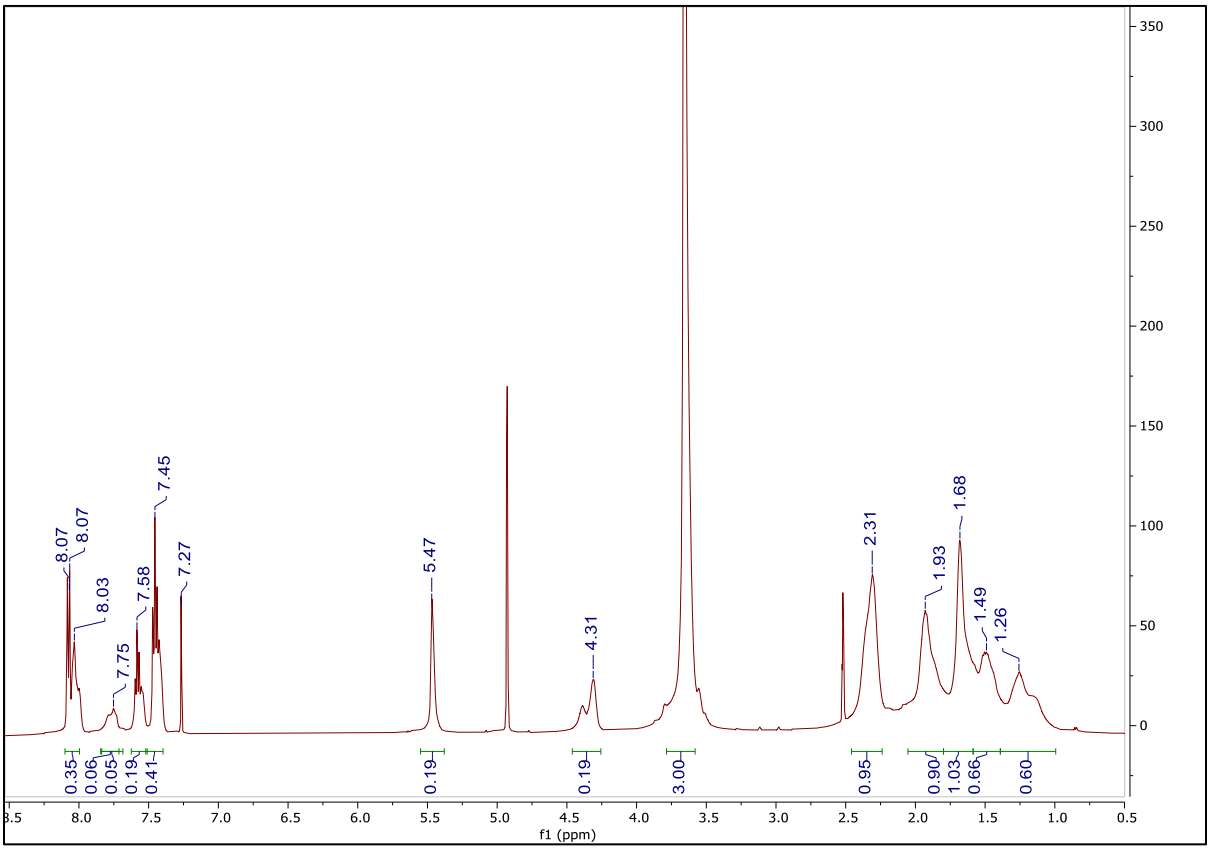

Figure A21: ^{1}H NMR spectrum of 1,4-disubstituted 1,2,3-triazole click product with propargyl benzoate attached (Table 3, Entry 7)

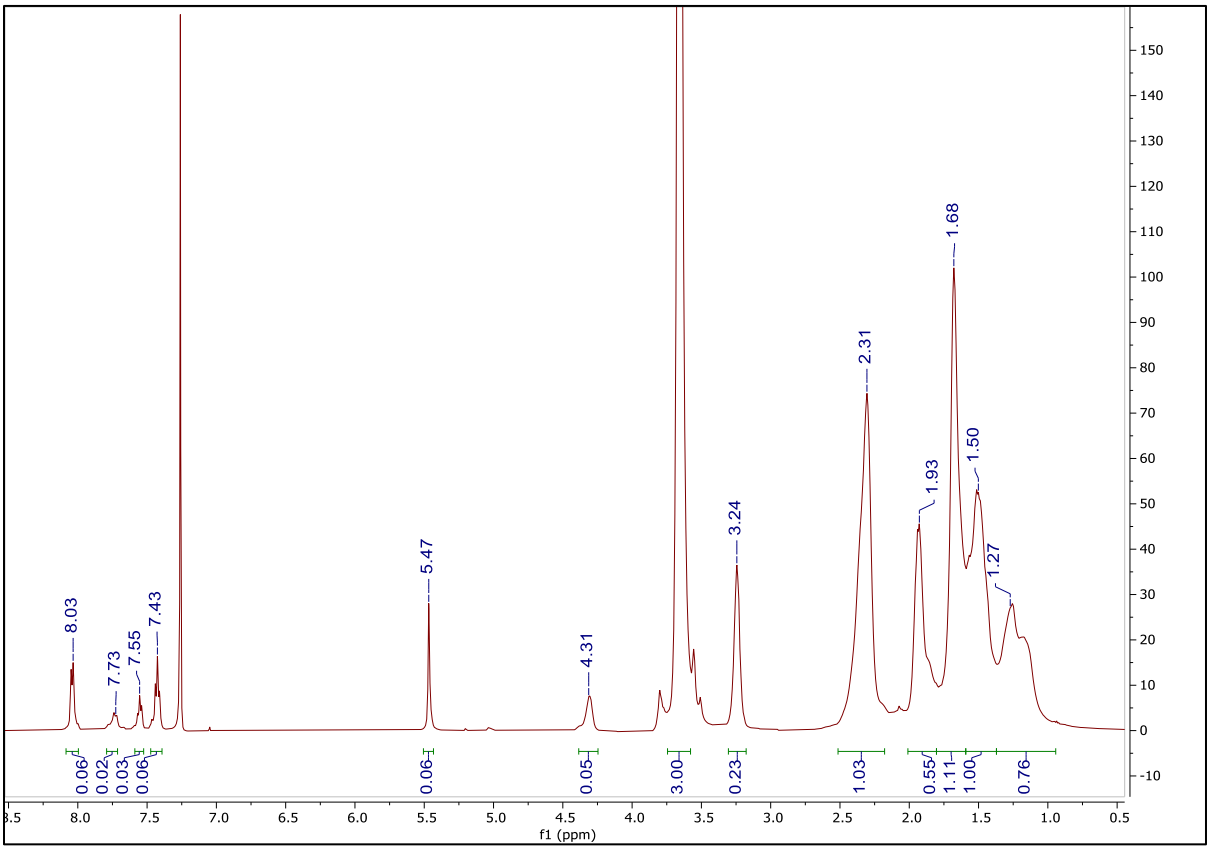

Figure A22: ^{1}H NMR spectrum of 1,4-disubstituted 1,2,3-triazole click product with propargyl benzoate attached (Table 3, Entry 8)

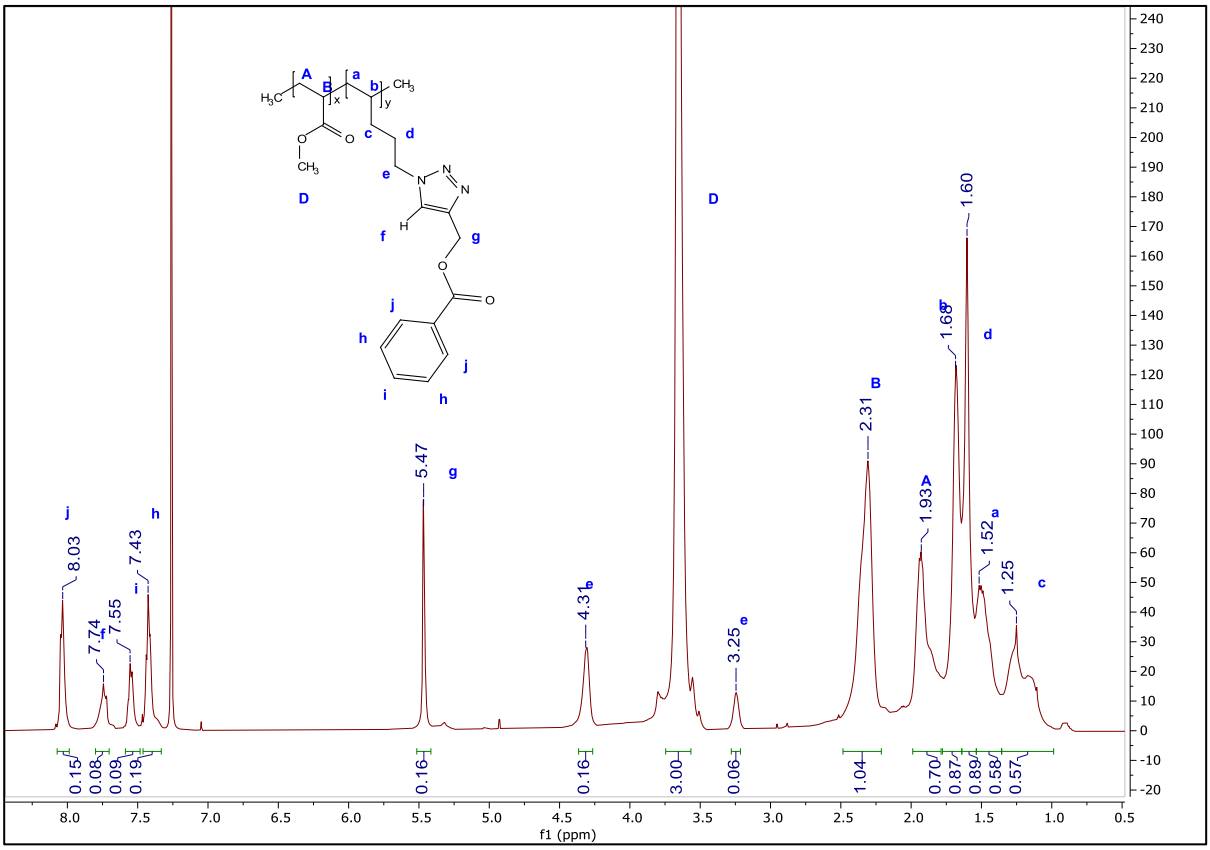

Figure A23: ^{1}H NMR spectrum of 1,4-disubstituted 1,2,3-triazole click product with propargyl benzoate attached (Table 3, Entry 9 / Table 4, Entry 3 / Table 5, Entry 9)

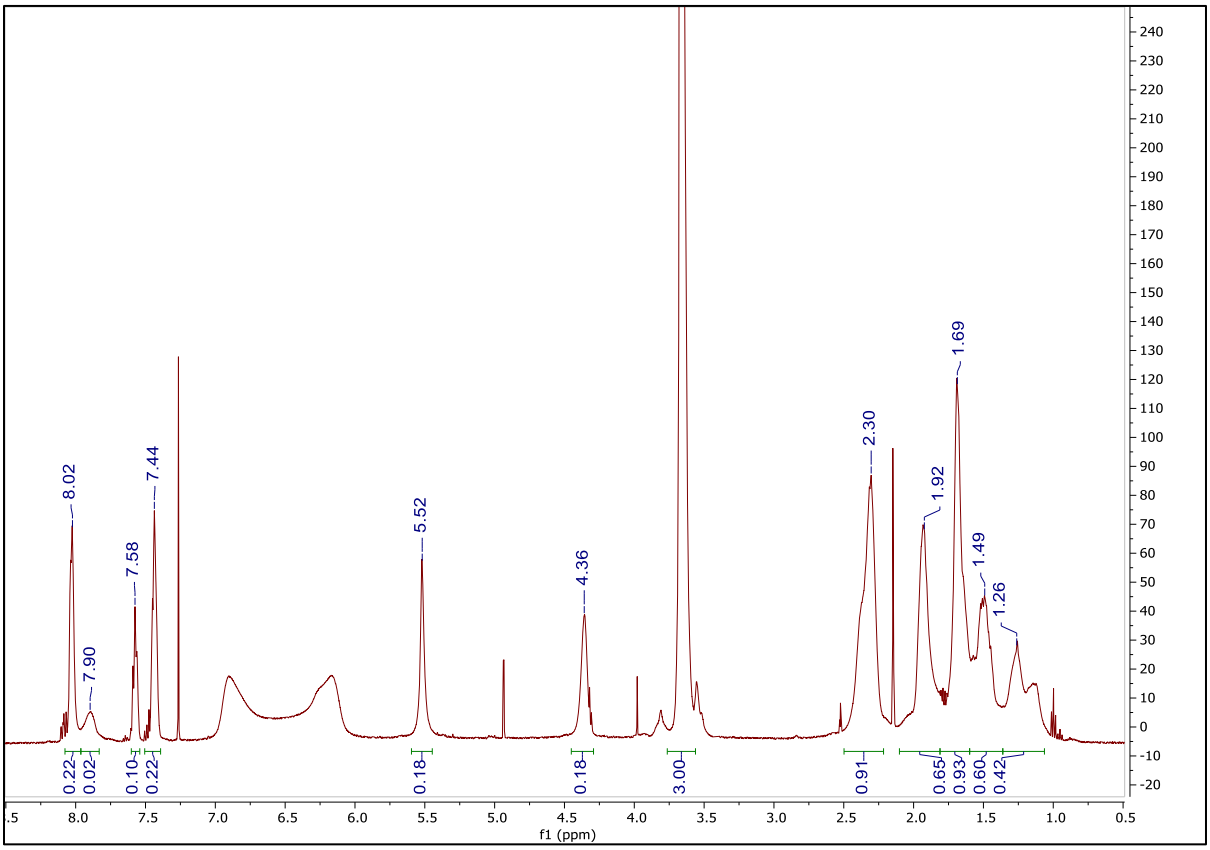

Figure A24: ^{1}H NMR spectrum of 1,4-disubstituted 1,2,3-triazole click product with propargyl benzoate attached (Table 3, Entry 10 / Table 4, Entry 4 / Table 5, Entry 10)

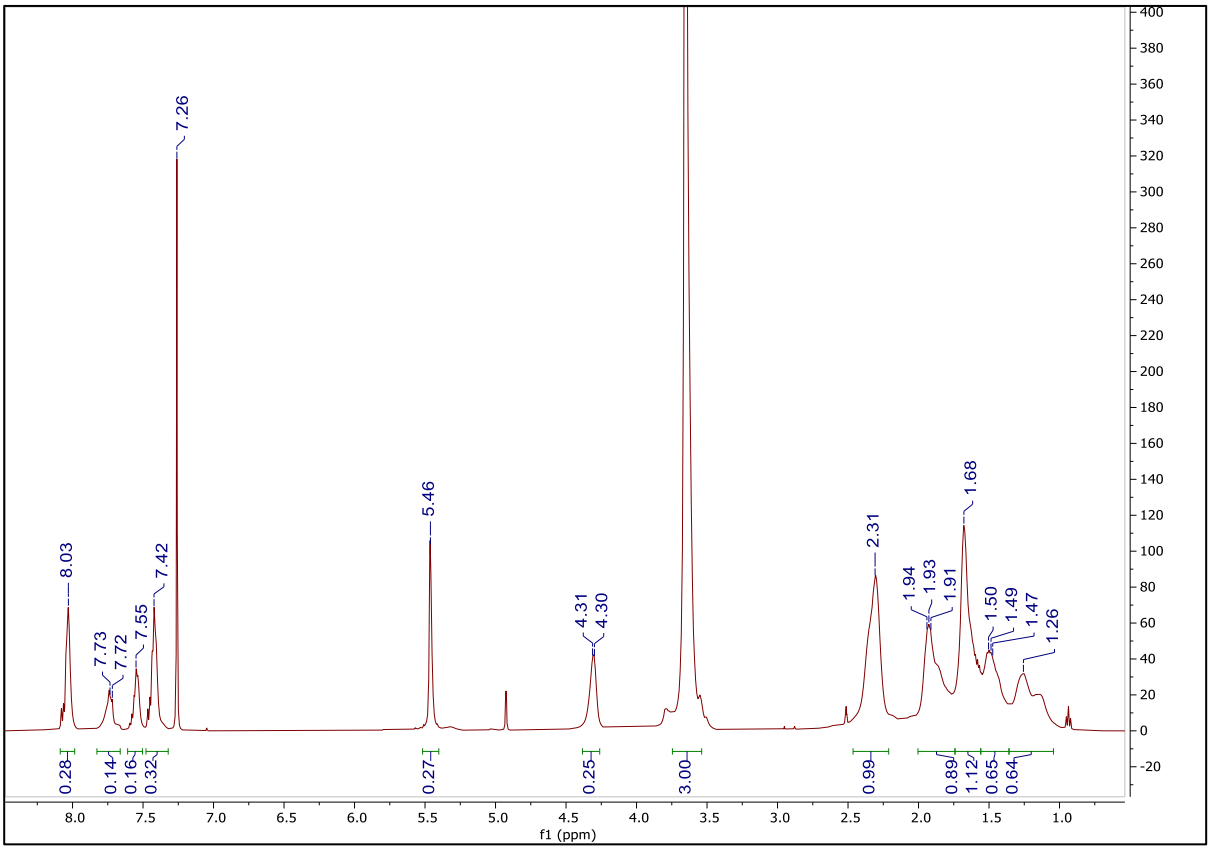

Figure A25: ^{1}H NMR spectrum of 1,4-disubstituted 1,2,3-triazole click product with propargyl benzoate attached (Table 3, Entry 11 / Table 4, Entry 5 / Table 5, Entry 11)

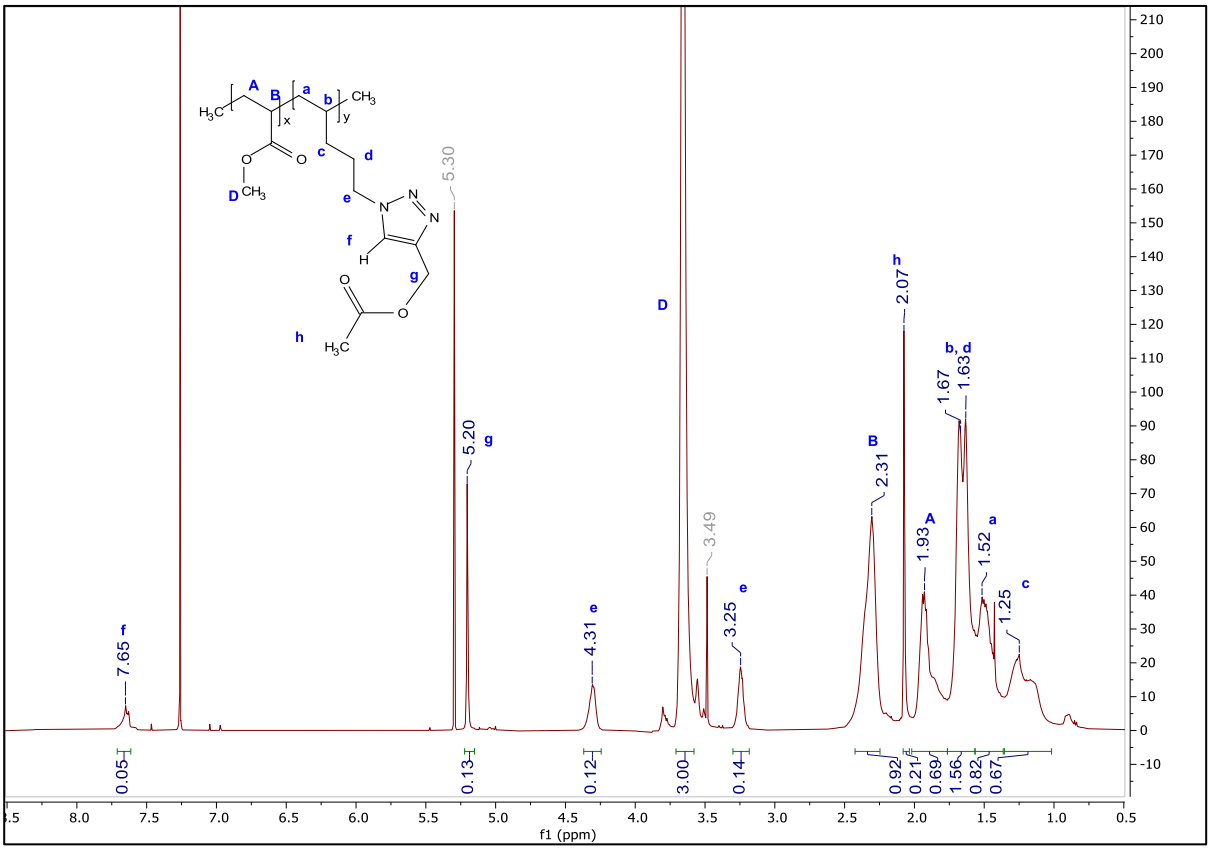

Figure A26: ^{1}H NMR spectrum of 1,4-disubstituted 1,2,3-triazole click product with propargyl acetate attached (Table 3, Entry 12)

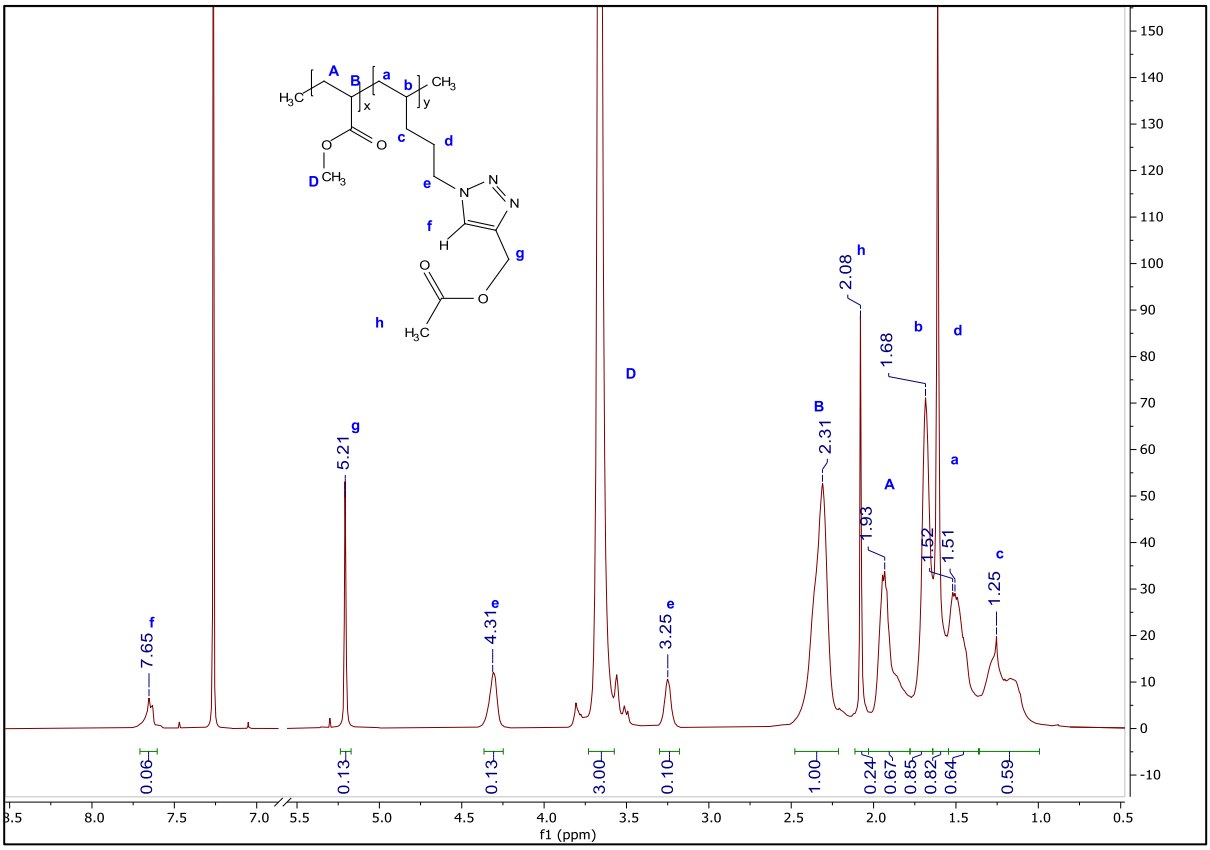

Figure A27: ^{1}H NMR spectrum of 1,4-disubstituted 1,2,3-triazole click product with propargyl acetate attached (Table 3, Entry 13)

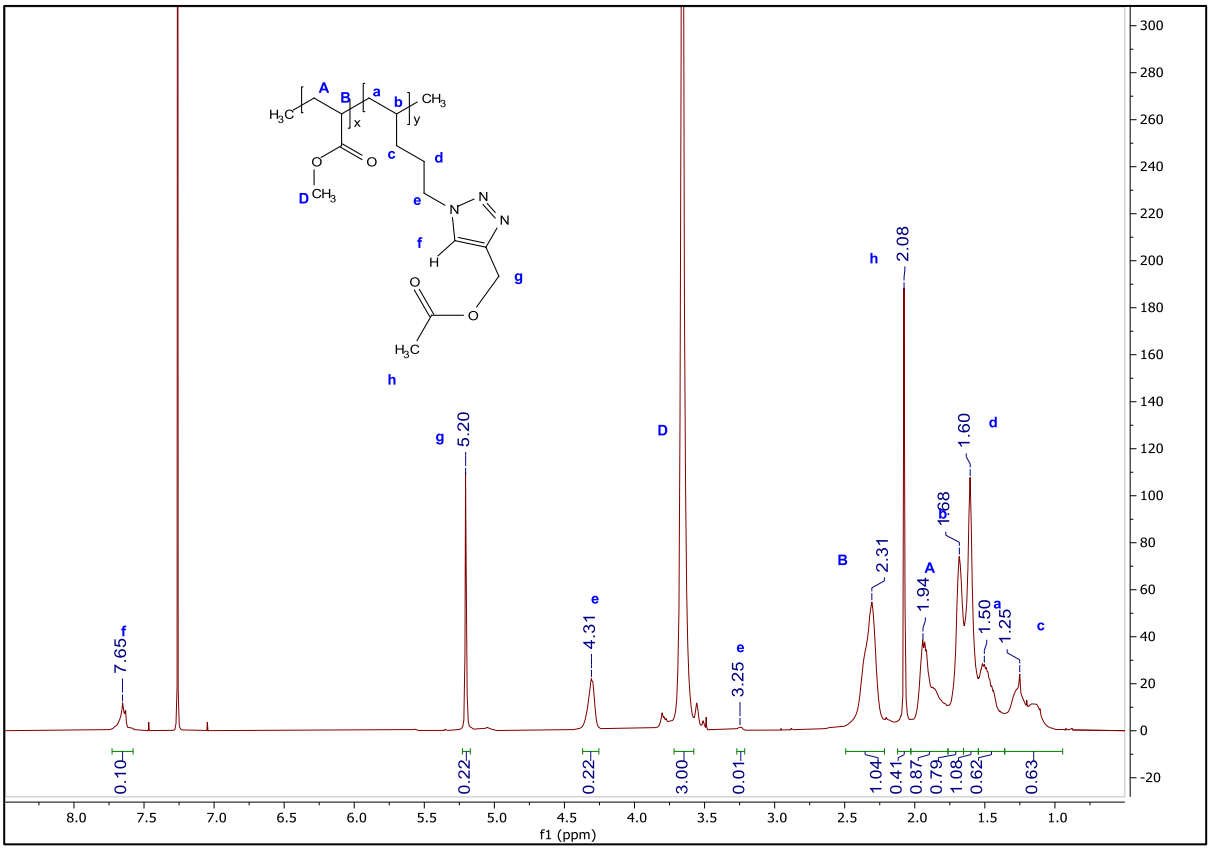

Figure A28: ^{1}H NMR spectrum of 1,4-disubstituted 1,2,3-triazole click product with propargyl acetate attached (Table 3, Entry 14 / Table 4, Entry 6 / Table 5, Entry 26)

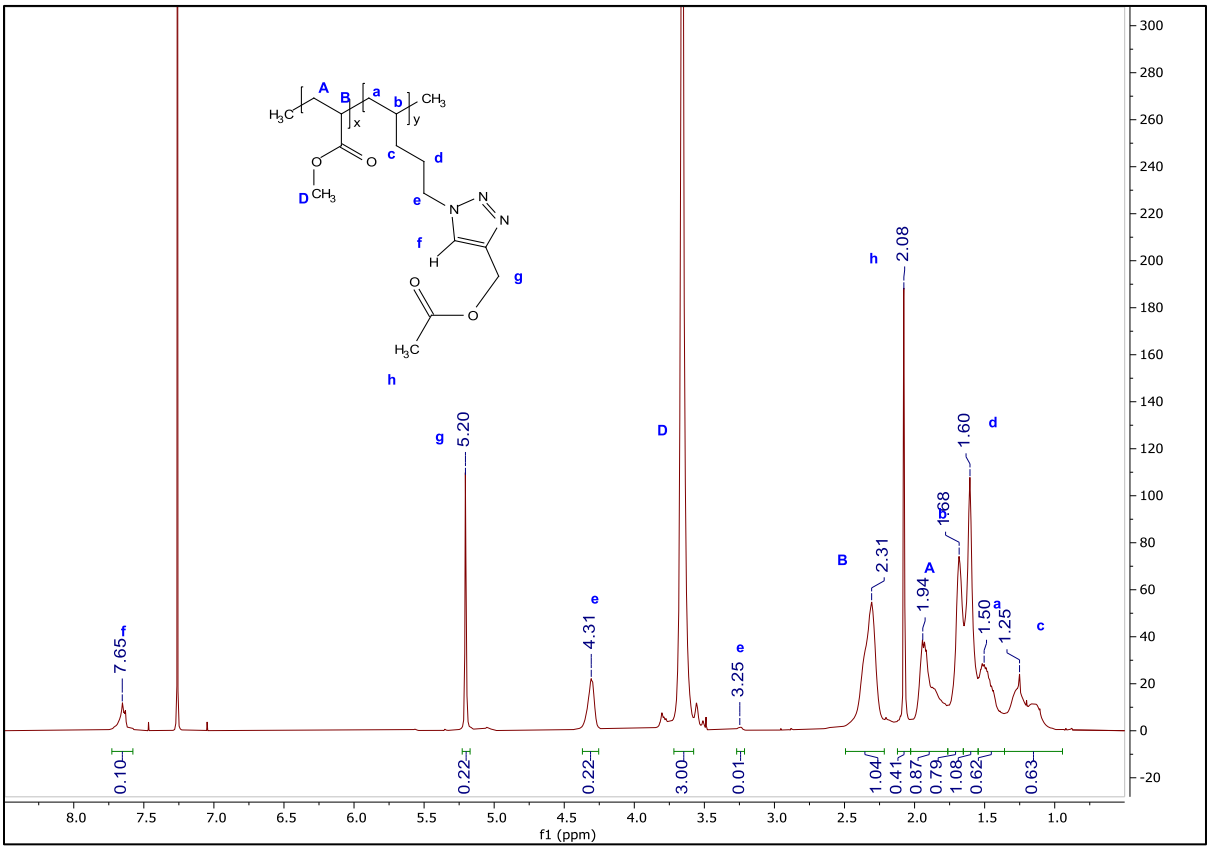

Figure A29: ^{1}H NMR spectrum of 1,4-disubstituted 1,2,3-triazole click product with propargyl acetate attached (Table 3, Entry 15 / Table 4, Entry 7 / Table 5, Entry 27)

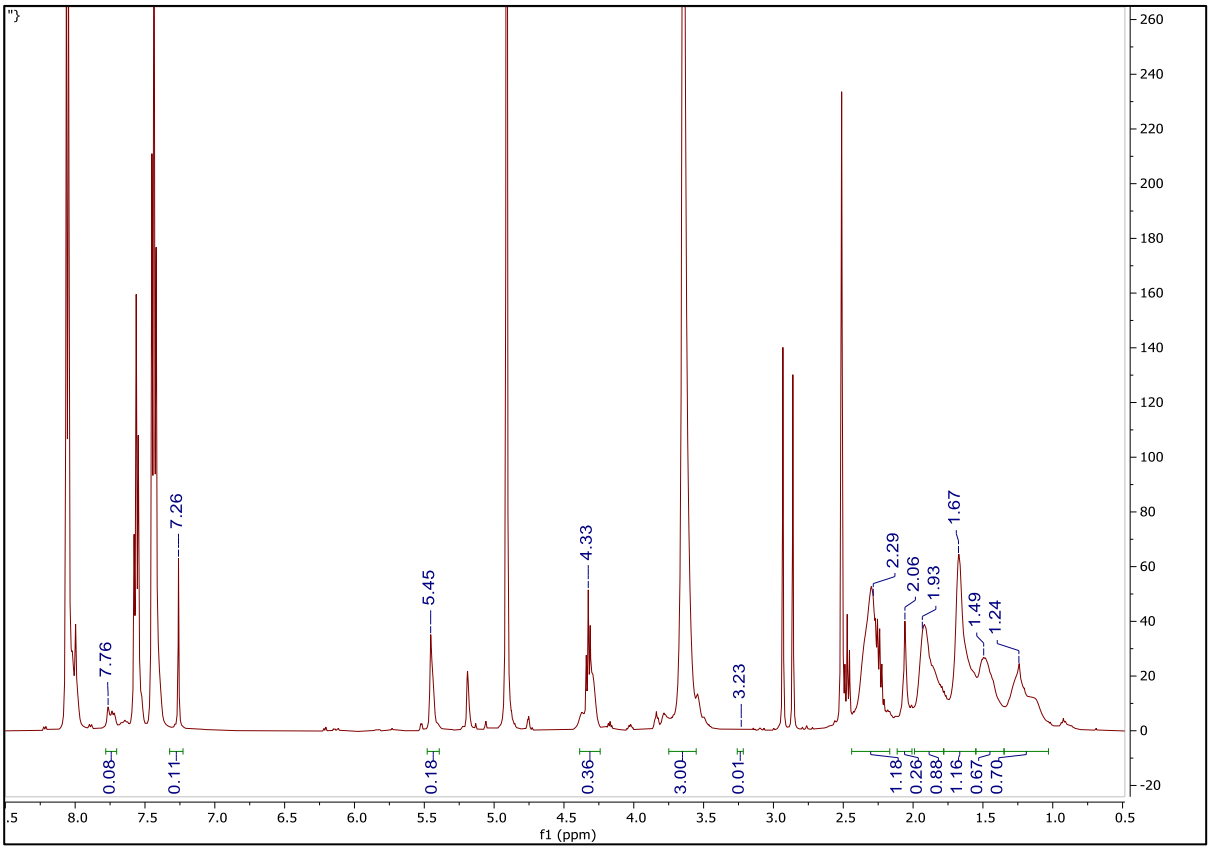

Figure A30: ^{1}H NMR spectrum of 1,4-disubstituted 1,2,3-triazole click product with propargyl acetate attached (Table 3, Entry 16 / Table 4, Entry 8 / Table 5, Entry 28)

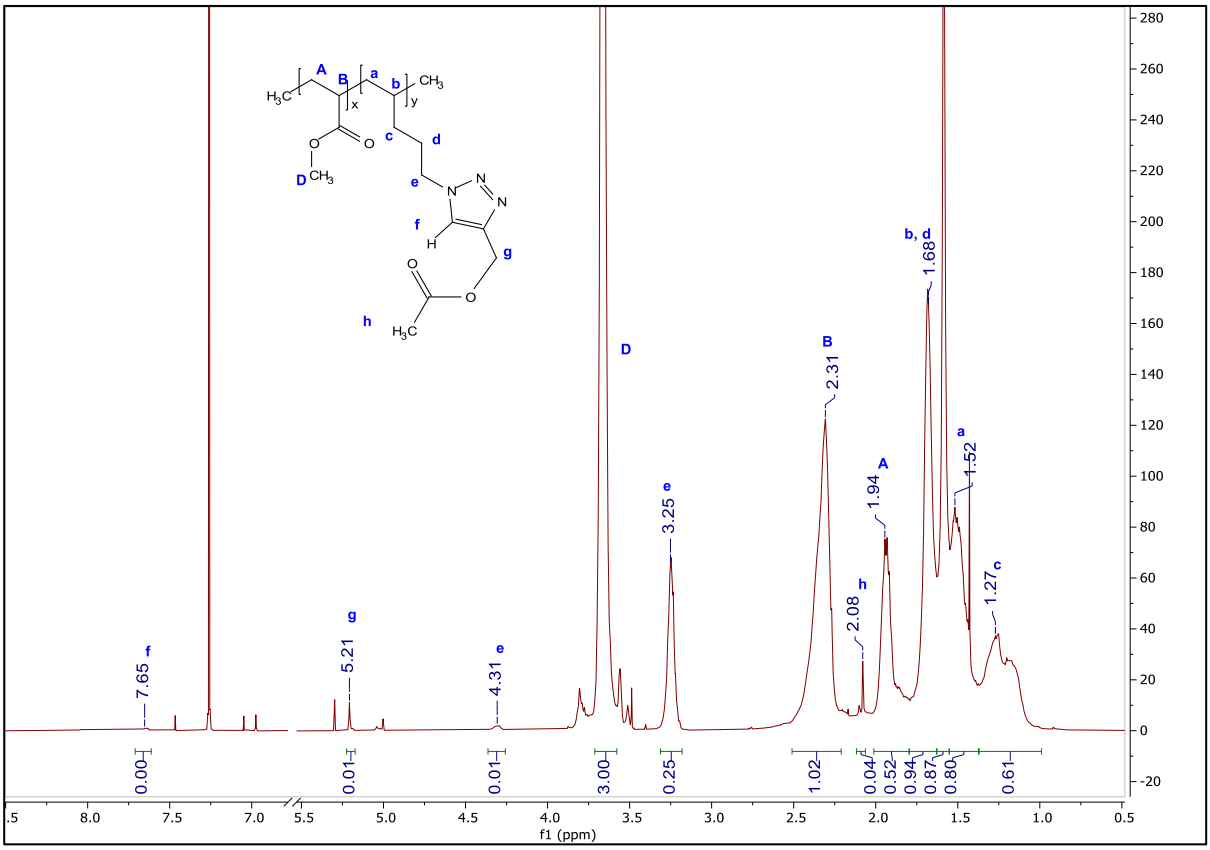

Figure A31: ^{1}H NMR spectrum of 1,4-disubstituted 1,2,3-triazole click product with propargyl acetate attached (Table 3, Entry 17)

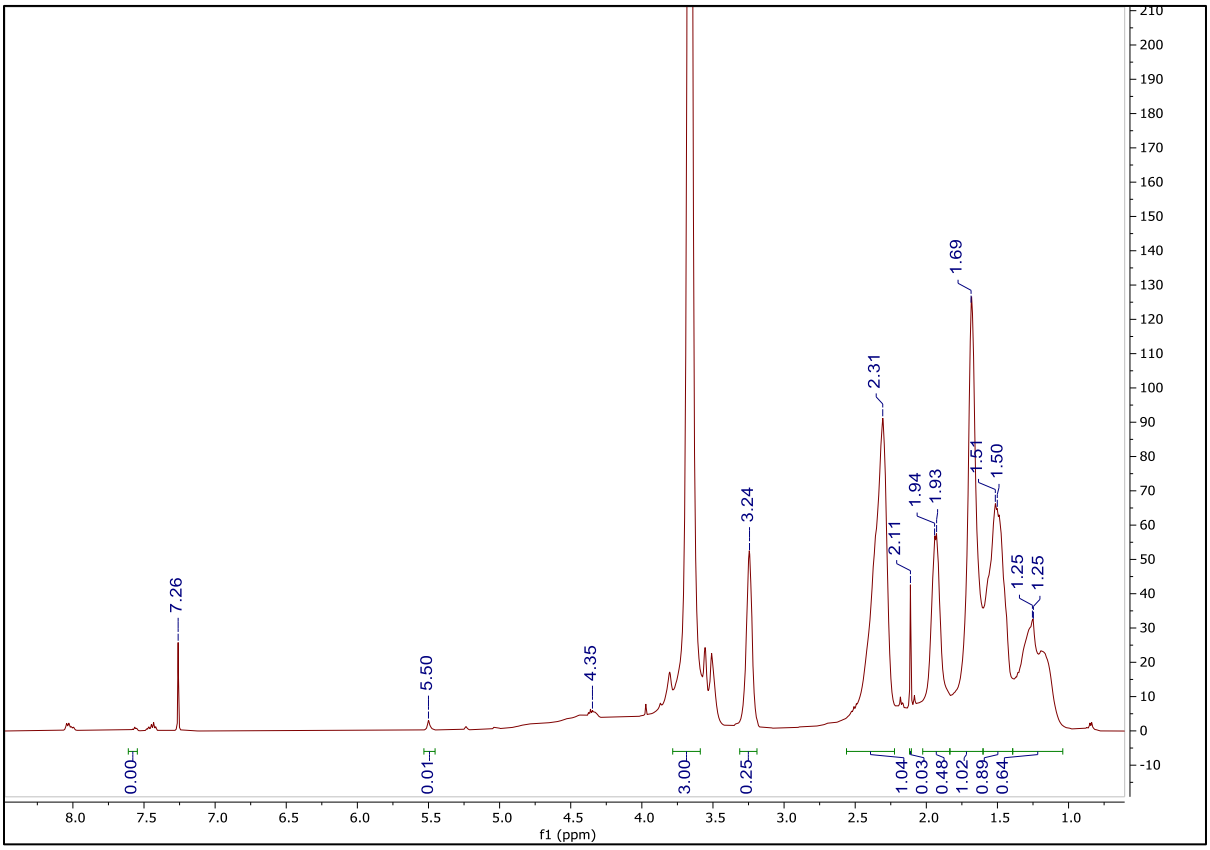

Figure A32: ^{1}H NMR spectrum of 1,4-disubstituted 1,2,3-triazole click product with propargyl acetate attached (Table 3, Entry 18)

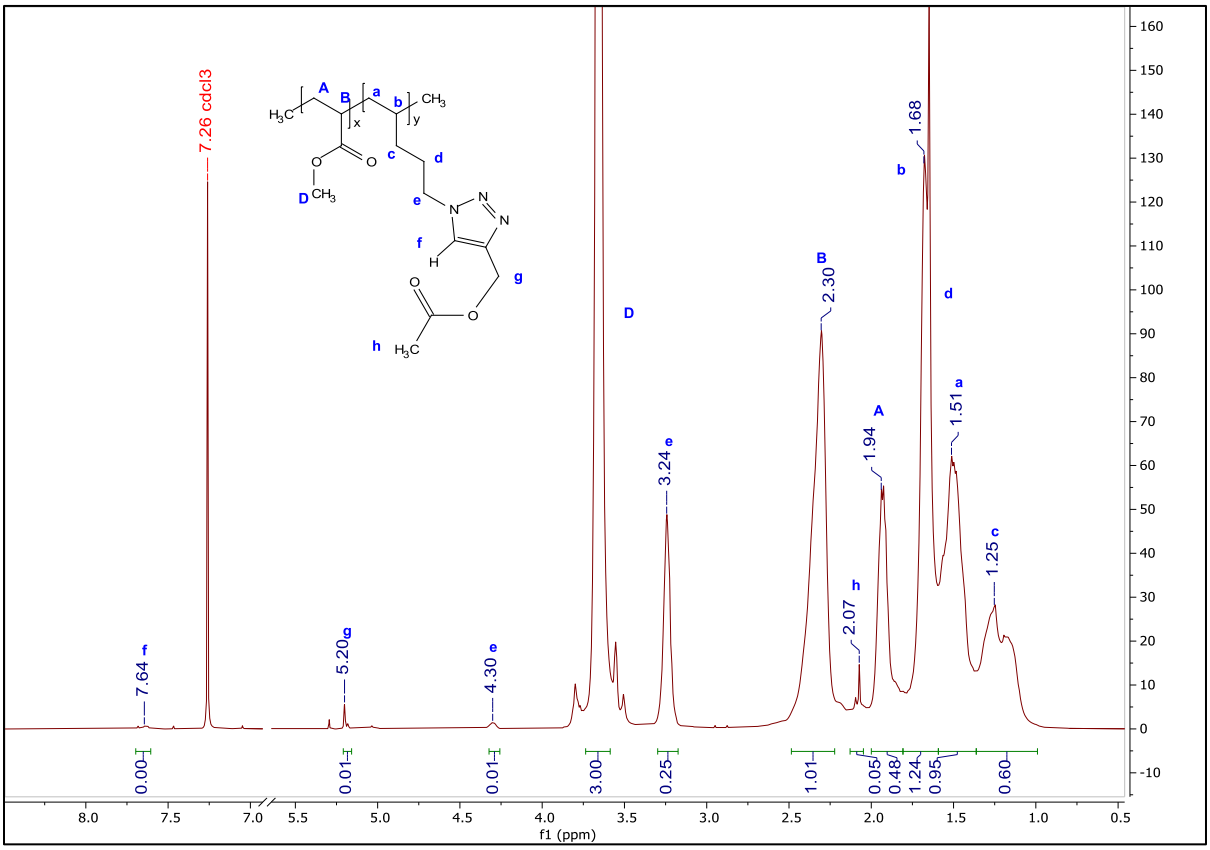

Figure A33: ^{1}H NMR spectrum of 1,4-disubstituted 1,2,3-triazole click product with propargyl acetate attached (Table 3, Entry 19 / Table 4, Entry 9 / Table 5, Entry 35)

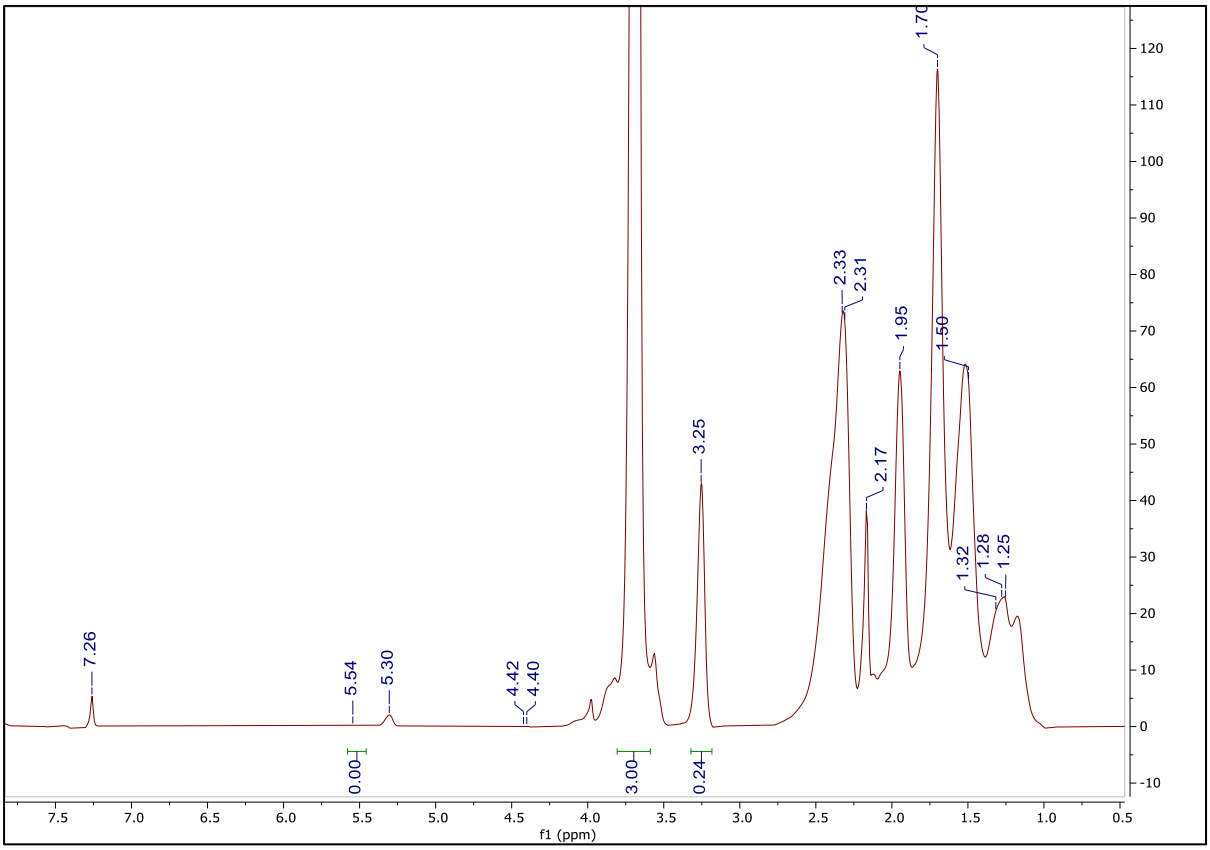

Figure A34: ^{1}H NMR spectrum of 1,4-disubstituted 1,2,3-triazole click product with propargyl acetate attached (Table 3, Entry 20 / Table 4, Entry 10 / Table 5, Entry 36)

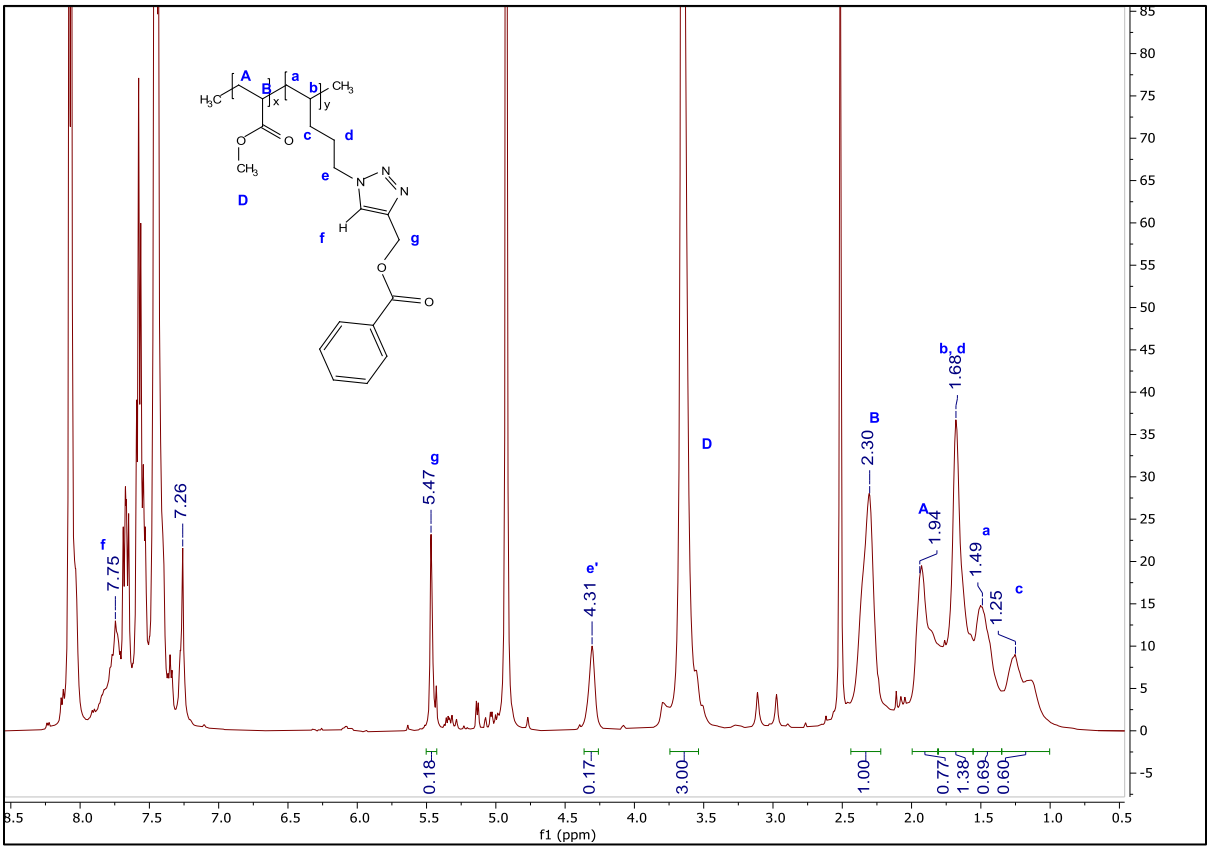

Figure A35: ^{1}H NMR spectrum of 1,4-disubstituted 1,2,3-triazole click product with propargyl benzoate attached (Table 4, Entry 11 / Table 5, Entry 18)

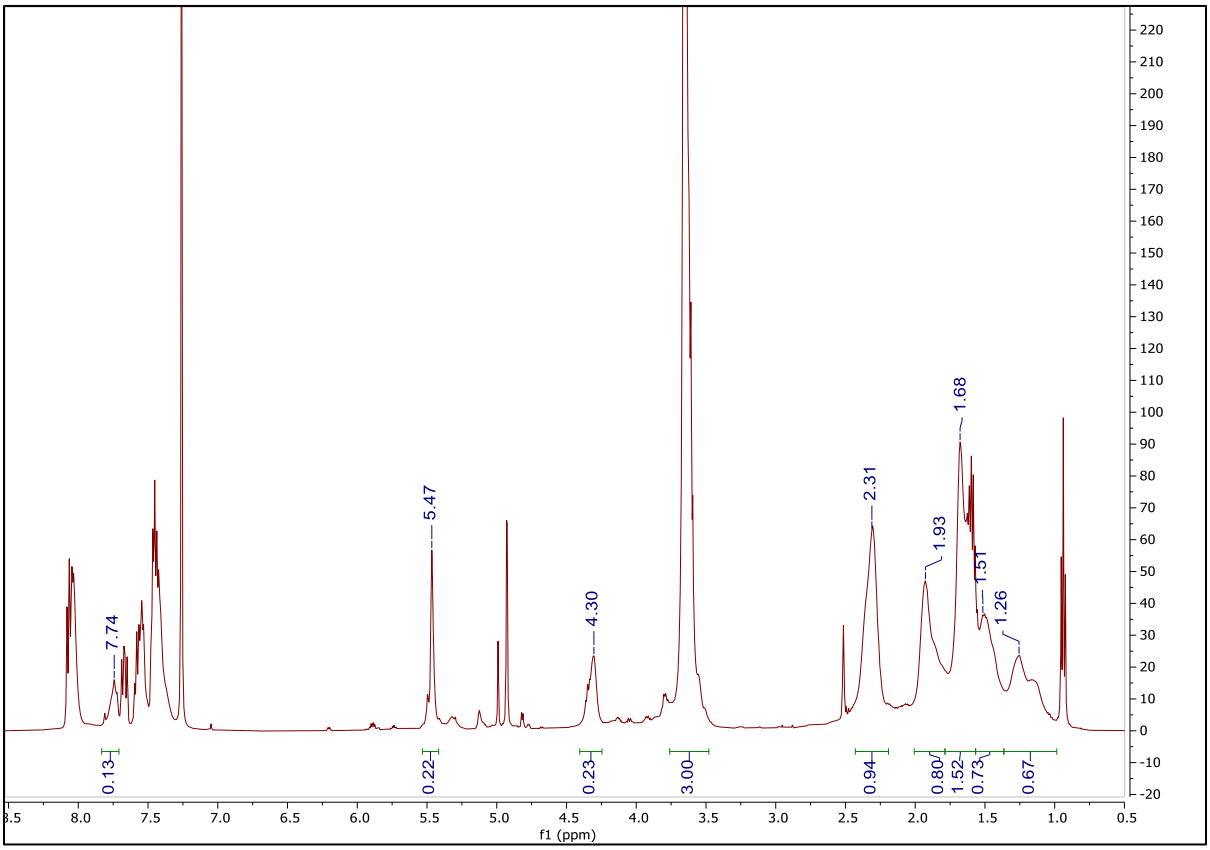

Figure A36: ^{1}H NMR spectrum of 1,4-disubstituted 1,2,3-triazole click product with propargyl benzoate attached (Table 4, Entry 12 / Table 5, Entry 19)

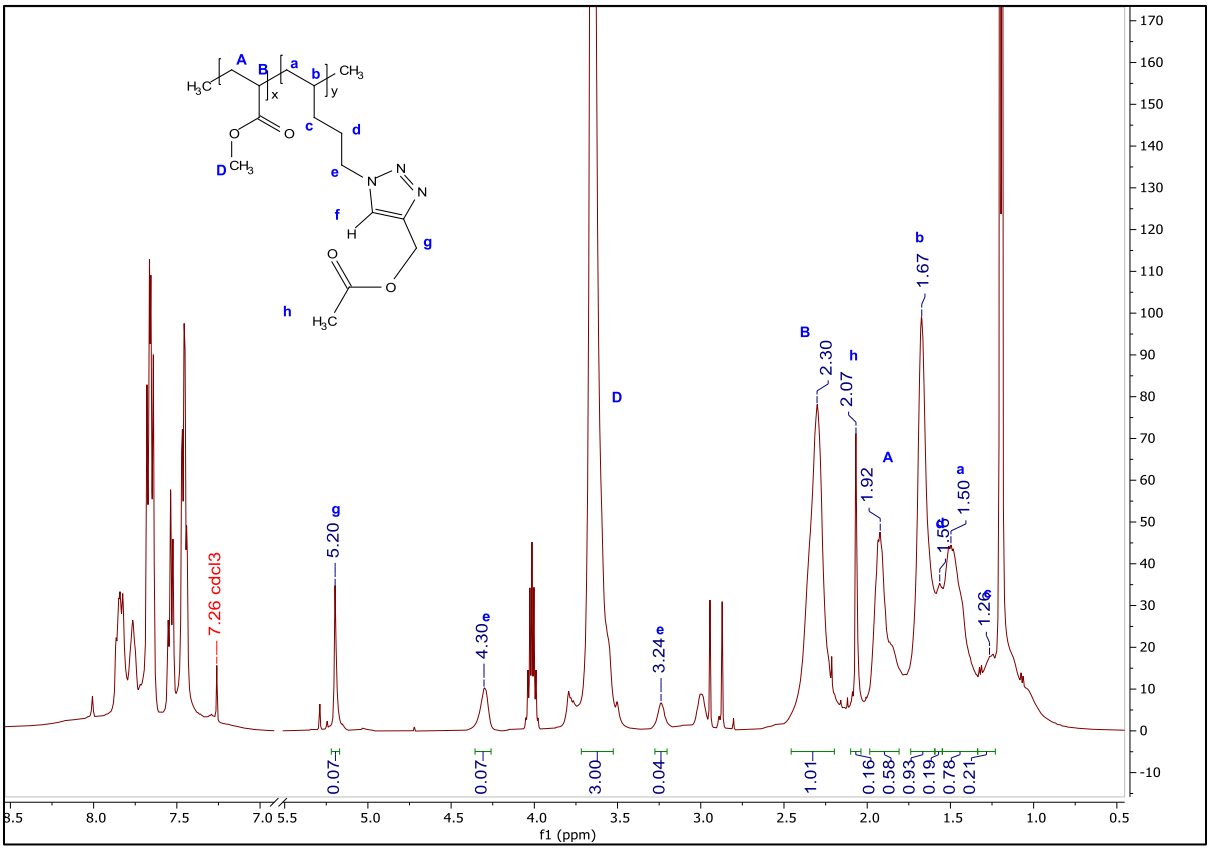

Figure A37: ^{1}H NMR spectrum of 1,4-disubstituted 1,2,3-triazole click product with propargyl acetate attached (Table 4, Entry 13 / Table 5, Entry 43)

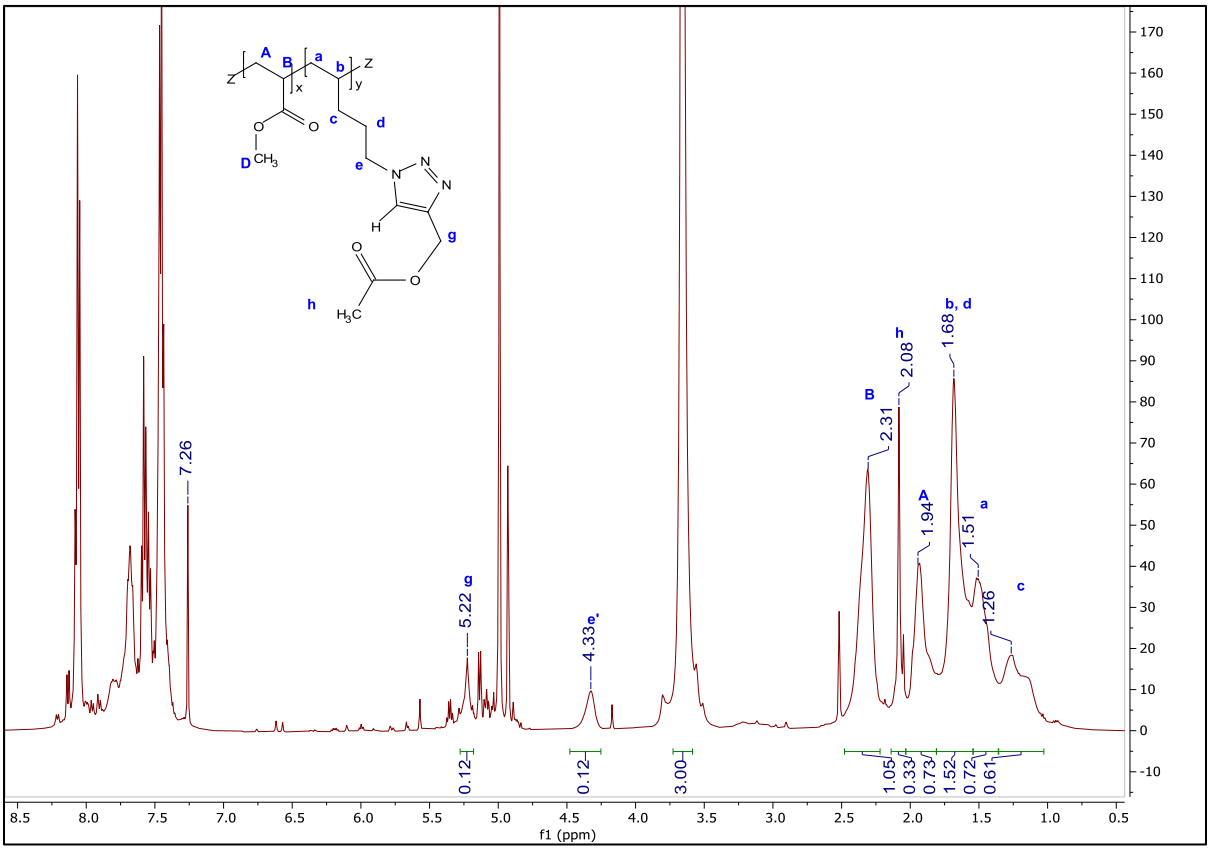

Figure A38: ^{1}H NMR spectrum of 1,4-disubstituted 1,2,3-triazole click product with propargyl acetate attached (Table 4, Entry 14 / Table 5, Entry 44)

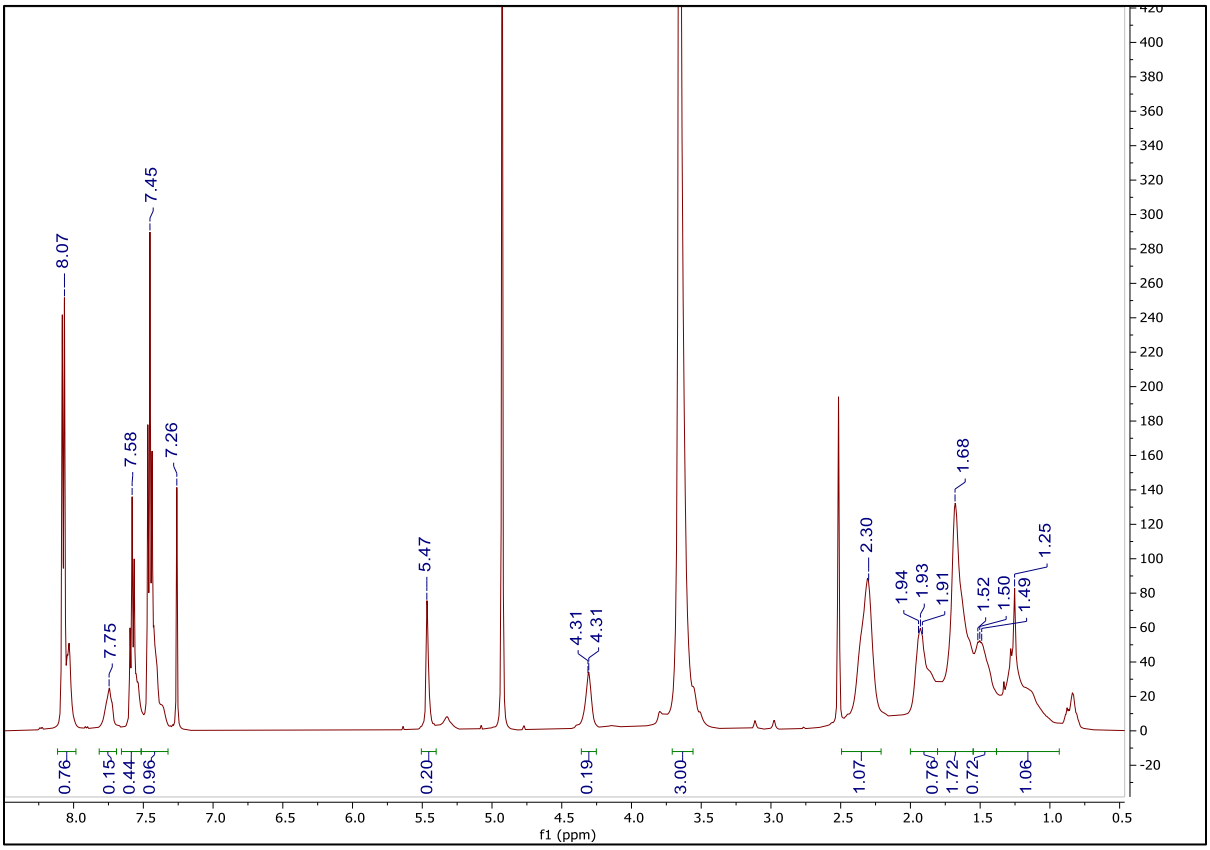

Figure A39: ^{1}H NMR spectrum of 1,4-disubstituted 1,2,3-triazole click product with propargyl benzoate attached (Table 5, Entry 3)

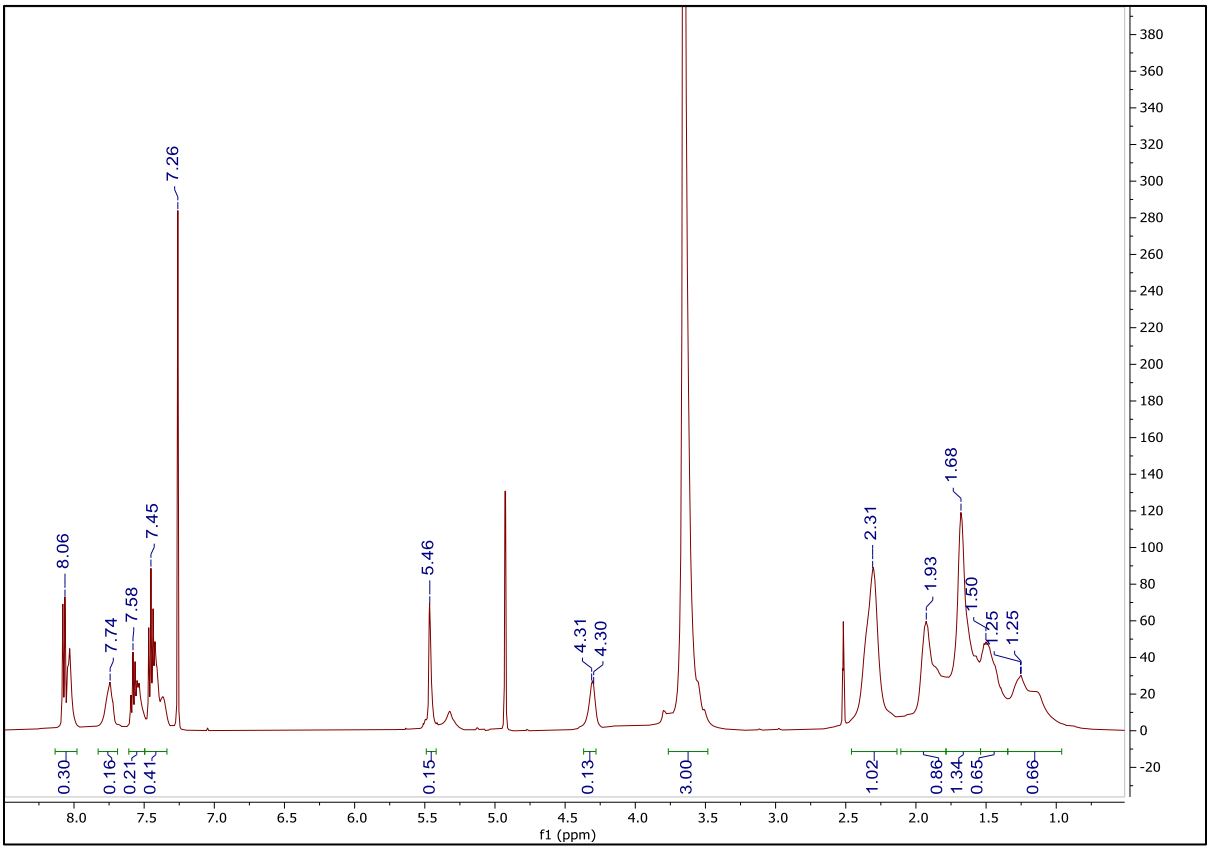

Figure A40: ^{1}H NMR spectrum of 1,4-disubstituted 1,2,3-triazole click product with propargyl benzoate attached (Table 5, Entry 4)

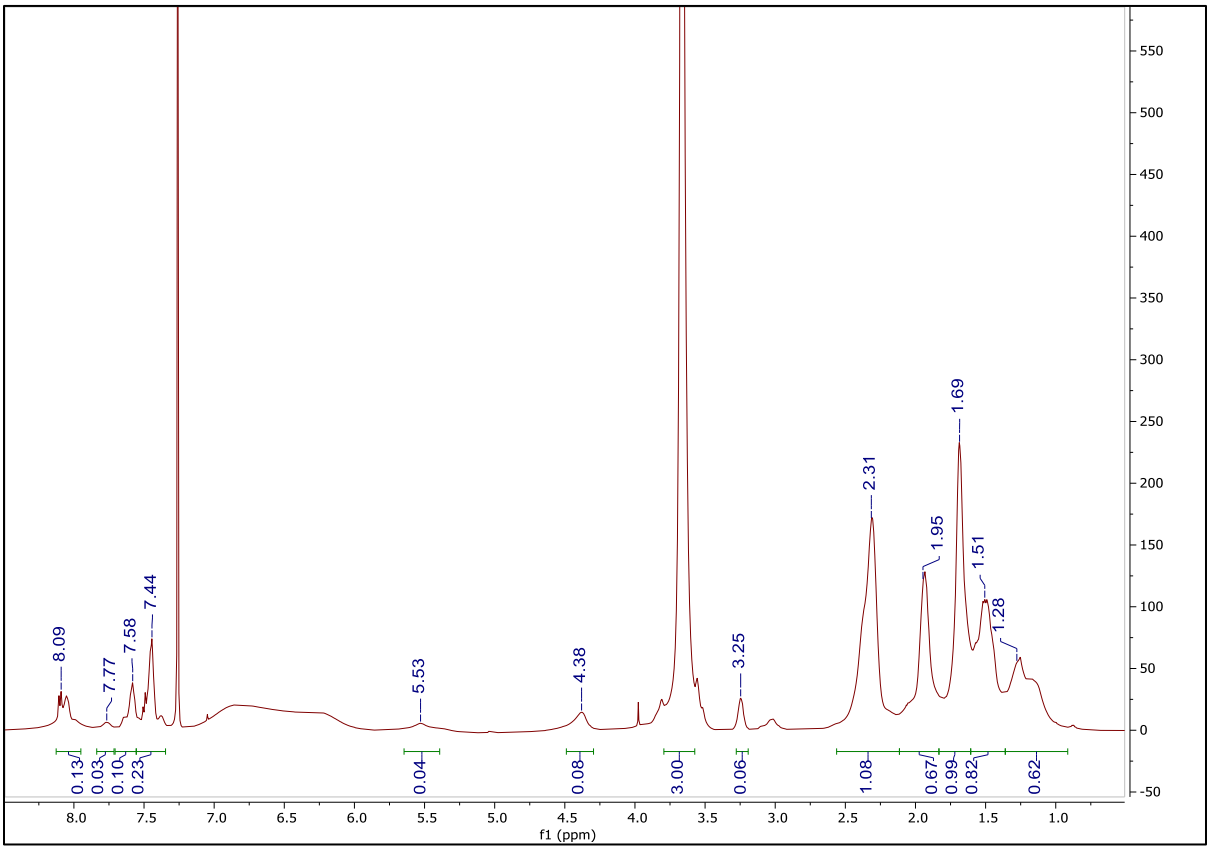

Figure A41: ^{1}H NMR spectrum of 1,4-disubstituted 1,2,3-triazole click product with propargyl benzoate attached (Table 5, Entry 5)

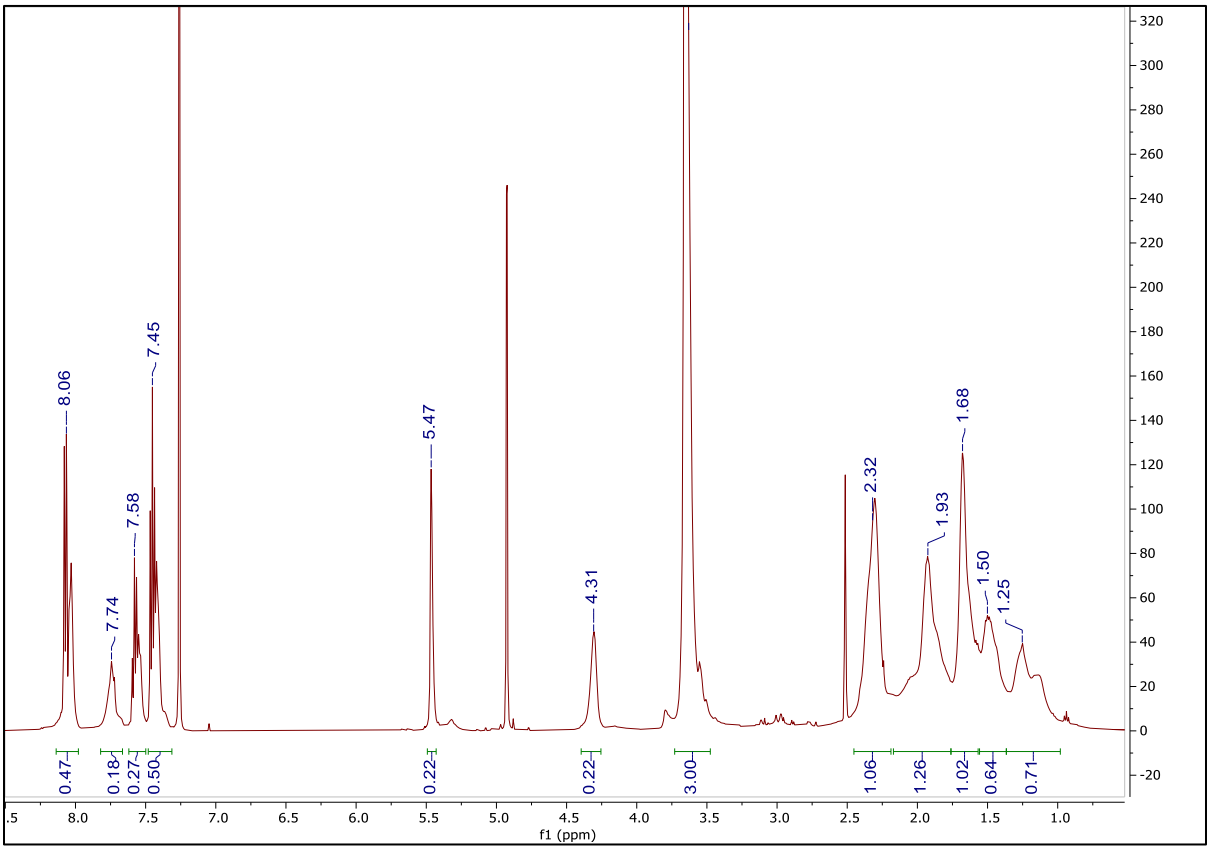

Figure A42: ^{1}H NMR spectrum of 1,4-disubstituted 1,2,3-triazole click product with propargyl benzoate attached (Table 5, Entry 6)

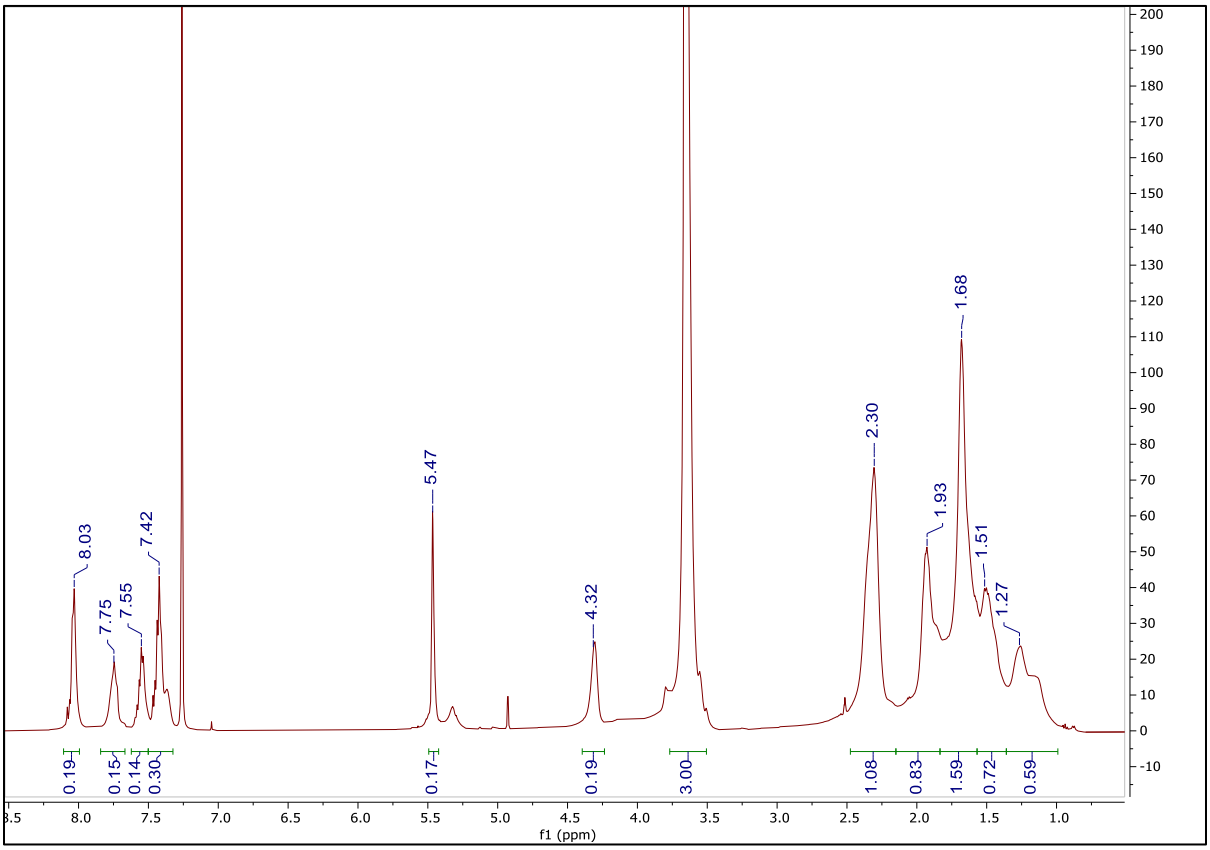

Figure A43: ^{1}H NMR spectrum of 1,4-disubstituted 1,2,3-triazole click product with propargyl benzoate attached (Table 5, Entry 7)

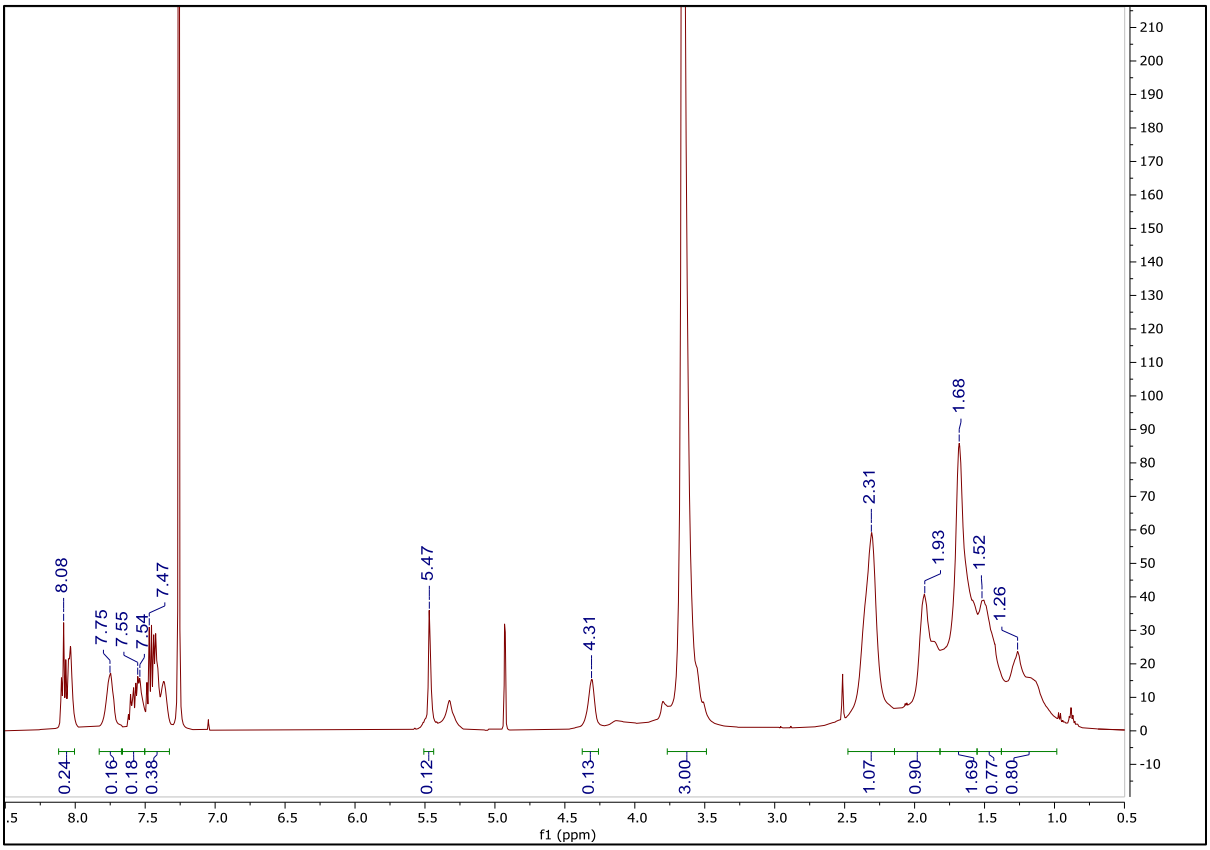

Figure A44: ^{1}H NMR spectrum of 1,4-disubstituted 1,2,3-triazole click product with propargyl benzoate attached (Table 5, Entry 8)

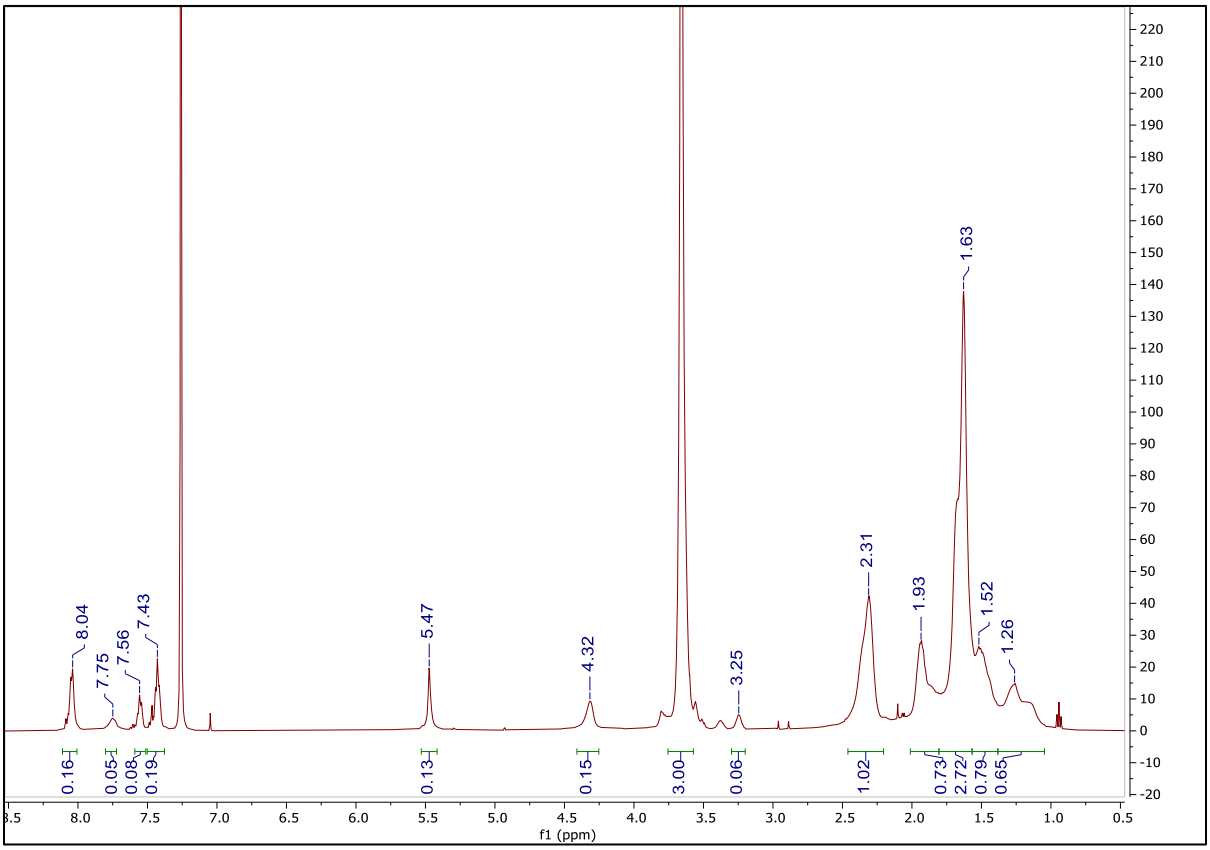

Figure A45: ^{1}H NMR spectrum of 1,4-disubstituted 1,2,3-triazole click product with propargyl benzoate attached (Table 5, Entry 12)

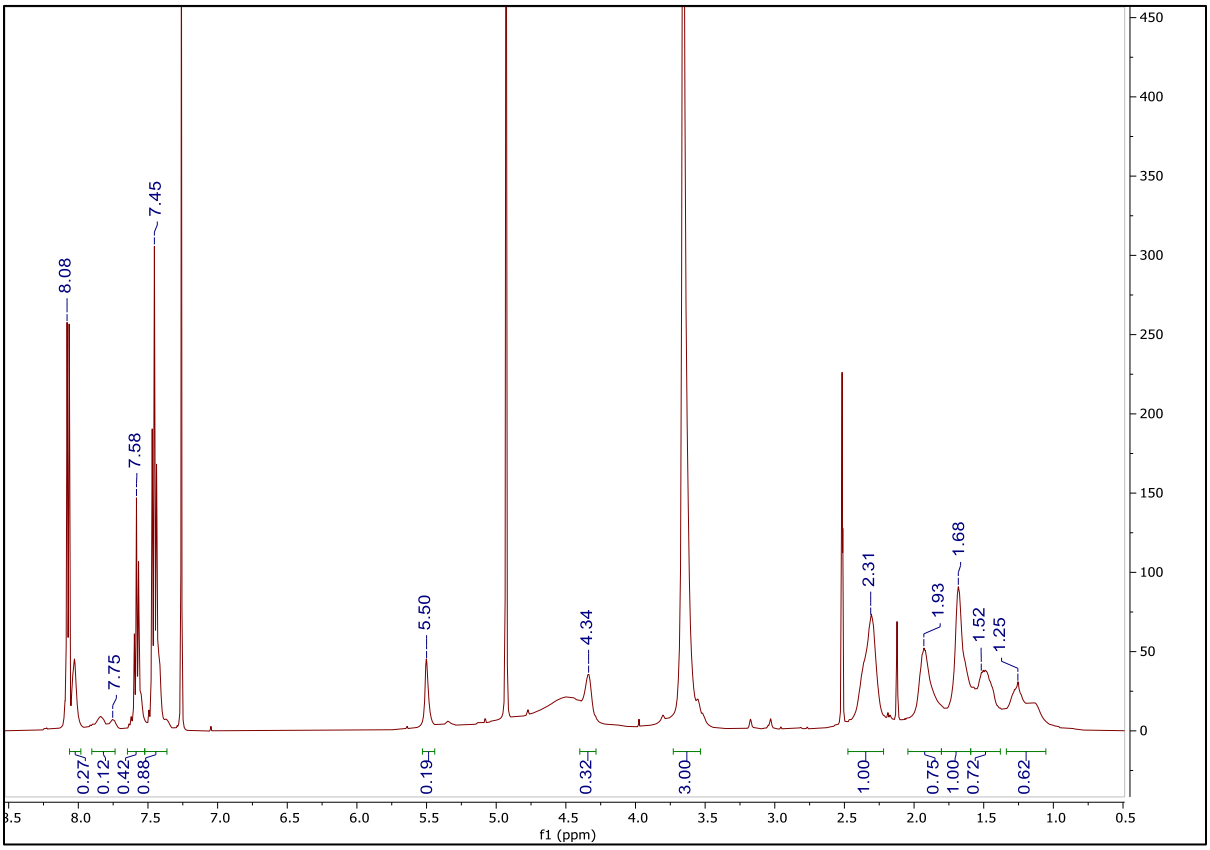

Figure A46: ^{1}H NMR spectrum of 1,4-disubstituted 1,2,3-triazole click product with propargyl benzoate attached (Table 5, Entry 13)

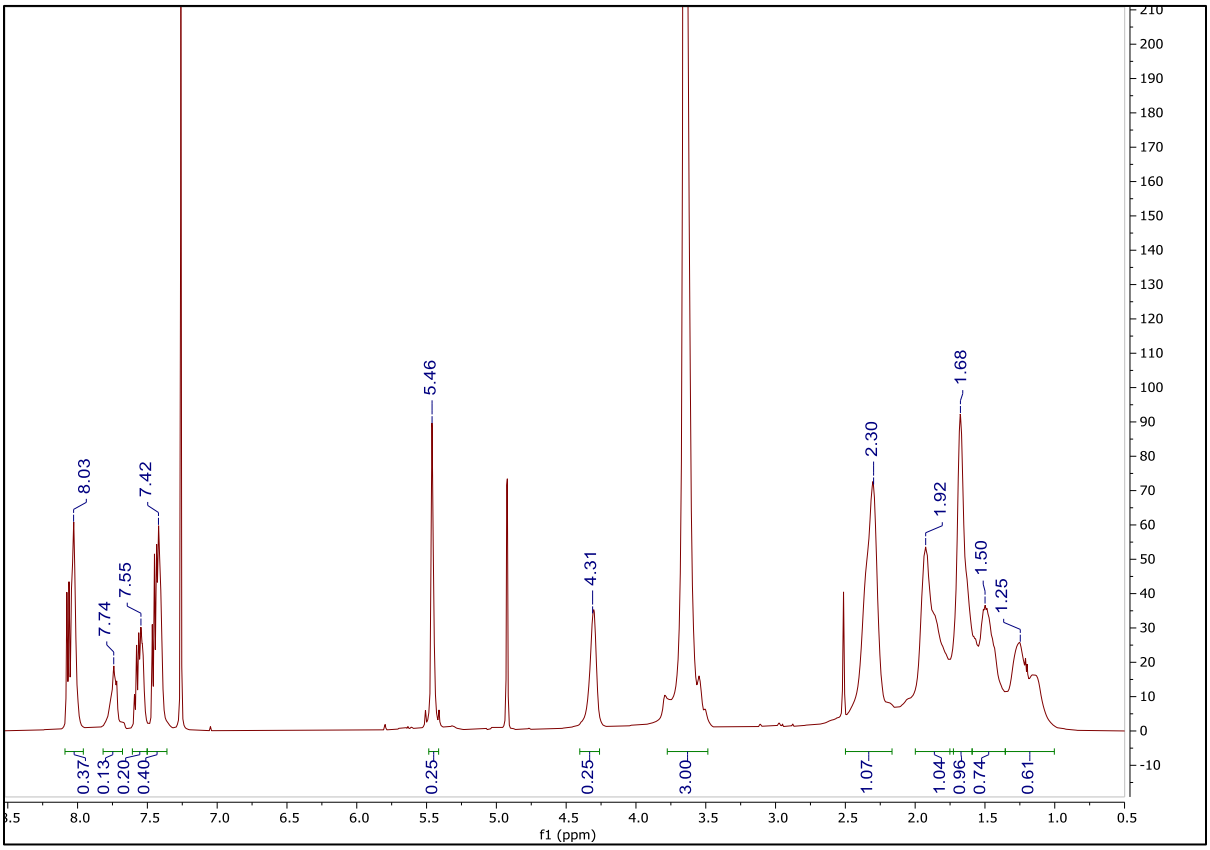

Figure A47: ^{1}H NMR spectrum of 1,4-disubstituted 1,2,3-triazole click product with propargyl benzoate attached (Table 5, Entry 14)

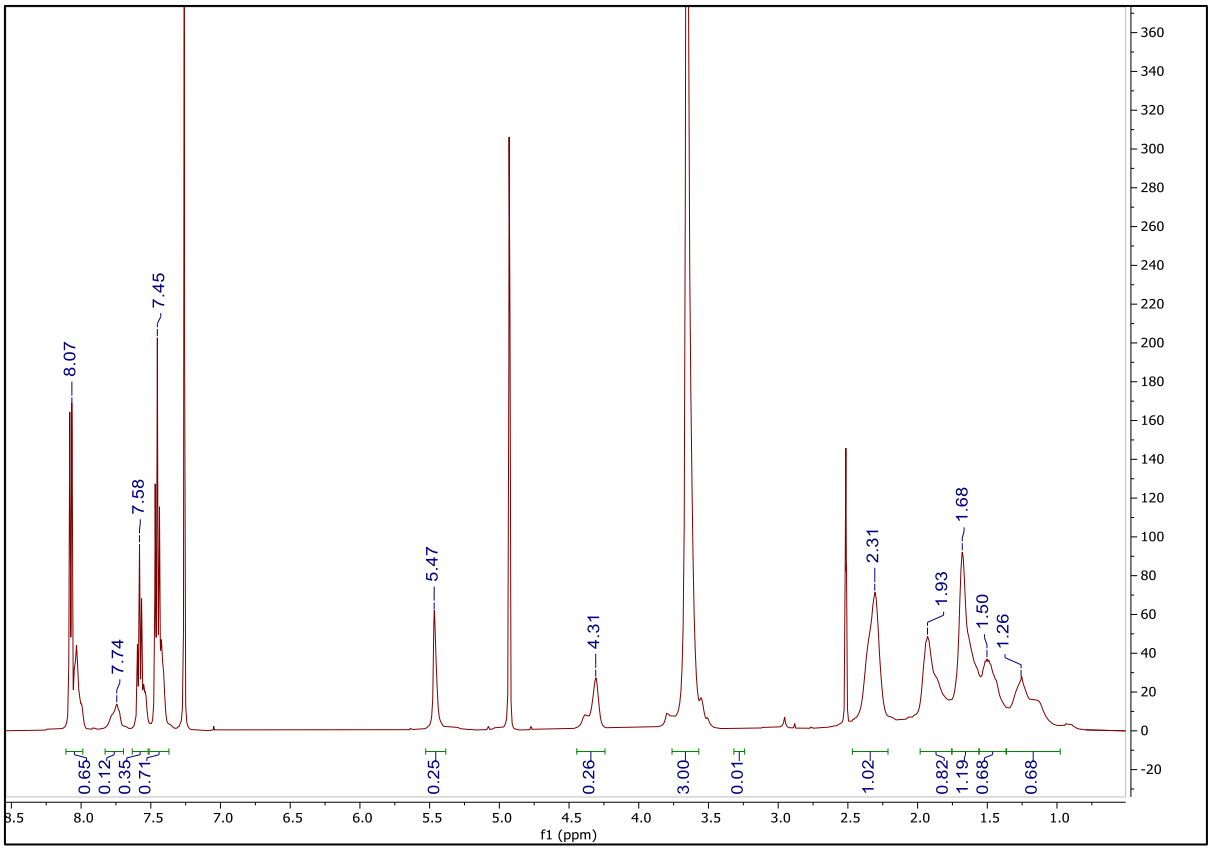

Figure A48: ^{1}H NMR spectrum of 1,4-disubstituted 1,2,3-triazole click product with propargyl benzoate attached (Table 5, Entry 15)

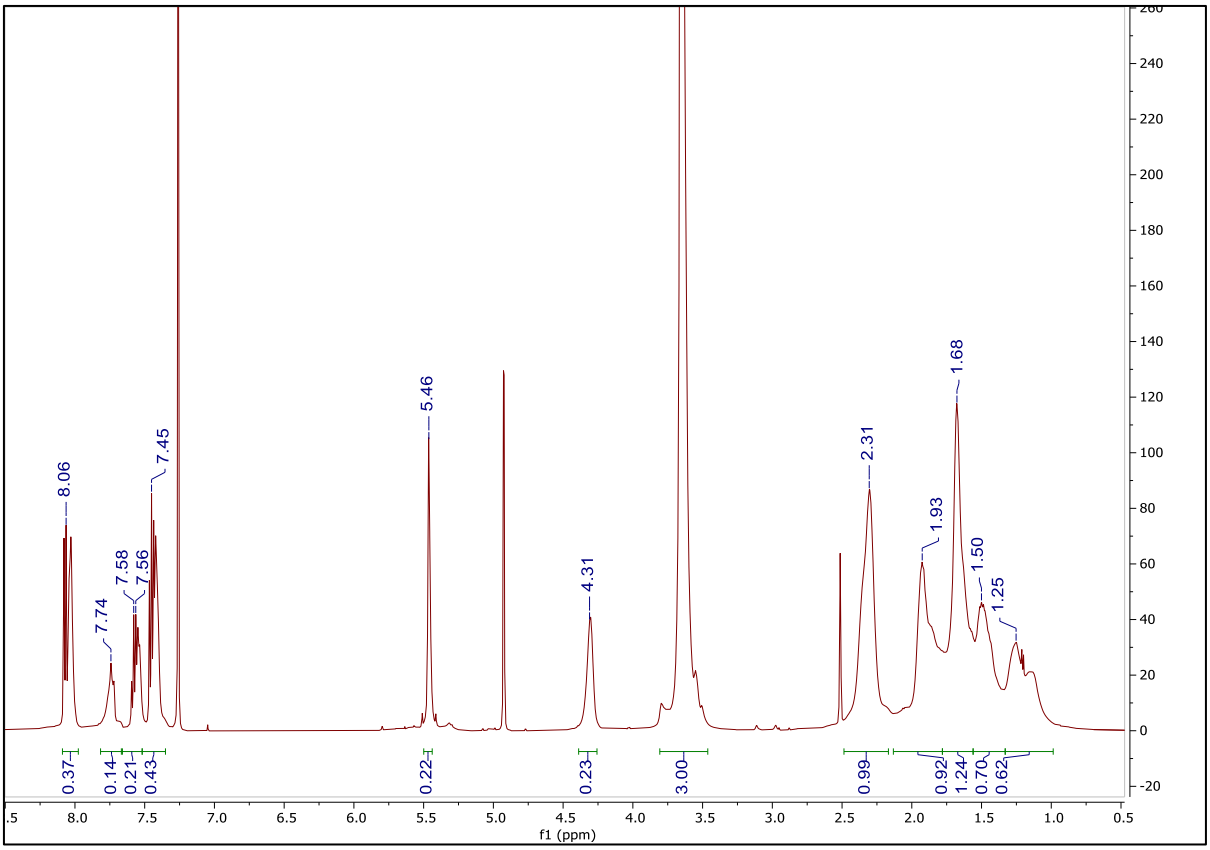

Figure A49: ^{1}H NMR spectrum of 1,4-disubstituted 1,2,3-triazole click product with propargyl benzoate attached (Table 5, Entry 16)

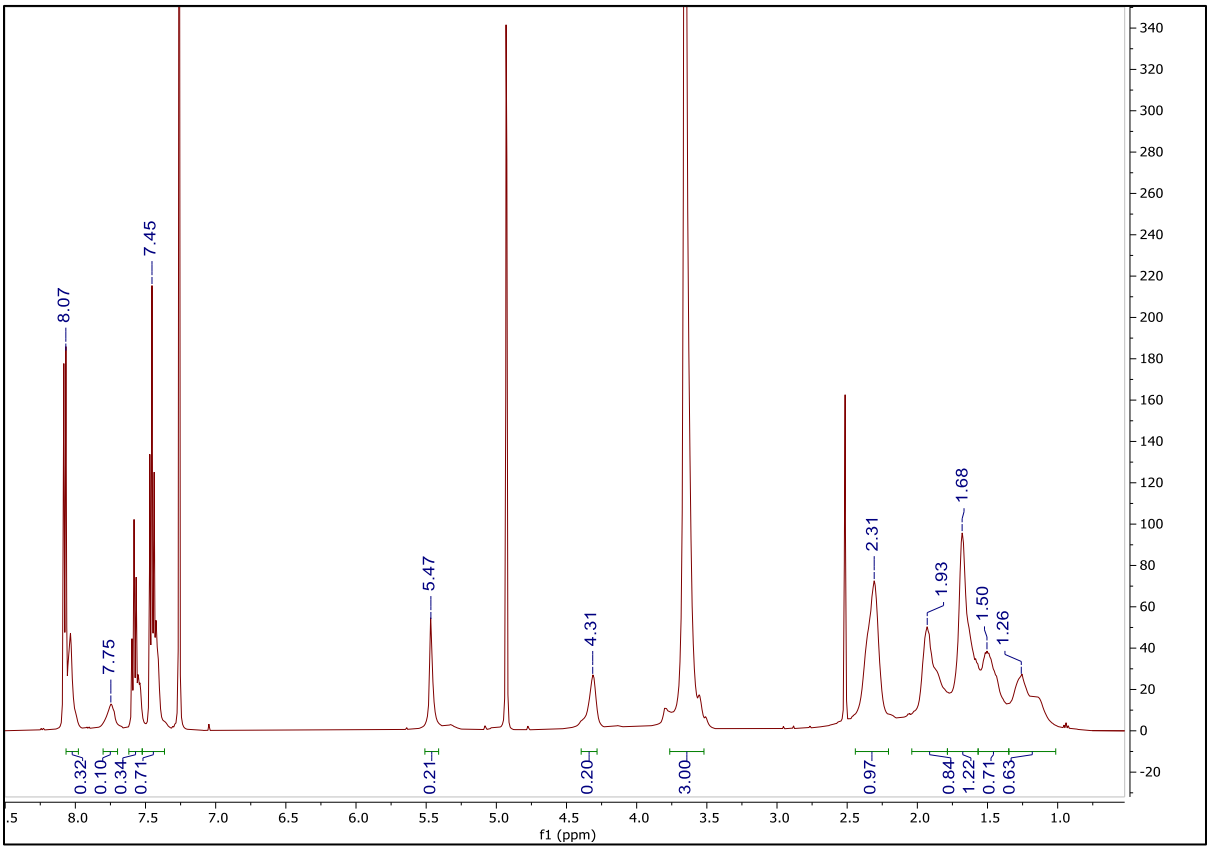

Figure A50: ^{1}H NMR spectrum of 1,4-disubstituted 1,2,3-triazole click product with propargyl benzoate attached (Table 5, Entry 17)

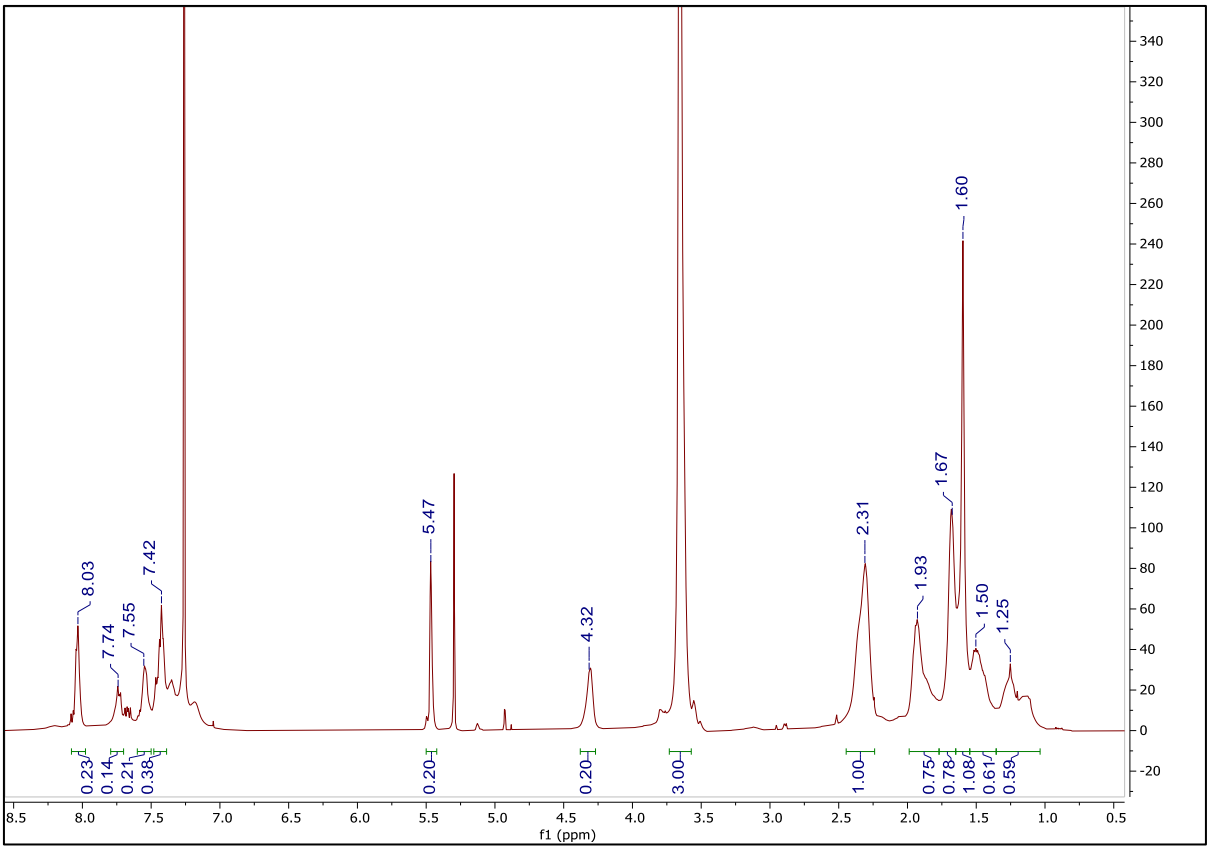

Figure A51: ^{1}H NMR spectrum of 1,4-disubstituted 1,2,3-triazole click product with propargyl benzoate attached (Table 5, Entry 20)

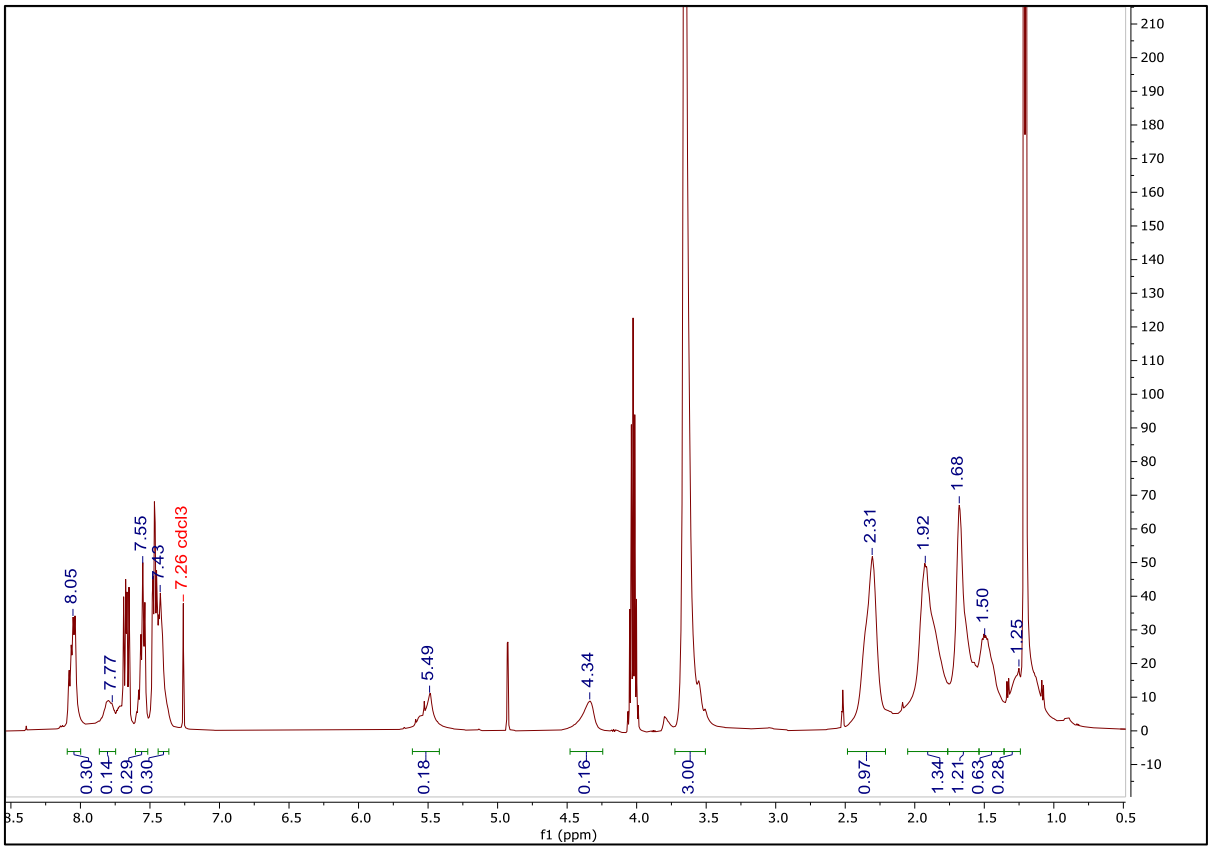

Figure A52: ^{1}H NMR spectrum of 1,4-disubstituted 1,2,3-triazole click product with propargyl benzoate attached (Table 5, Entry 21)

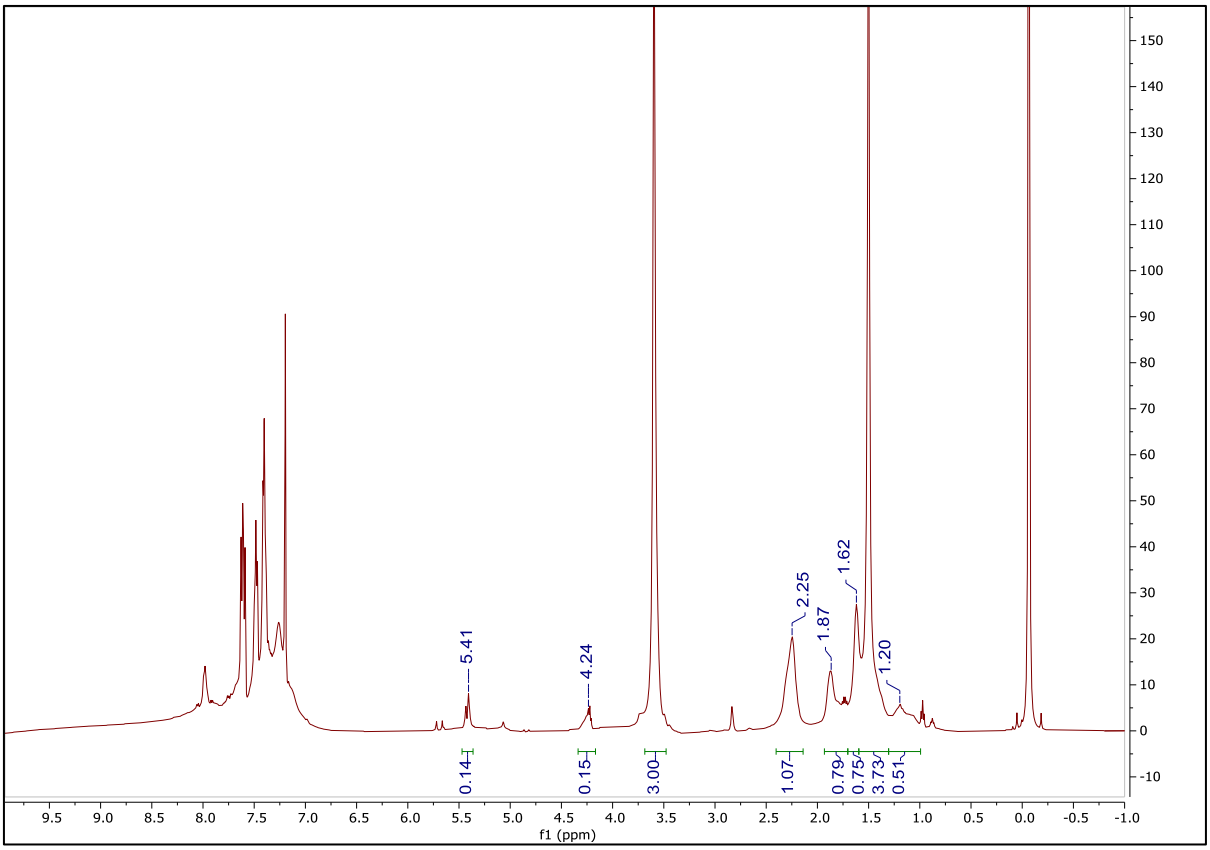

Figure A53: ^{1}H NMR spectrum of 1,4-disubstituted 1,2,3-triazole click product with propargyl benzoate attached (Table 5, Entry 22)

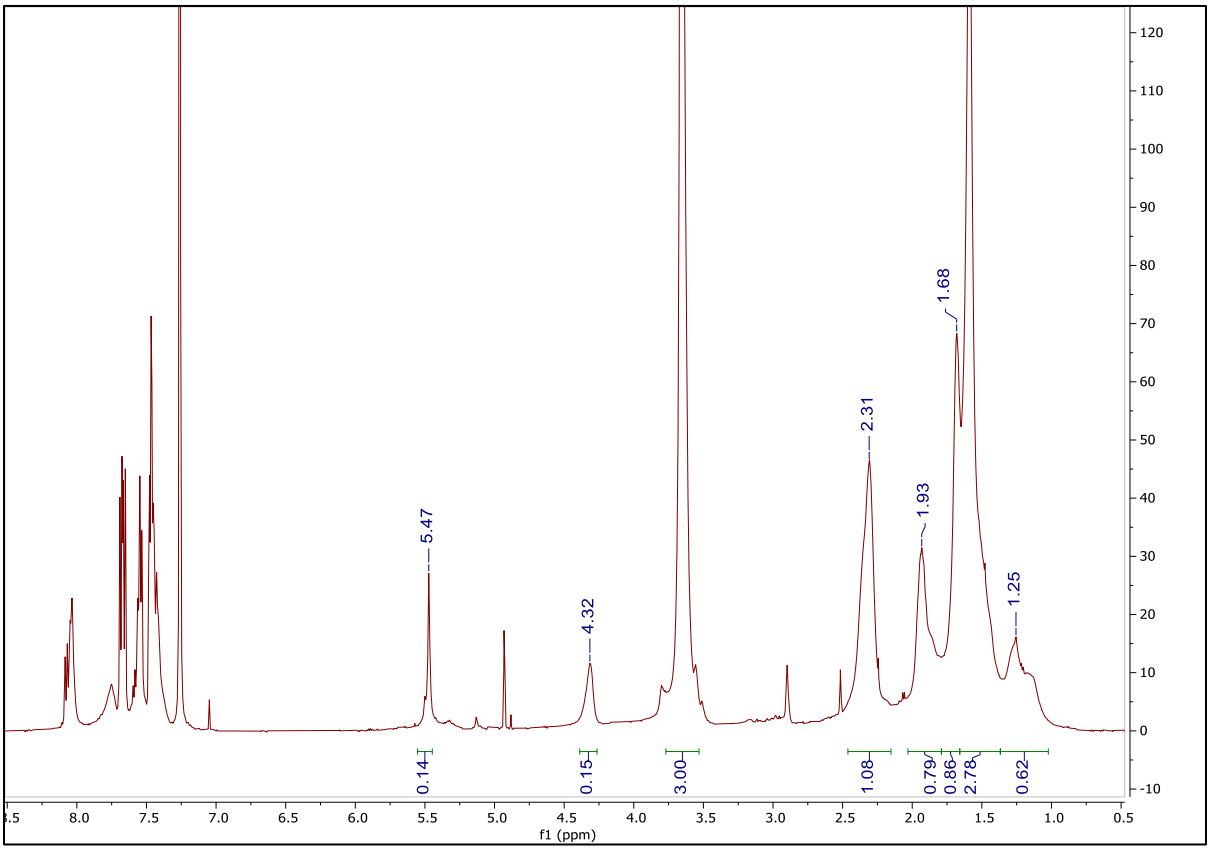

Figure A54: ^{1}H NMR spectrum of 1,4-disubstituted 1,2,3-triazole click product with propargyl benzoate attached (Table 5, Entry 23)

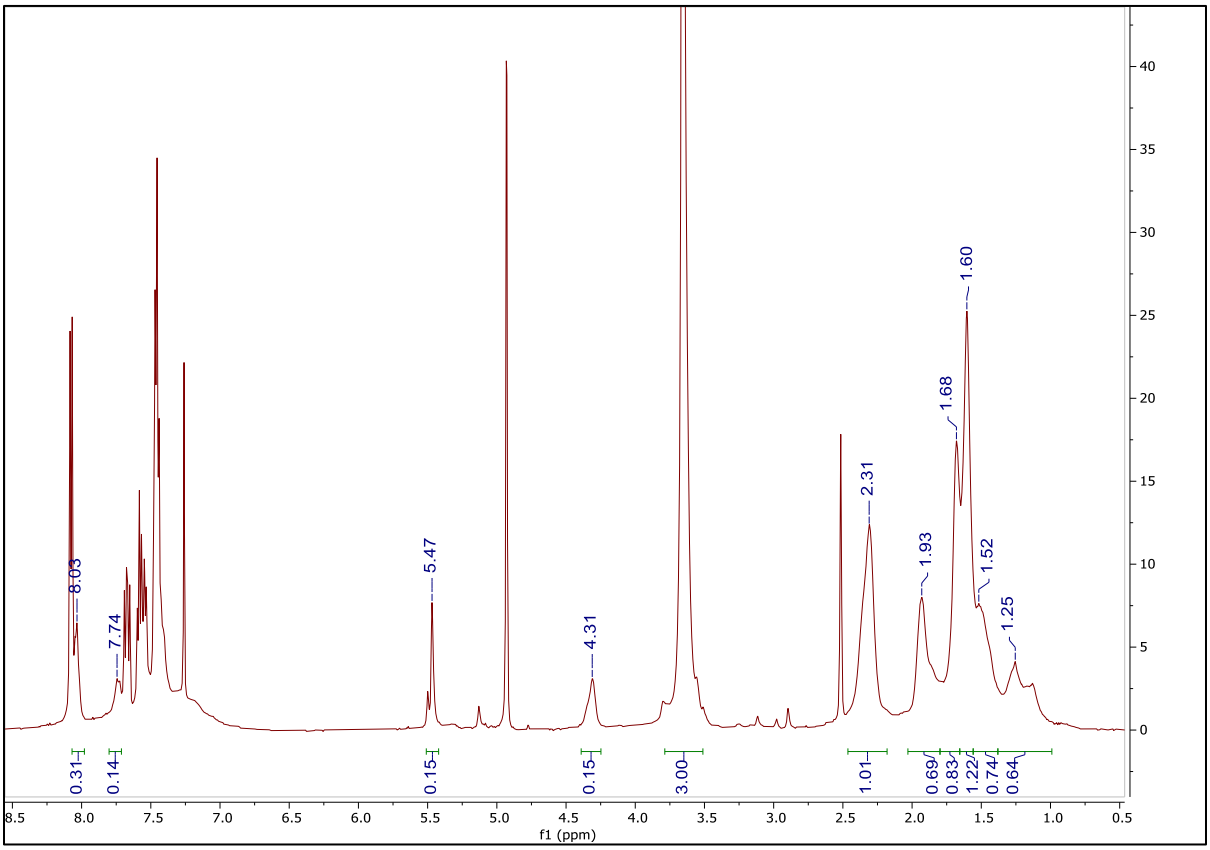

Figure A55: ^{1}H NMR spectrum of 1,4-disubstituted 1,2,3-triazole click product with propargyl benzoate attached (Table 5, Entry 24)

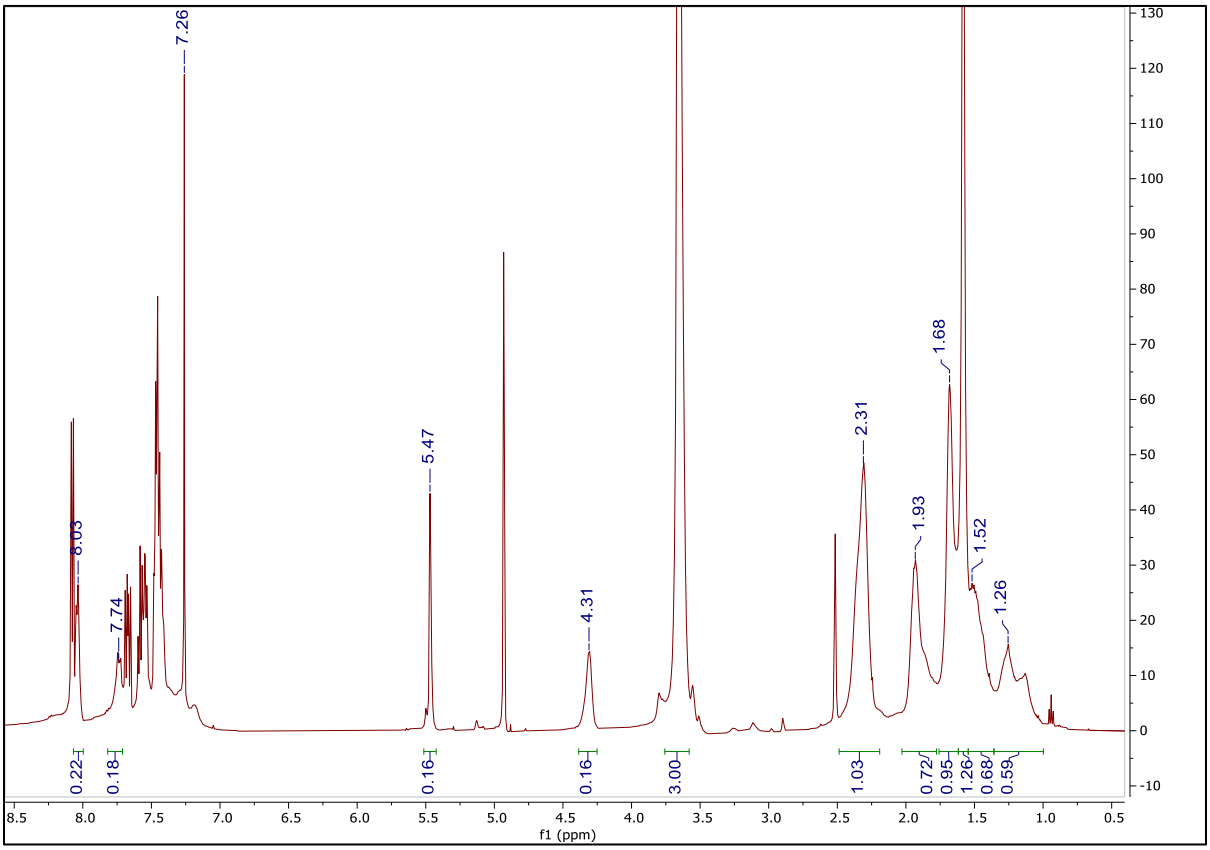

Figure A56: ^{1}H NMR spectrum of 1,4-disubstituted 1,2,3-triazole click product with propargyl benzoate attached (Table 5, Entry 25)

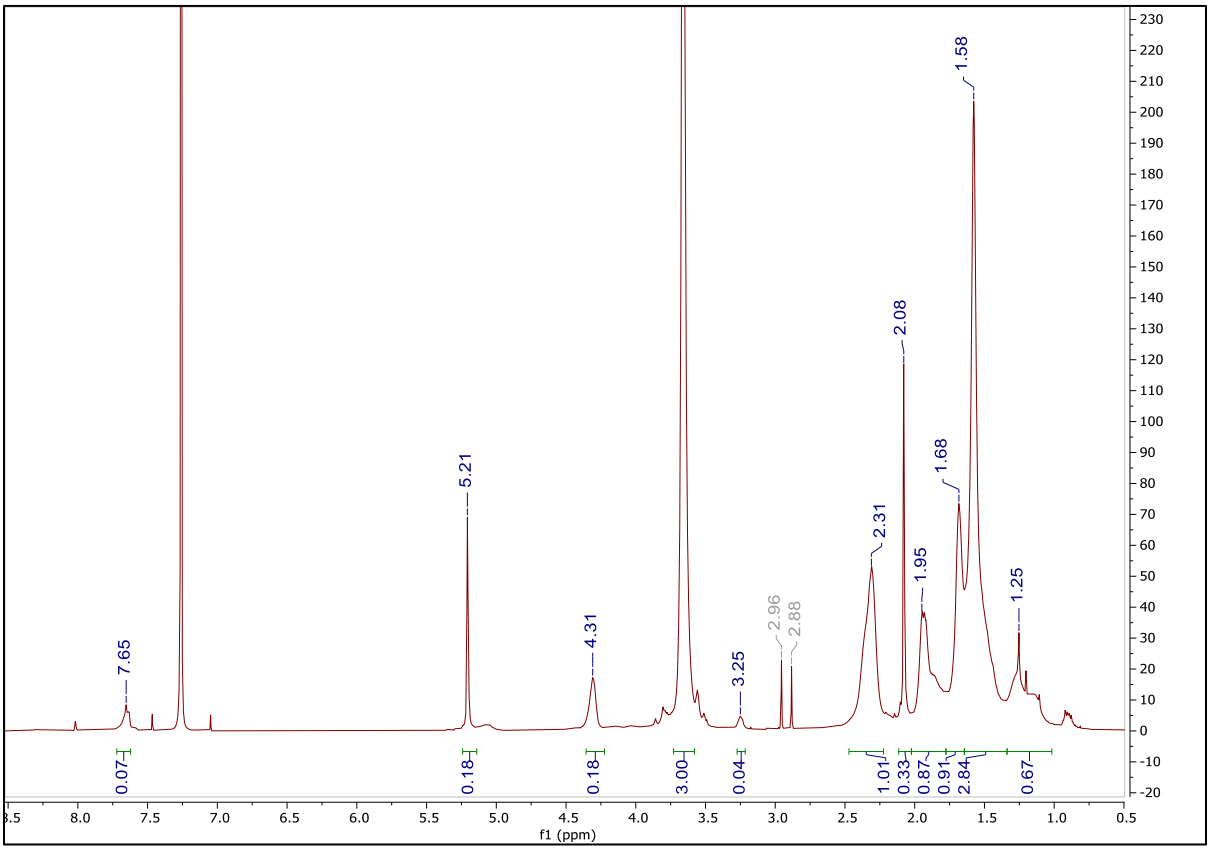

Figure A57: ^{1}H NMR spectrum of 1,4-disubstituted 1,2,3-triazole click product with propargyl acetate attached (Table 5, Entry 29)

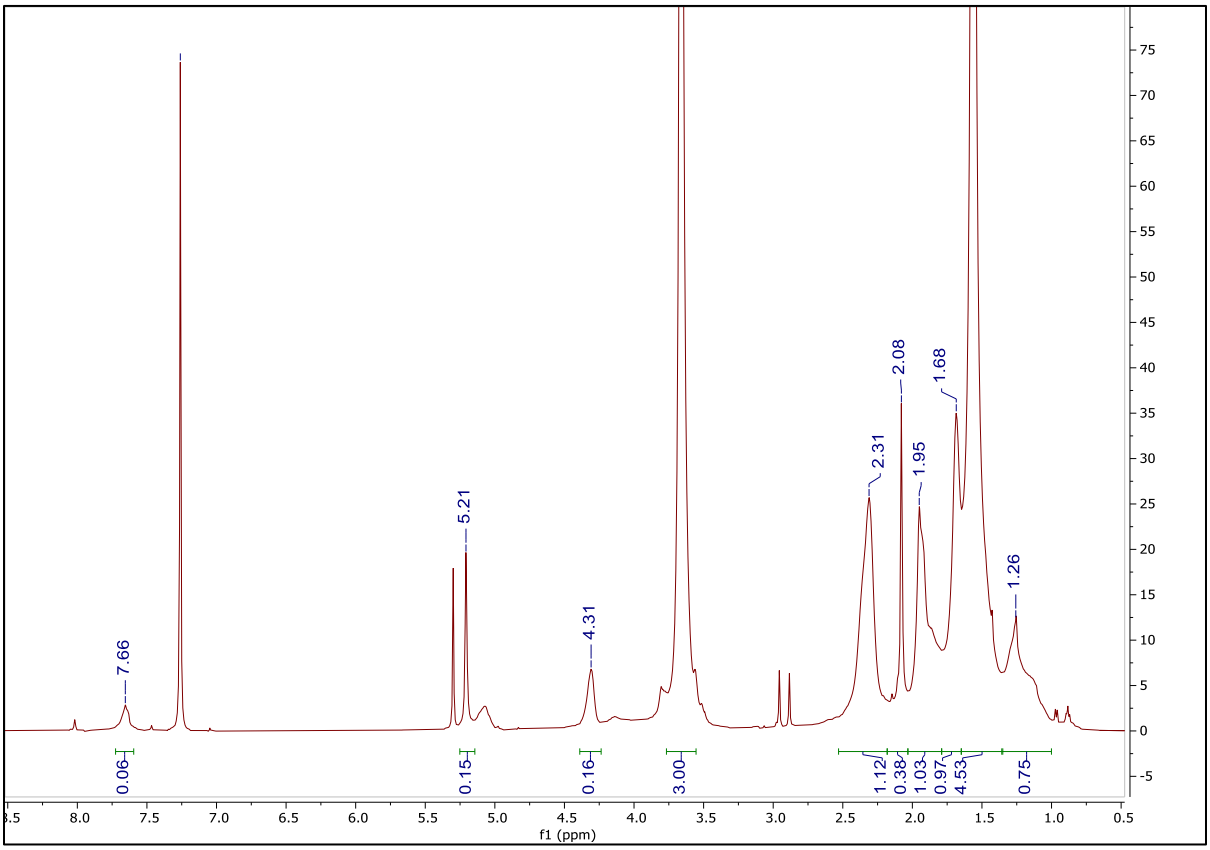

Figure A58: ^{1}H NMR spectrum of 1,4-disubstituted 1,2,3-triazole click product with propargyl acetate attached (Table 5, Entry 30)

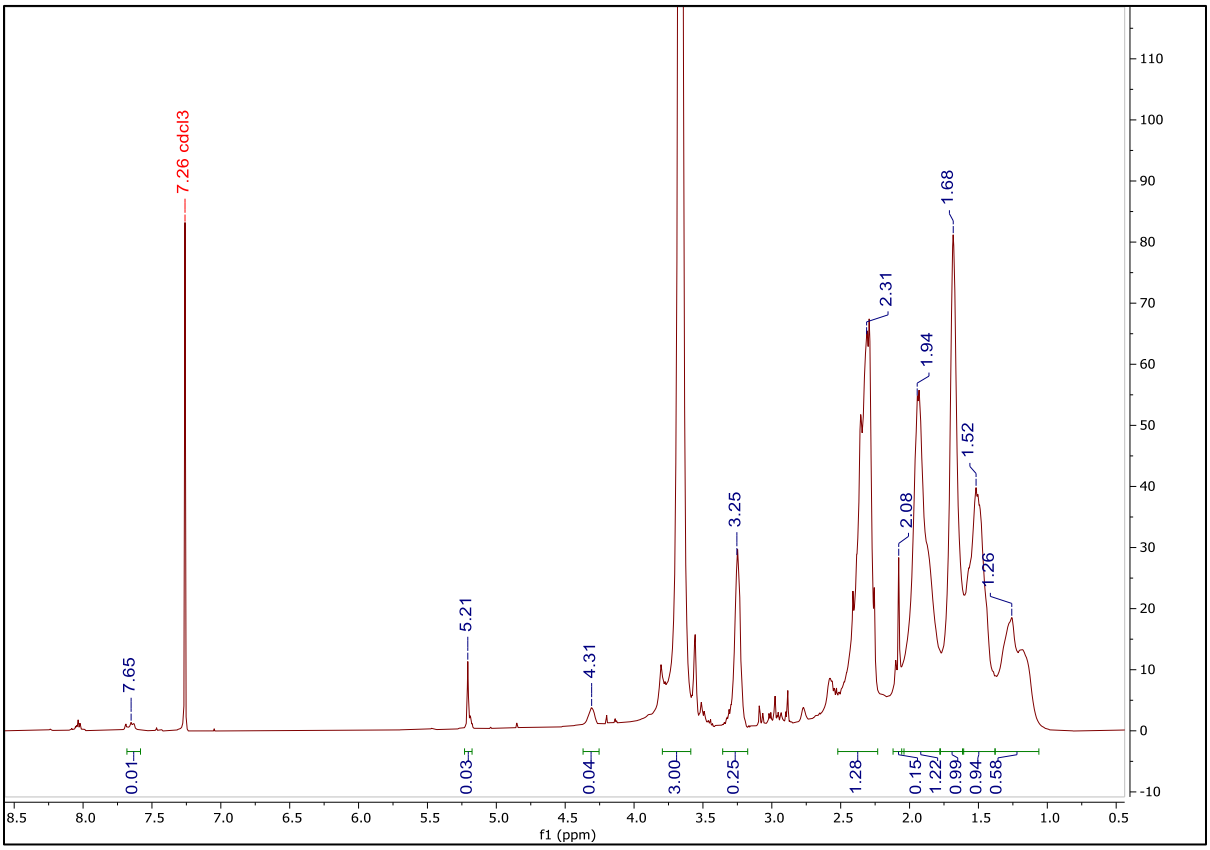

Figure A59: ^{1}H NMR spectrum of 1,4-disubstituted 1,2,3-triazole click product with propargyl acetate attached (Table 5, Entry 31)

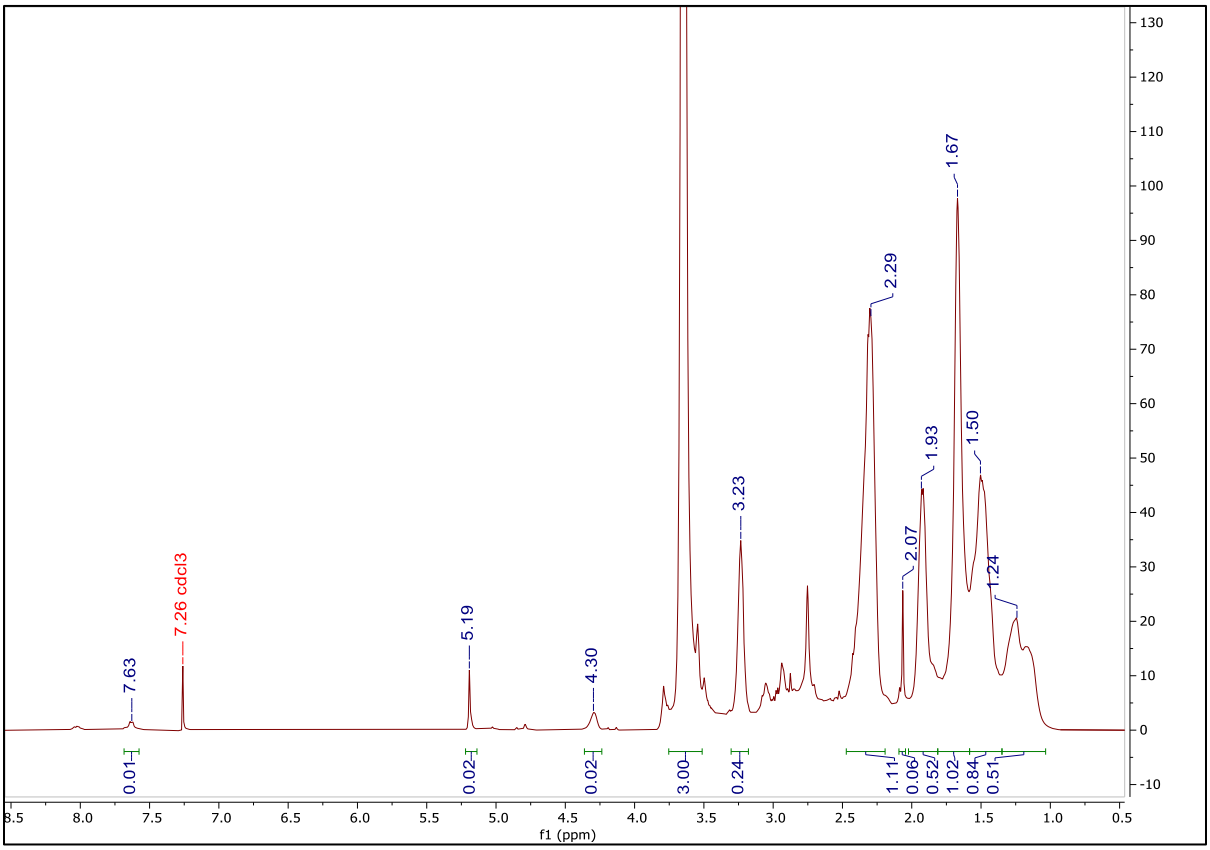

Figure A60: ^{1}H NMR spectrum of 1,4-disubstituted 1,2,3-triazole click product with propargyl acetate attached (Table 5, Entry 32)

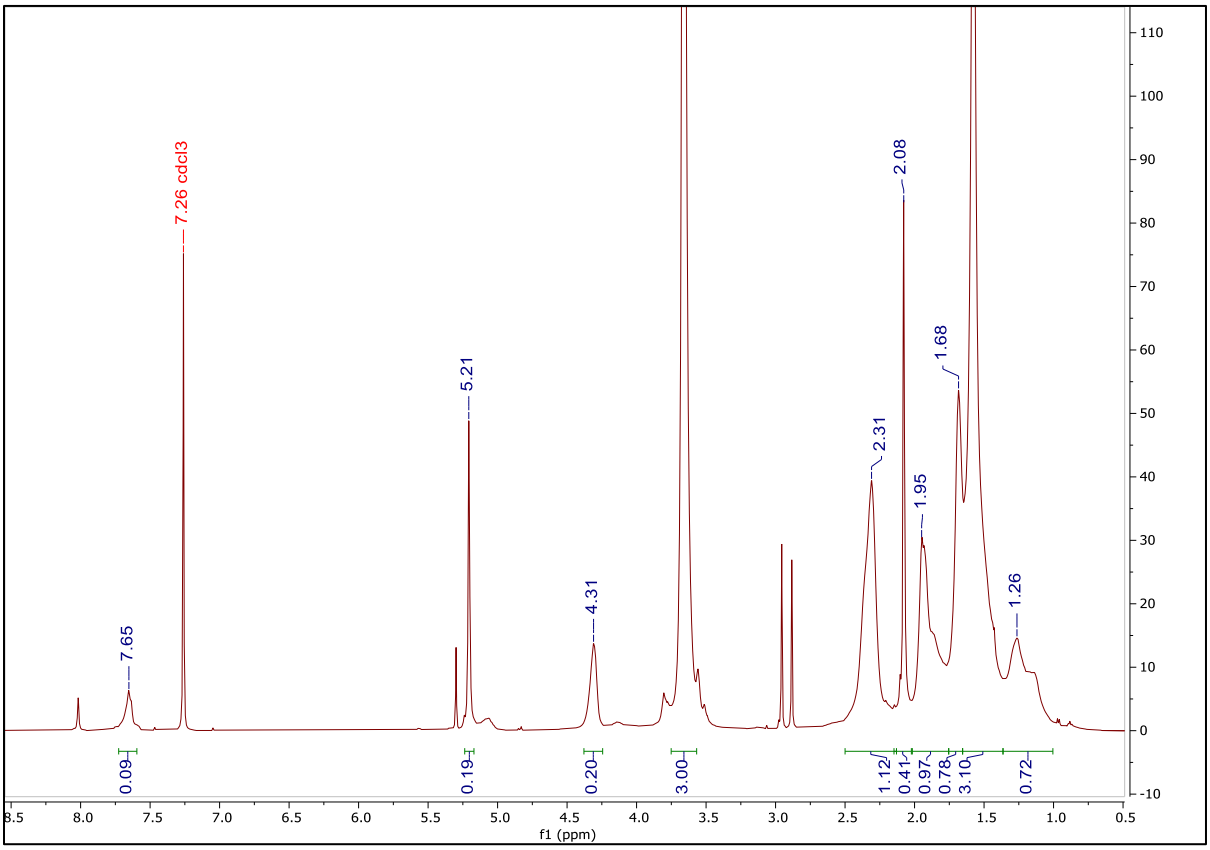

Figure A61: ^{1}H NMR spectrum of 1,4-disubstituted 1,2,3-triazole click product with propargyl acetate attached (Table 5, Entry 33)

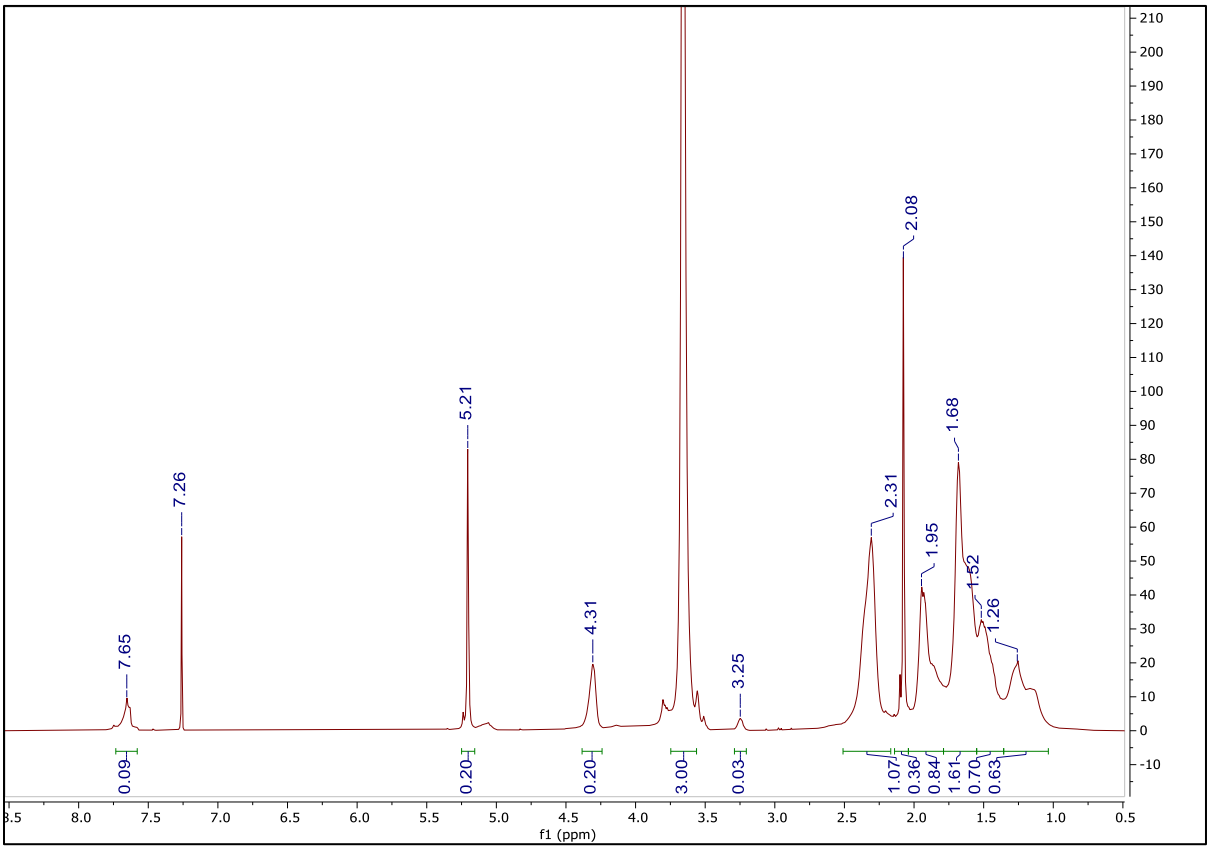

Figure A62: ^{1}H NMR spectrum of 1,4-disubstituted 1,2,3-triazole click product with propargyl acetate attached (Table 5, Entry 34)

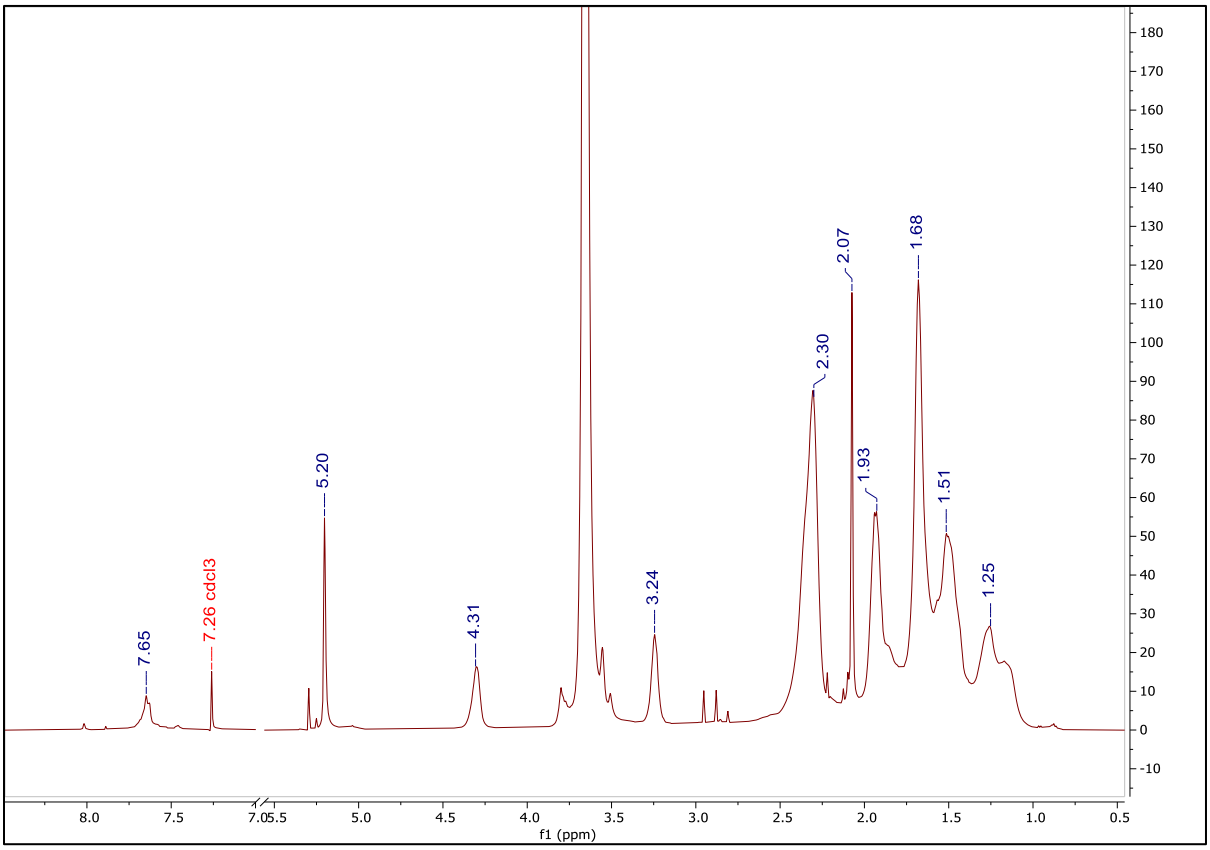

Figure A63: ^{1}H NMR spectrum of 1,4-disubstituted 1,2,3-triazole click product with propargyl acetate attached (Table 5, Entry 37)

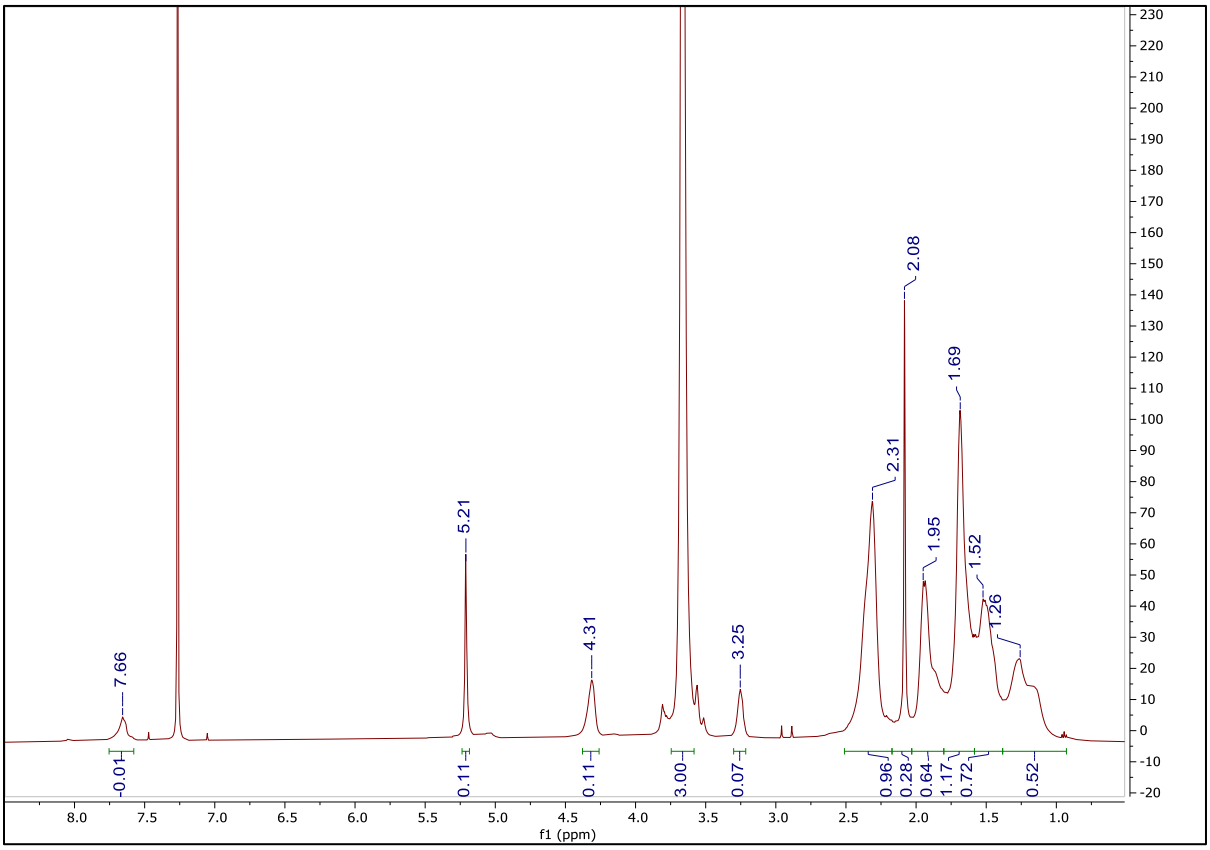

Figure A64: ^{1}H NMR spectrum of 1,4-disubstituted 1,2,3-triazole click product with propargyl acetate attached (Table 5, Entry 38)

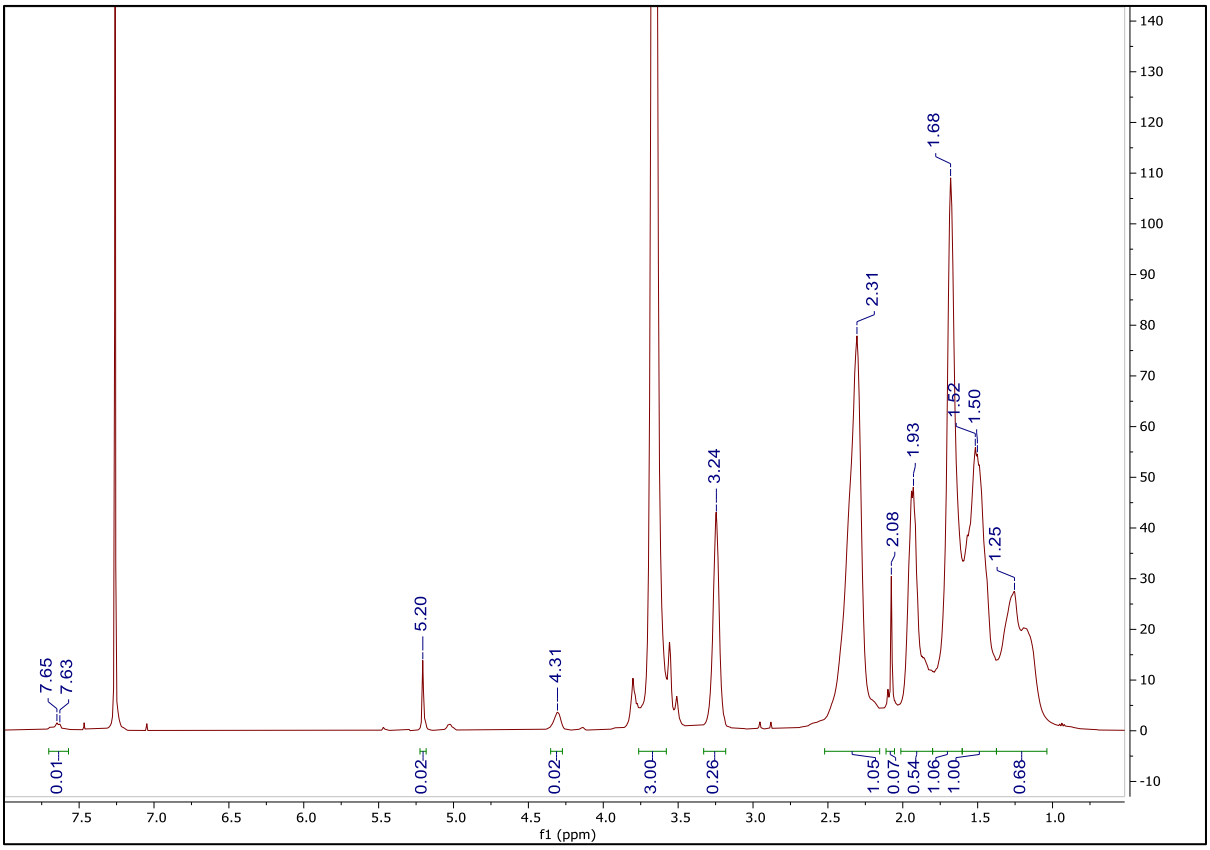

Figure A65: ^{1}H NMR spectrum of 1,4-disubstituted 1,2,3-triazole click product with propargyl acetate attached (Table 5, Entry 39)

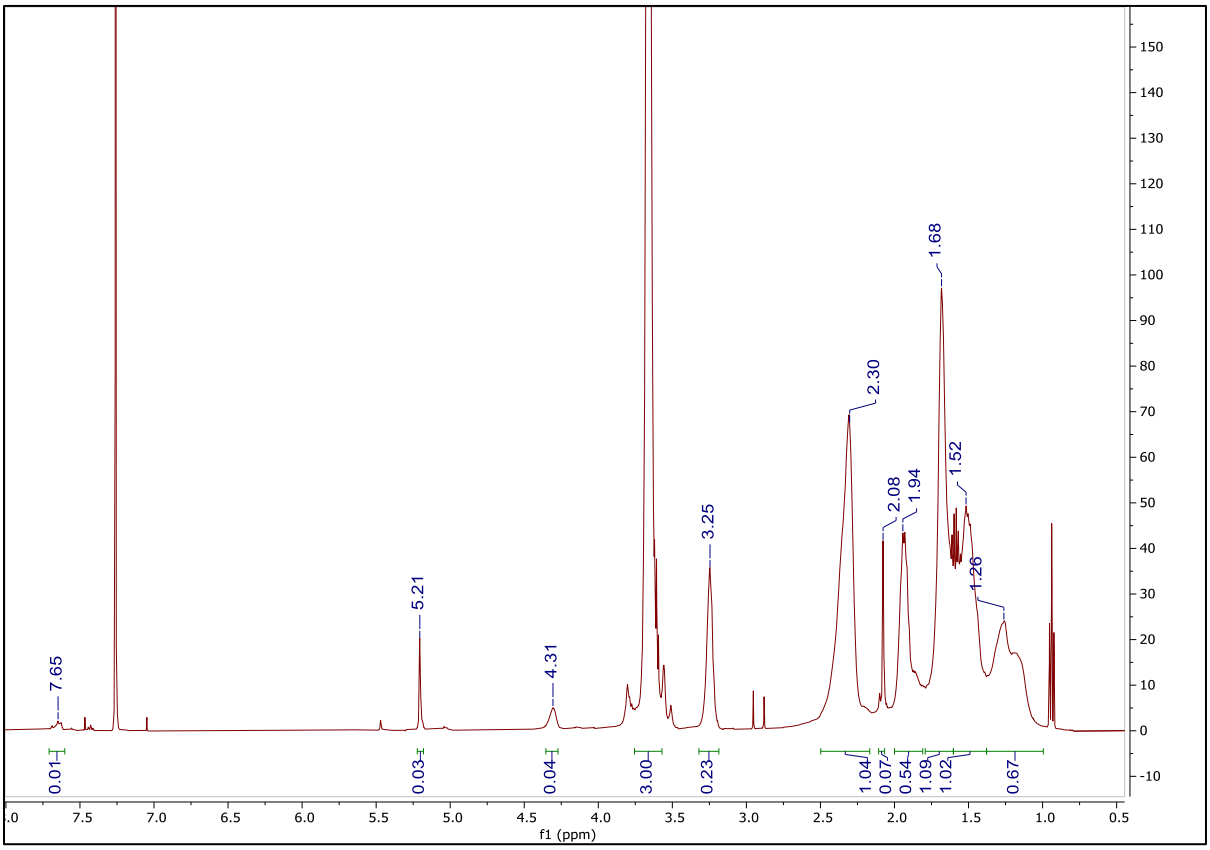

Figure A66: ^{1}H NMR spectrum of 1,4-disubstituted 1,2,3-triazole click product with propargyl acetate attached (Table 5, Entry 40)

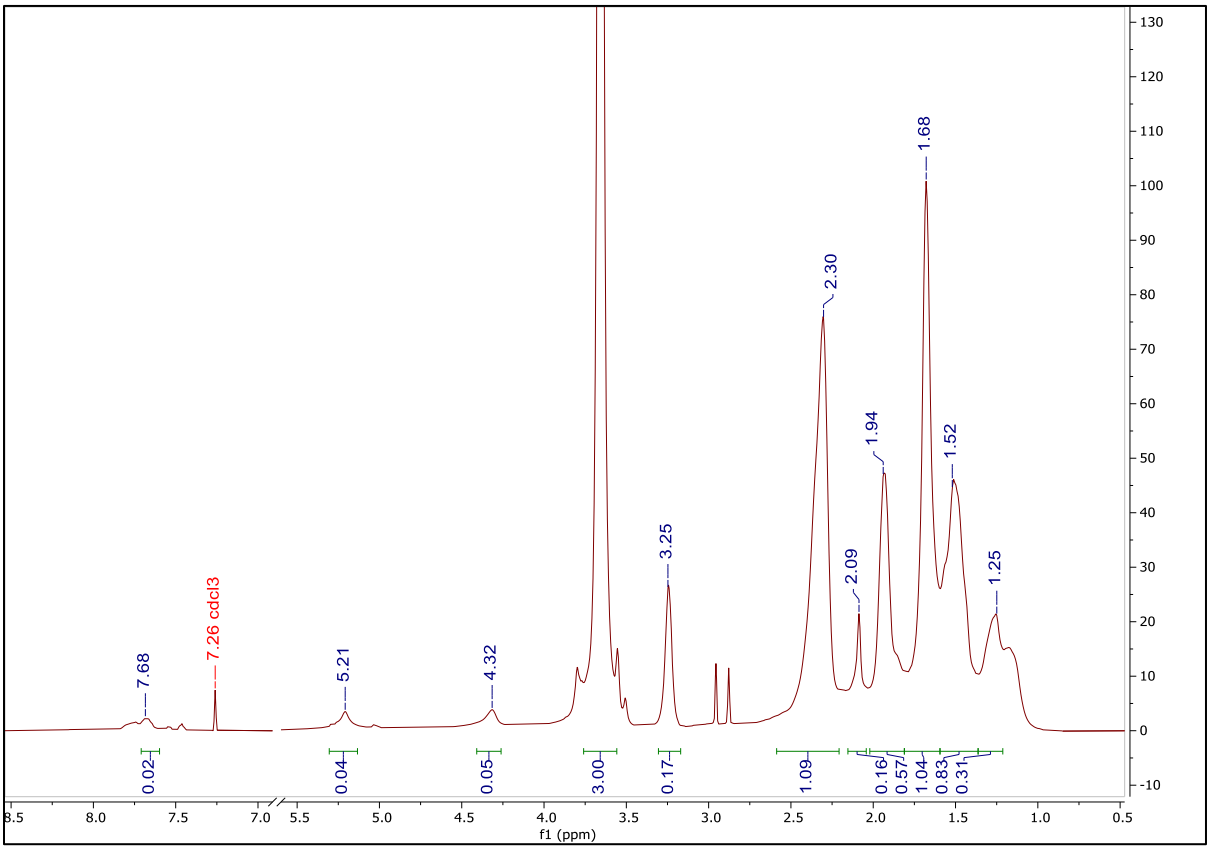

Figure A67: ^{1}H NMR spectrum of 1,4-disubstituted 1,2,3-triazole click product with propargyl acetate attached (Table 5, Entry 41)

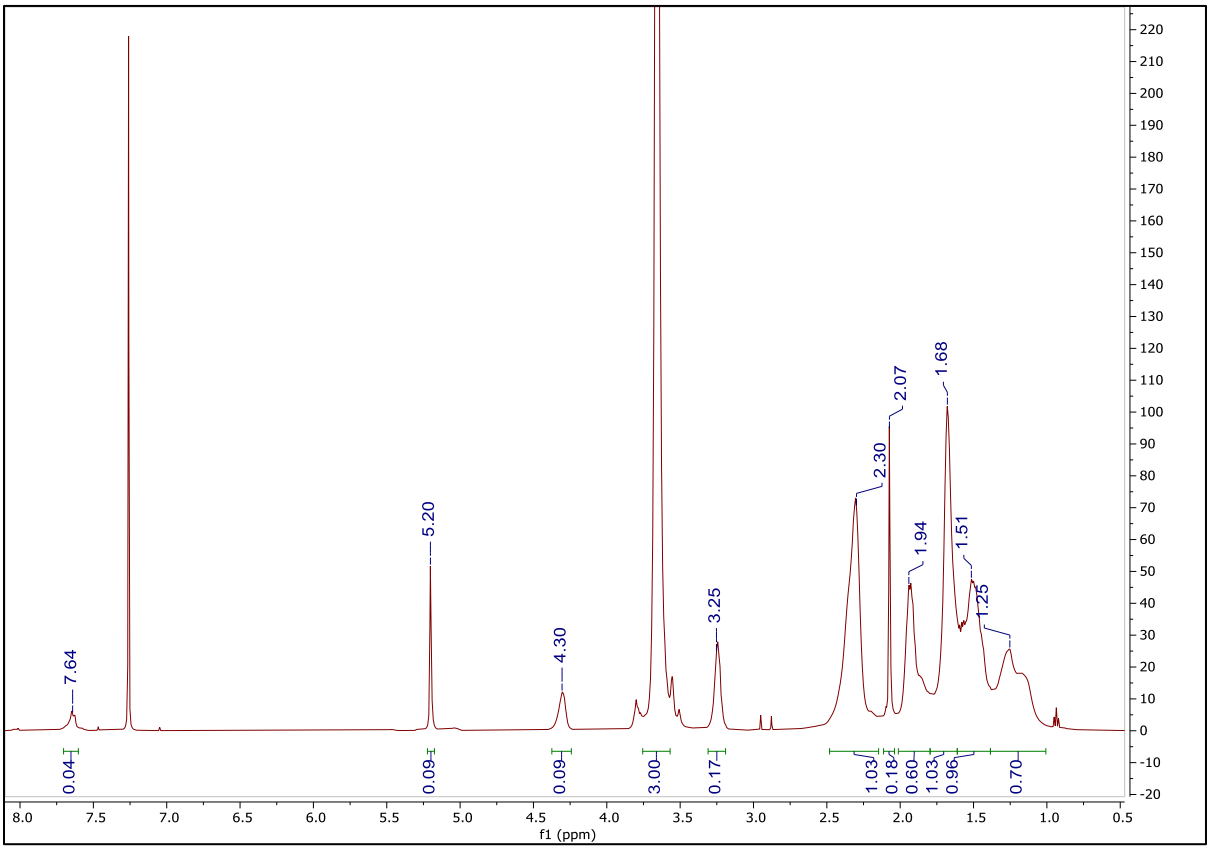

Figure A68: ^{1}H NMR spectrum of 1,4-disubstituted 1,2,3-triazole click product with propargyl acetate attached (Table 5, Entry 42)

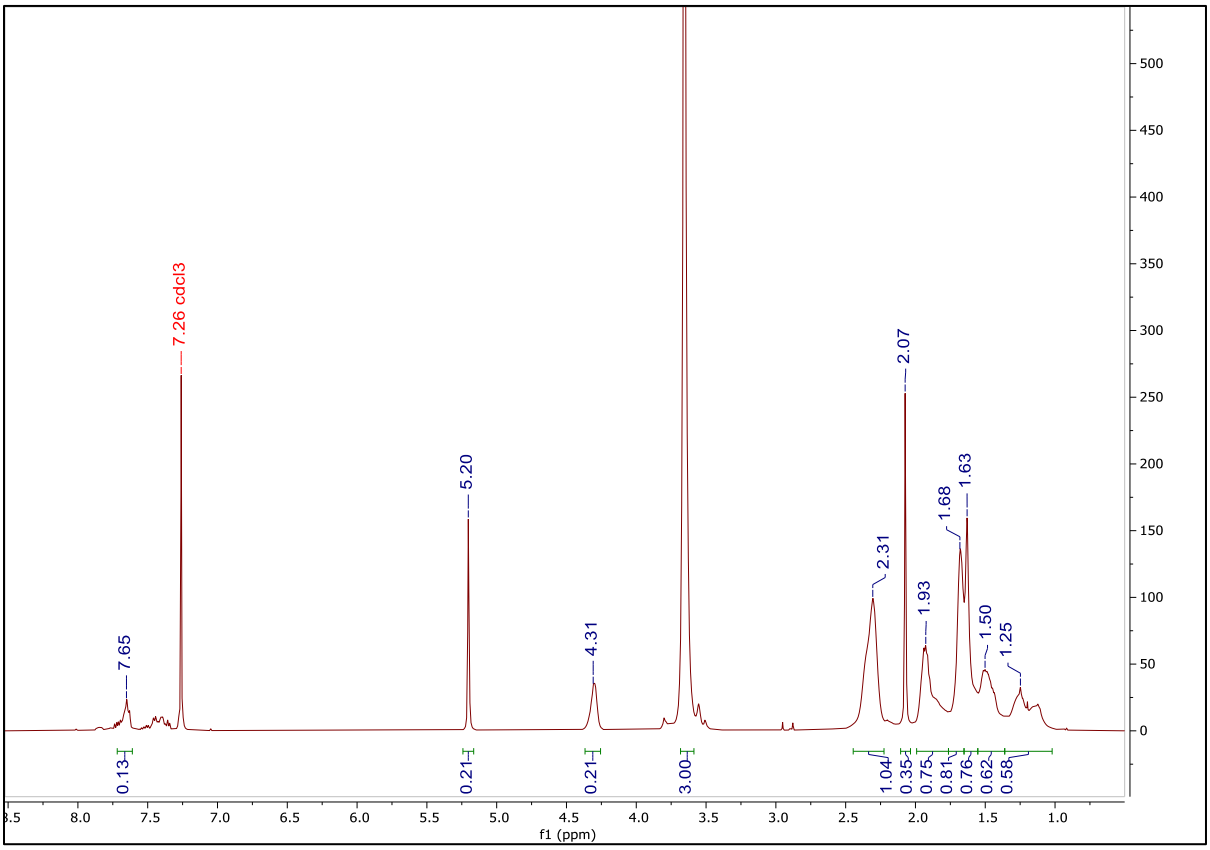

Figure A69: ^{1}H NMR spectrum of 1,4-disubstituted 1,2,3-triazole click product with propargyl acetate attached (Table 5, Entry 45)

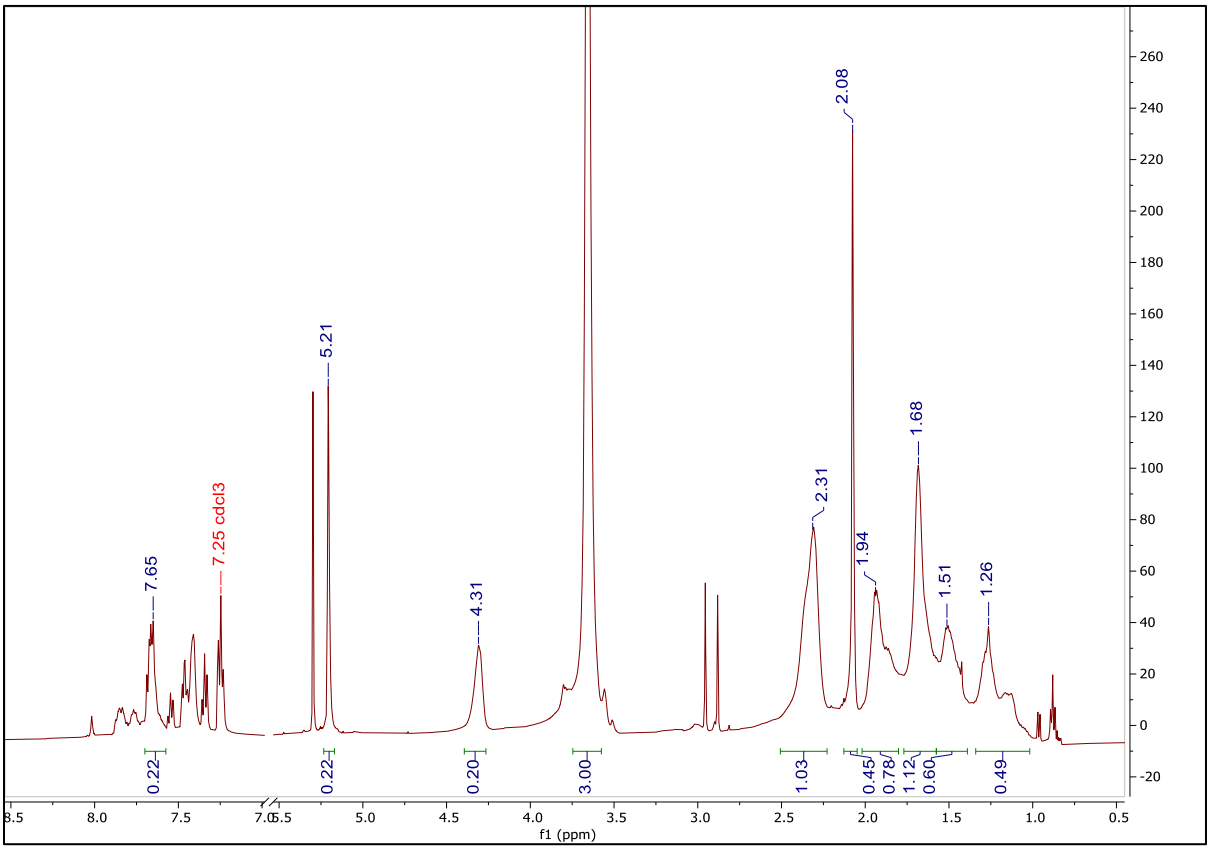

Figure A70: ^{1}H NMR spectrum of 1,4-disubstituted 1,2,3-triazole click product with propargyl acetate attached (Table 5, Entry 46)

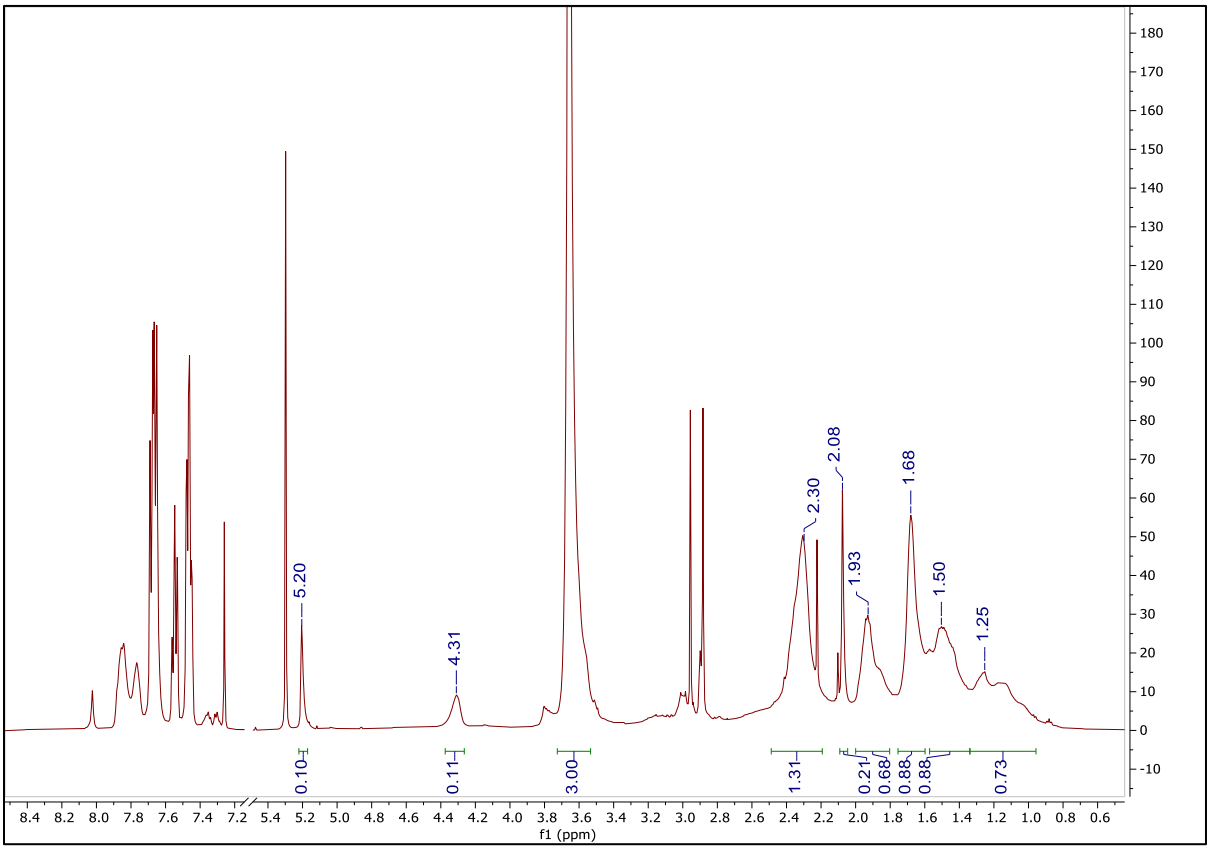

Figure A71: ^{1}H NMR spectrum of 1,4-disubstituted 1,2,3-triazole click product with propargyl acetate attached (Table 5, Entry 47)

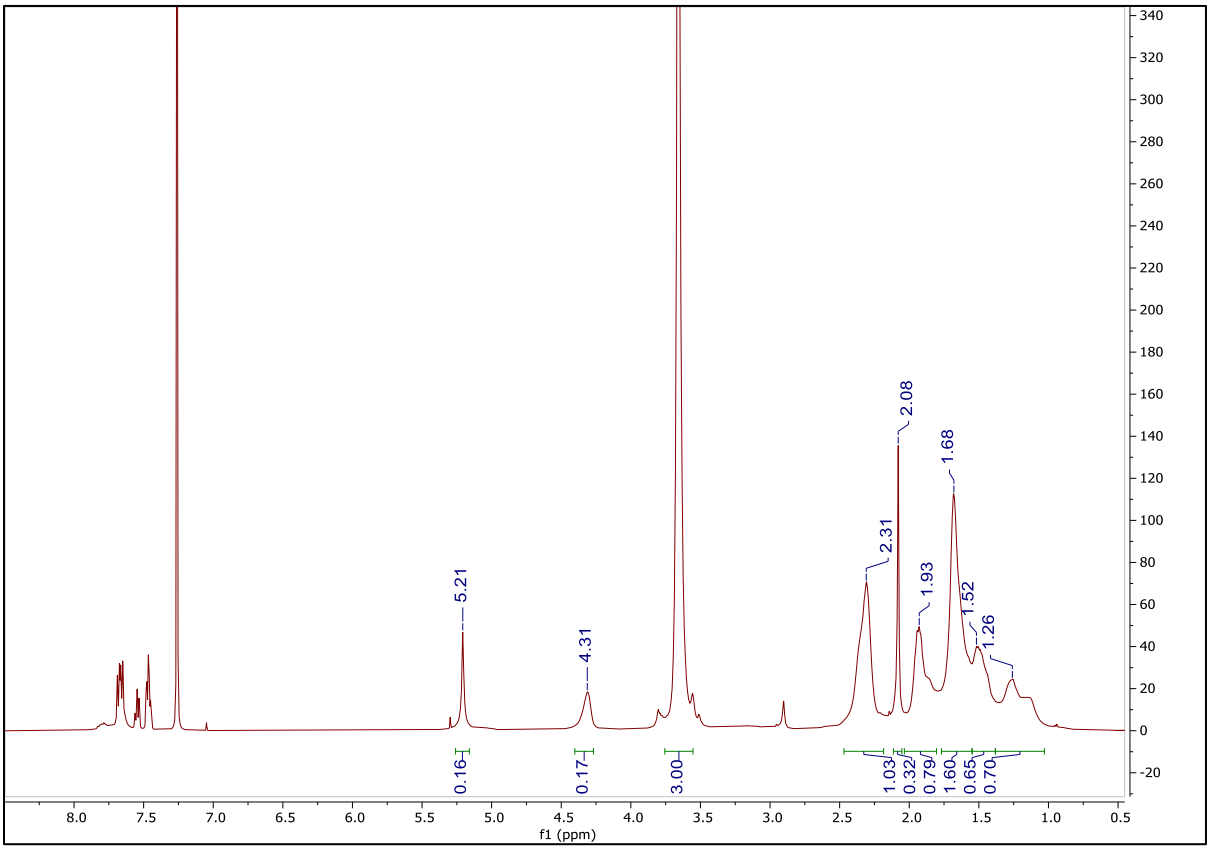

Figure A72: ^{1}H NMR spectrum of 1,4-disubstituted 1,2,3-triazole click product with propargyl acetate attached (Table 5, Entry 48)

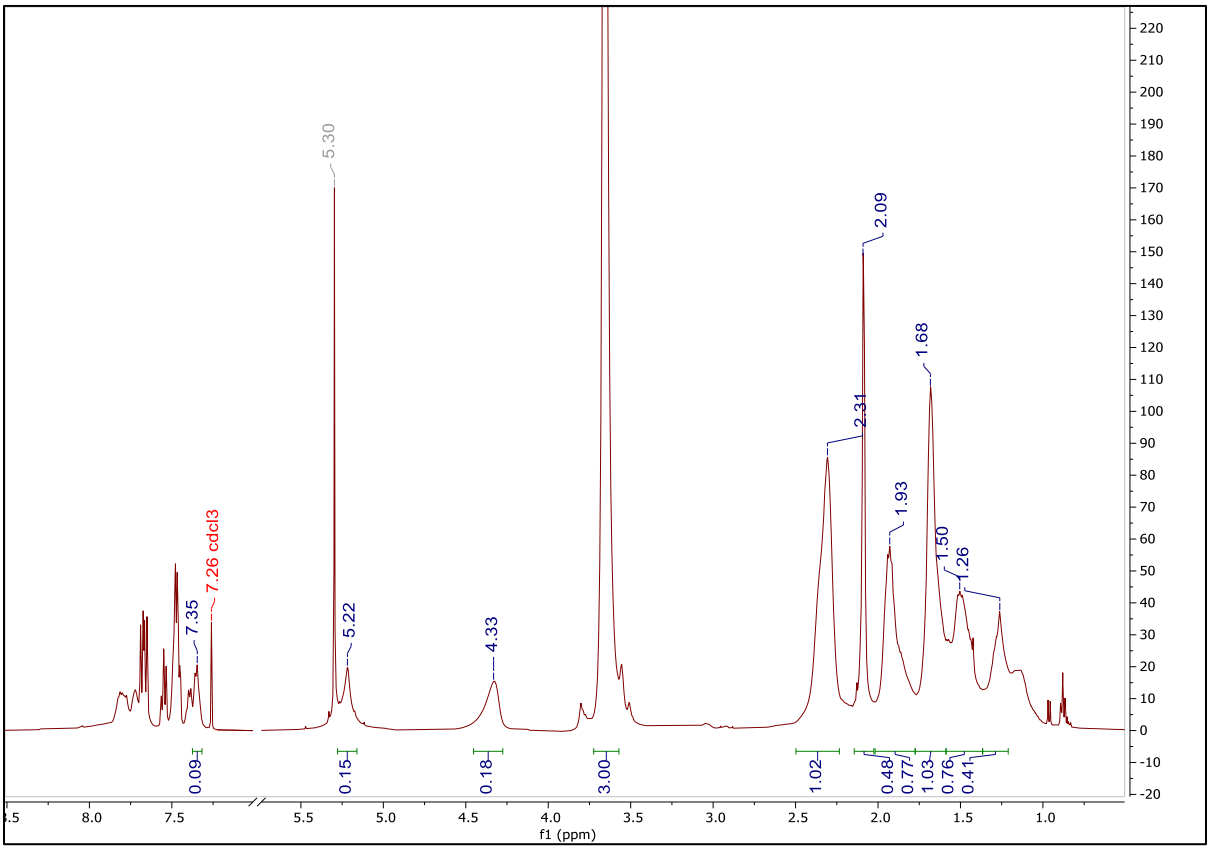

Figure A73: ^{1}H NMR spectrum of 1,4-disubstituted 1,2,3-triazole click product with propargyl acetate attached (Table 5, Entry 49)

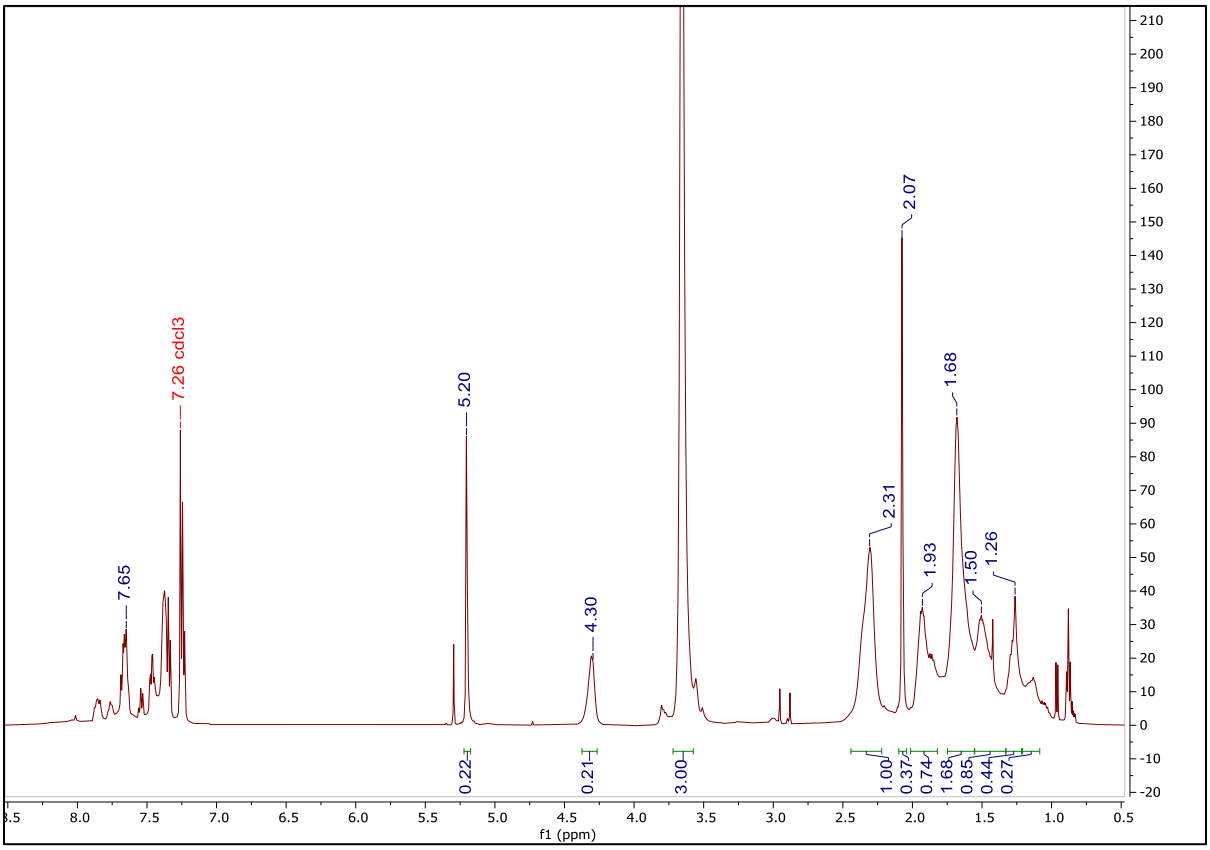

Figure A74: ^{1}H NMR spectrum of 1,4-disubstituted 1,2,3-triazole click product with propargyl acetate attached (Table 5, Entry 50)

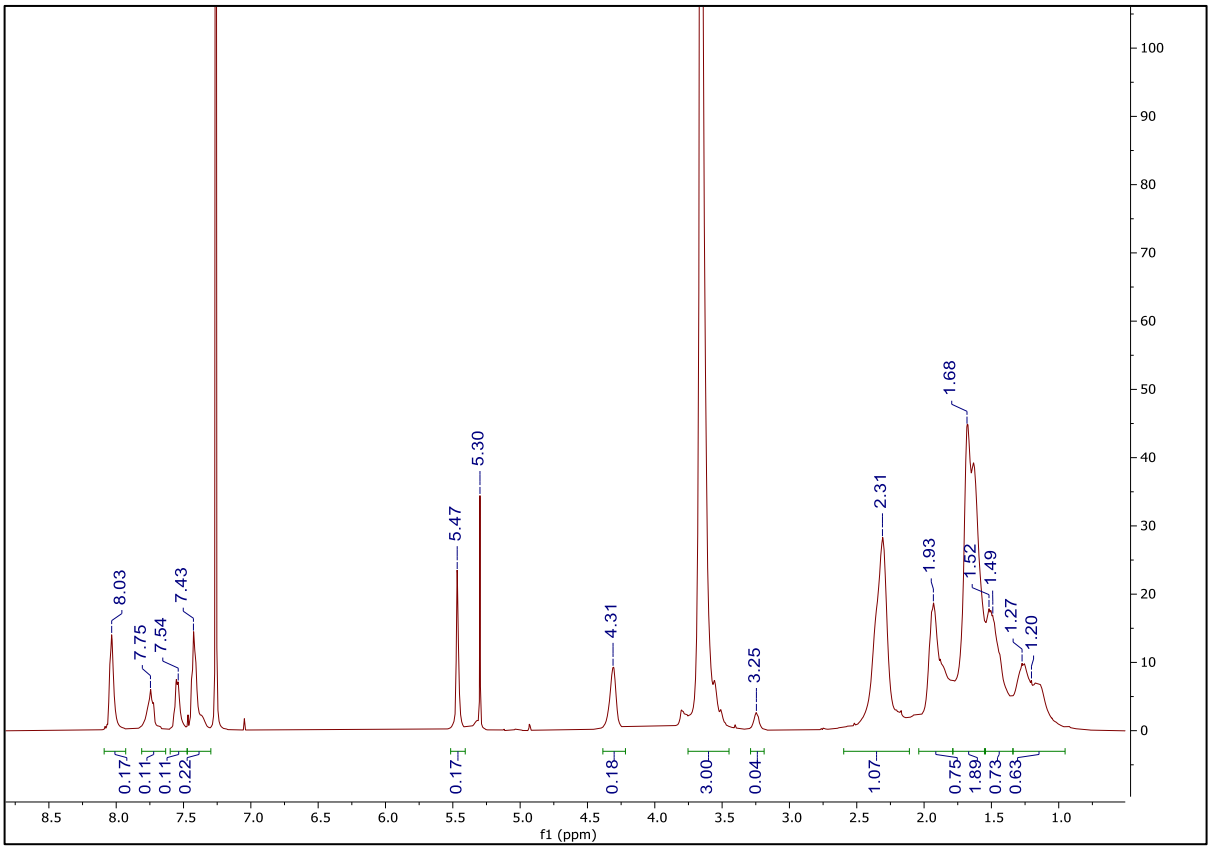

Figure A75: ^{1}H NMR spectrum of 1,4-disubstituted 1,2,3-triazole click product with propargyl acetate attached (Table 6, Entry 1)

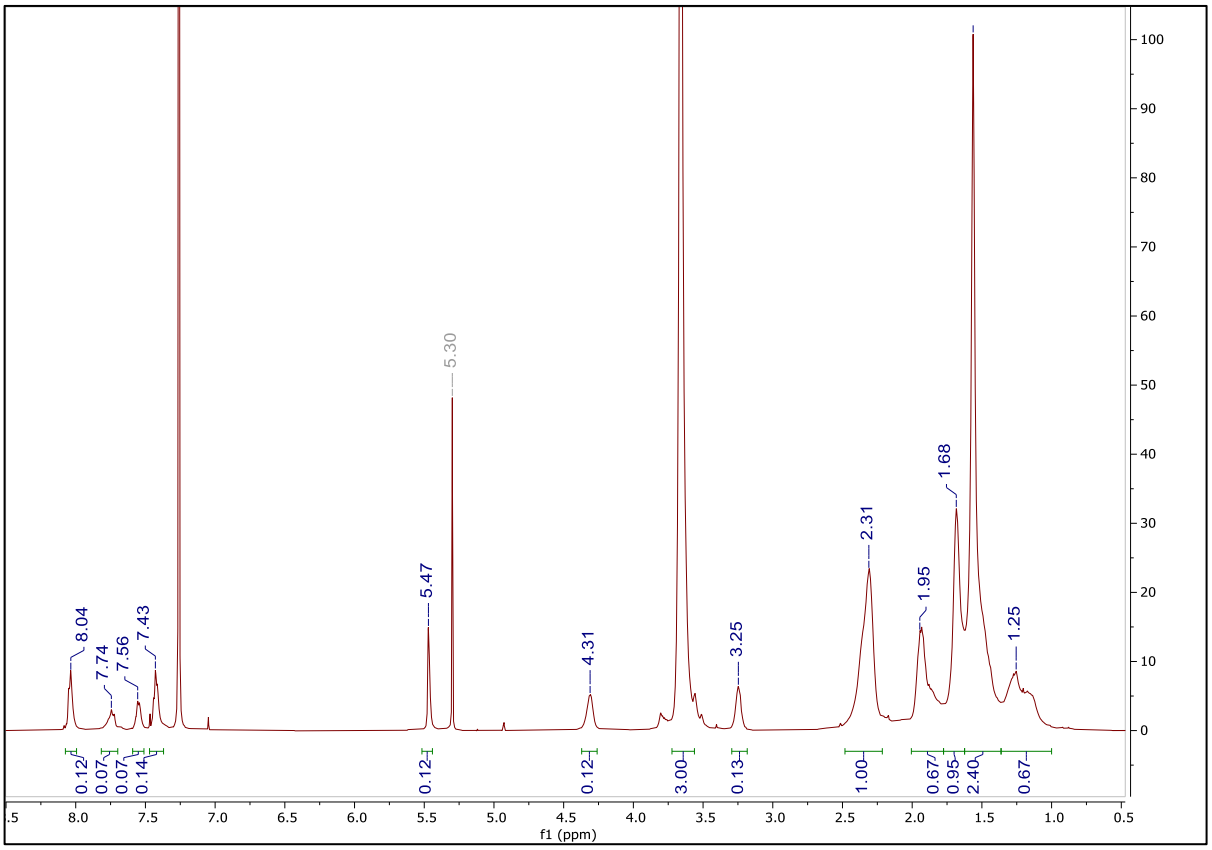

Figure A76: ^{1}H NMR spectrum of 1,4-disubstituted 1,2,3-triazole click product with propargyl acetate attached (Table 6, Entry 2)

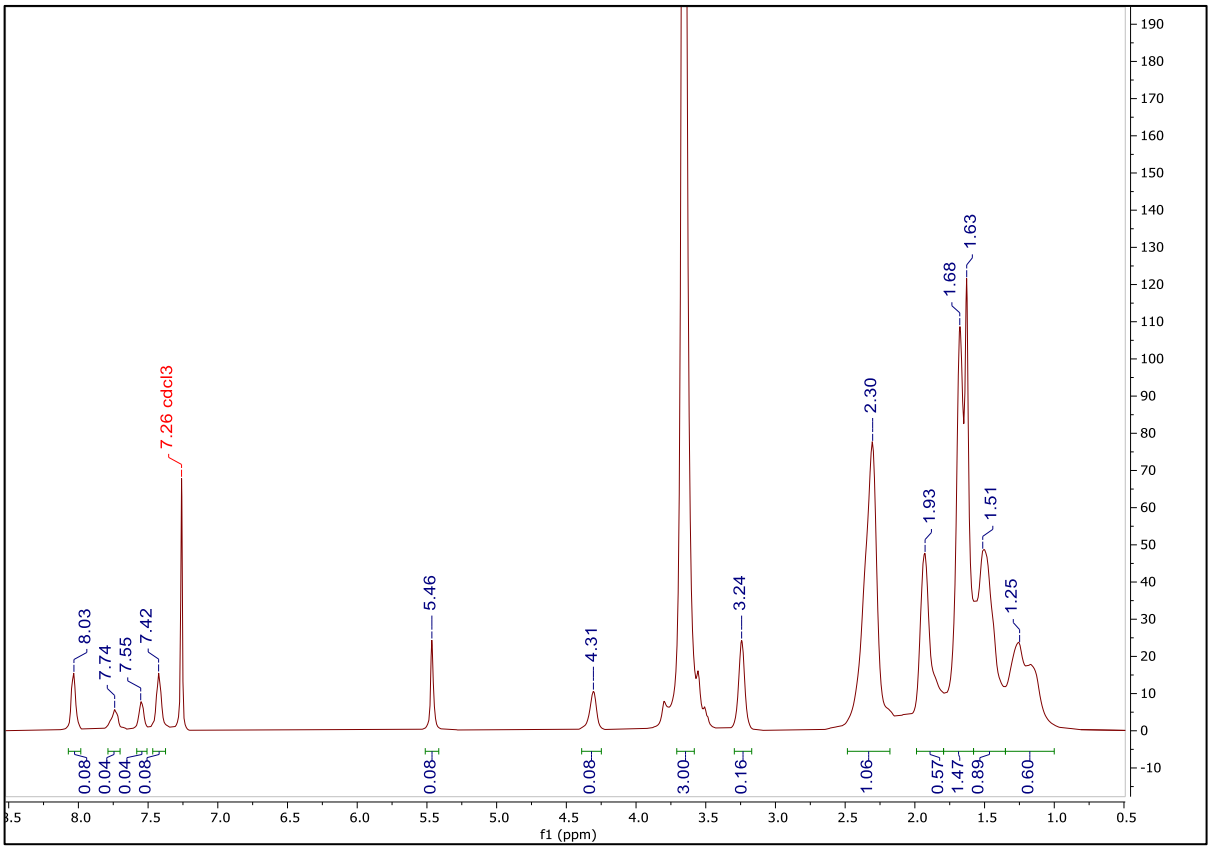

Figure A77: ^{1}H NMR spectrum of 1,4-disubstituted 1,2,3-triazole click product with propargyl acetate attached (Table 6, Entry 3)

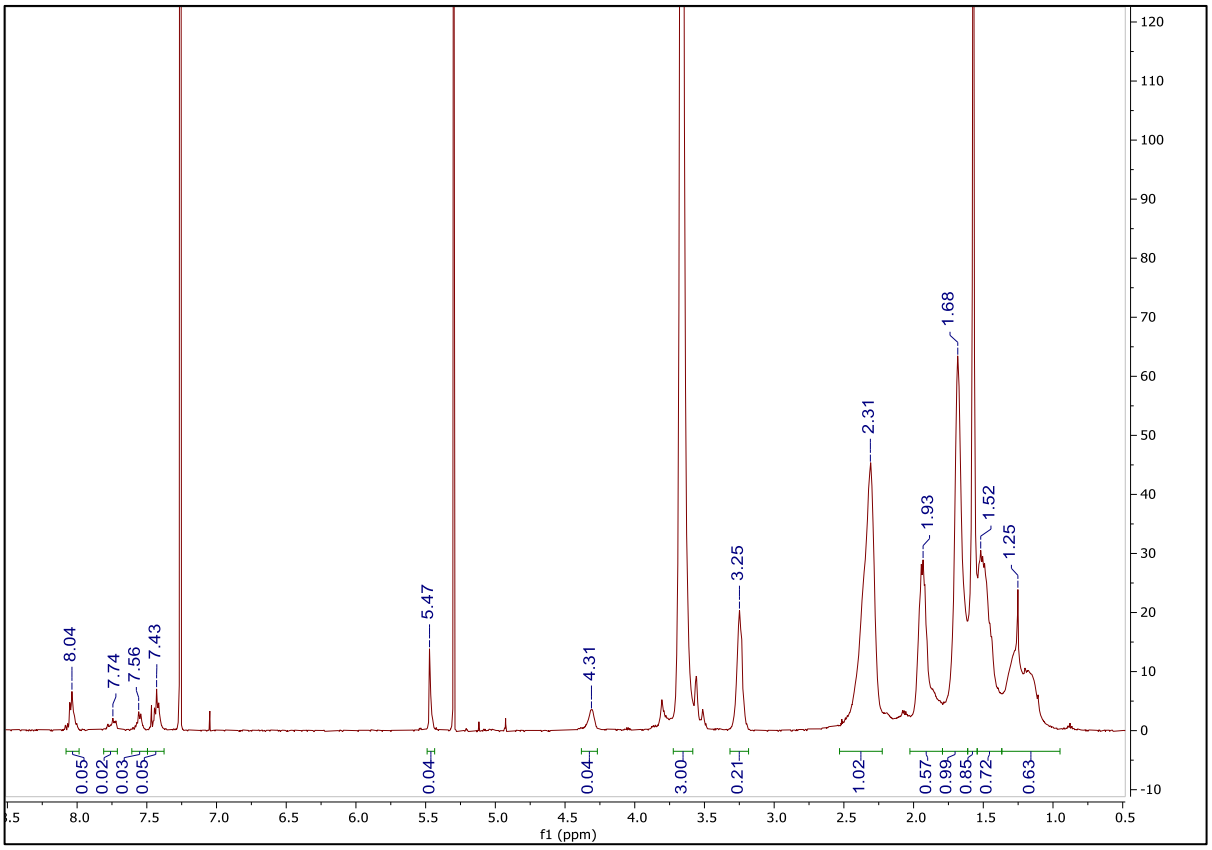

Figure A78: ^{1}H NMR spectrum of 1,4-disubstituted 1,2,3-triazole click product with propargyl acetate attached (Table 6, Entry 4)

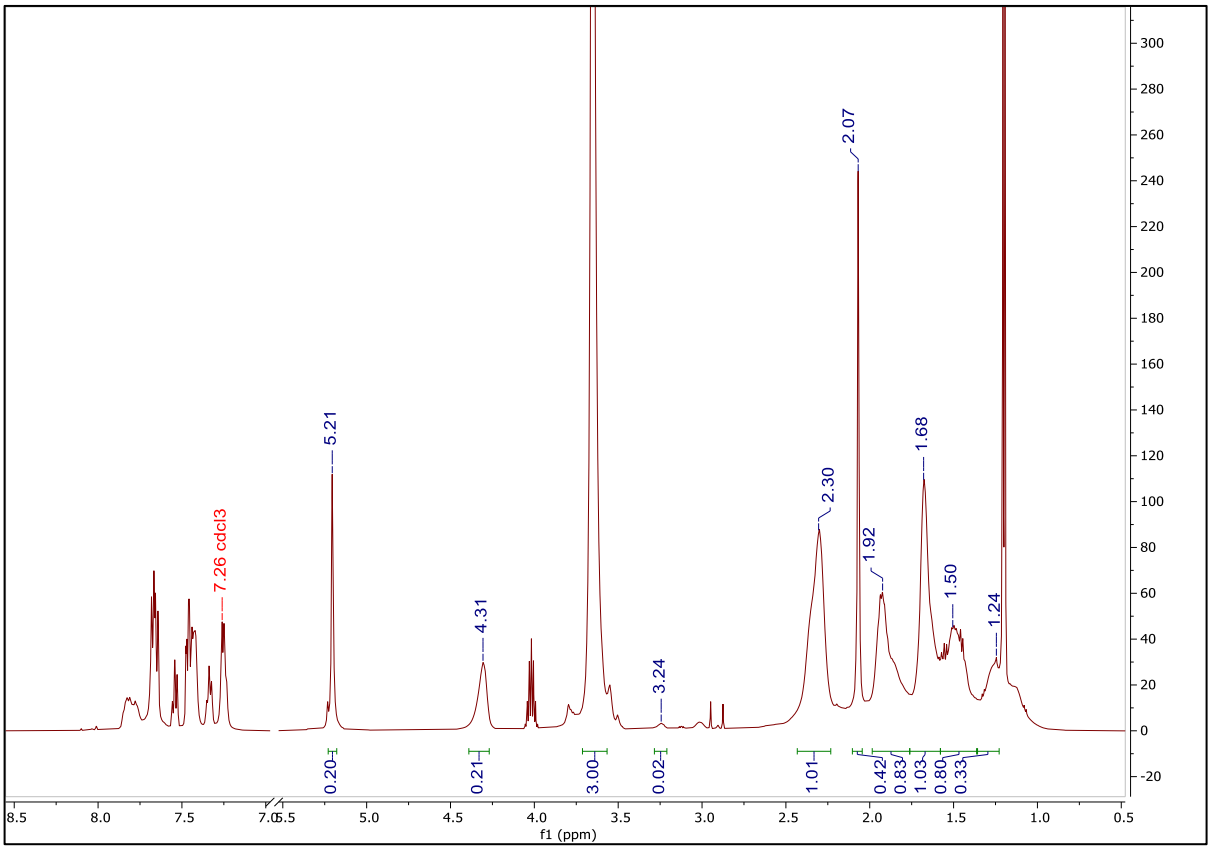

Figure A79: ^{1}H NMR spectrum of 1,4-disubstituted 1,2,3-triazole click product with propargyl acetate attached (Table 6, Entry 5)

References

1. Lenz, R.W., Marchessault, R.H. Bacterial Polyesters: Biosynthesis, Biodegradable Plastics and Biotechnology. *Biomacromol*. **2005**. 6 (1).
2. Keshavarz T., Roy, I. Polyhydroxyalkanoates: bioplastics with a green agenda. *Curr Opin Microbiol.* **2010**. 13. 321-326
3. Urtuvia V., Villegas P. Gonzalez M., Seeger M. Bacterial production of the biodegradable plastics Polyhydroxyalkanoates. *Intern J Biol Macromol.* **2014**. 70. 208-213
4. Obruca S., Marova I., Stankova M., Mravcova L., Svoboda Z. Effect of ethanol and hydrogen peroxideon poly(3-hydroxybutyrate) biosynthetic pathway in Cupriavidus necator H16. *World J Microbiol Biotechnol.* **2010**. 26. 1261-1267
5. Lakshman K., Shamala T.R. Enhanced biosynthesis of polyhydroxyalkanoates in a mutant strain of Rhizobium meliloti. *Biotechnol Letters*. **2003**. 25, 115
6. Raza Z.A., Abid S., Banat I.M., Polyhydroxyalkanoates: Characteristics, production, recent developments and applications. *Inter Biodeter Biodeg.* **2018**. 126.45-56
7. Ali I., Jamil N. Polyhydroxyalkanoates: Current applications in the medical field. *Front. Biol.* **2016**. 11. 19-27
8. Lutz, F. Zarafshani, Z. Efficient construction of therapeutics, bioconjugates, biomaterials and bioactive surfaces using azide–alkyne “click” chemistry, *Adv. Drug Deliv. Rev*. **2008**. 60. 958–970
9. Kolb, H.C. Sharpless, K.B. The growing impact of click chemistry on drug discovery, Drug Discovery Today. **2003**. 8 (24). 1128 – 1137

10. Nkrumah-Agyeefi, S. Chemical Modification of Poly(hydroxyalkanoate)s (PHA)s via "Click" Chemistry. PhD Dissertation. University of Alabama in Huntsville. Huntsville, Alabama. **2018**.

11. Lee S.Y., Choi J-I., Wong H.H. Recent advances in polyhydroxyalkanoate production by bacterial fermentation: mini-review. *Intern J Biol Macromol.* **1999**. 25. 31-36

12. Verlinden R.A.J., Hill D.J., Kenward M.A., Williams C.D., Radecka I. Bacterial synthesis of biodegradable Polyhydroxyalkanoates. *J Appl Microbiol.* **2007**. 102. 1437-1449

13. Lemoigne M. Products of dehydration and of polymerization of beta-hydroxybutyric acid. *Bull Soc Chim Biol*. **1926**. 8. 770-782

14. Tsuge T. Metabolic Improvements and Use of Inexpensive Carbon Sources in Microbial Production of Polyhydroxyalkanoates. *J Biosci Bioeng.* **2002**. 94. 579-584

15. Chaudhry W.N., Jamil N., Ali I., Ayaz M.H., Hasnain S. Screening for polyhydroxyalkanoate (PHA)-producing bacterial strains and comparison of PHA production from various inexpensive carbon sources. *Ann Microbiol.* **2011**. 61. 623-629

16. Rehm B.H.A., Steinbüchel A., Biochemical and genetic analysis of PHA synthases and other proteins required for PHA synthesis. *Intern J Biol Macromol.* **1999**. 25. 3-19

17. Zou, H., Shi M., Zhang T., Li Le., Li, L., Xian M., Natural and engineered polyhydroxyalkanoate (PHA) synthase: key enzyme in biopolyester production. *Appl Microbiol Biotechnol*. **2017**. 101. 7417-7426

18. Tsuge, T., Hyakutake, M., Mizuno, K. Class IV polyhydroxyalkanoate (PHA) synthases and PHA-producing Bacillus. *Appl. Microbiol. Biotechnol.* **2015**. 99. 6231-6240

19. Tsuge, T. Fundamental factors determining the molecular weight of polyhydroxyalkanoate during biosynthesis. *Polym J.* **2016**. 48. 1051-1057

20. Ikada, Y., Tsuji, H. Biodegradable polyesters for medical and ecological applications. *Macromol. Rapid Commun.* **2000**. 21. 117-132

21. Kobayashi, T., Uchino, K., Abe, T., Yamazaki, Y., Saito, T. Novel Intracellular 3-Hydroxybutyrate-Oligomer Hydrolase in Wautersia eutropha H16. *J. Bacteriol*. **2005**. 187 (15). 5129-5135

22. Eggers, J., Steinbuchel, A. Poly(3-Hydroxybutyrate) Degradation in Ralstonia eutropha H16 Is Mediated Stereoselectively to (S)-3-Hydroxybutyryl Coenzyme A (CoA) via Crotonyl-CoA. *J. Bacteriol*. **2013**. 195 (14). 3213-3223

23. Ong, S.Y., Chee, J. Y., Sudesh, K. Degradation of Polyhydroxyalkanoate (PHA): a Review. *J. Sib. Fed. Univ. Biol.* **2017**. 10 (2), 211-225

24. Luzier, W. Materials derived from biomass/biodegradable materials. *Proc. Natl. Acad. Sci.* **1992**. 89. 839-842

25. Shah, A.A., Hasan, F., Hameed, A., Ahmed, S. Biological degradation of plastics: A comprehensive review. *Biotechnol. Adv.* **2008**. 26. 246-265

26. Mergaert, J. Webb, A., Anderson, C., Wouters, A., Swings, J. Microbial degradation of poly (3-hydroxybutyrate) and poly (3-hydroxybutyrate-*co*-3-hydroxyvalerate) in soils. *Appl. Environ.l Microbiol.* **1993**. 59 (10). 3233-3238

27. Mukai, K., Yamada, K., Doi, Y. Efficient hydrolysisof polyhydroxyalkanoates by Pseudomonas stutzeri YM1414 isolated from lake water. *Polymer Degrad. Stab.* **1994**. 43. 319-327

28. Kasuya, K., Doi, Y., Yao, T. Enzymatic degradation of poly[(R)-3-hydroxybutyrate]by Comarnonas testosteroni ATSU of soil bacterium. *Polymer Degrad. Stab*. **1994**. 45. 379-386.

29. Lee S.Y., Choi J.I. Production and degradation of polyhydroxyalkanoates in waste environment. *Waste Management.* **1999.** 19 (2). 133-139

30. Ong, S.Y., Sudesh, K. Effects of polyhydroxyalkanoate degradation on soil microbial community. *Polymer Degrad. Stabil.* **2016**. 131. 9-19

31. Lee, S. Y. Bacterial Polyhydroxyalkanoates. *Biotechnol. Biol.* **1996**. 49. 1-14

32. Bugnicourt, E., Cinelli, P., Lazzeri, A., Alvarez, V. Polyhydroxyalkanoate (PHA): Review of synthesis, characteristics, processing and potential applications in packaging, *Express Polymer Let*. **2004**. 8 (11). 791–808

33. Kim, Y.B., Lenz, R.W., Fuller, R.C., Poly-3-Hydroxyalkanoates containing unsaturated repeating units produced by pseudomonas oleovorans, *J. Polym. Sci. Part A Polymer Chem.* **1995**. 33. 1367–1374

34. Curley, J.M., Hazer, B., Lenz, R.W., Fuller, R.C. Production of Poly(3-hydroxyalkanoates) Containing Aromatic Substituents by Pseudomonas oleovorans. *Macromol*. **1996**. 29. 1762–1766

35. Chen, GQ., Wang, Y. Medical applications of biopolyesters Polyhydroxyalkanoates. *Chinese J. Polymer Sci.* **2013**. 31 (5). 719-736

36. Nobles, G.A.R., Marchessault, R.H., Maysinger, D. Polyhydroxyalkanoates: Materials for Delivery Systems. *Drug Deliv.* **1998**. 5. 167-177

37. Bissery, M.C., Valeriote,F.A., Thies, C. Therapeutic efficacy of CCNU-loaded microspheres prepared from poly (D,L) lactide (PLA) or poly-B-hydroxybutyrate (PHB) against Lewis lung (LL) carcinoma. *Proceed. Am. Assoc. Canc. Res*. **1985**. 26.

38. Gould, P.L., Holland, S.J., Tighe, B.J. Polymers for biodegradable medical devices. IV. Hydroxybutyrate-valerate copolymers as non-disintegrating matrices for controlled release oral dosage forms, Int. J. Pharm. **1987**. 38. 231–237

39. Yagmurlu, M.F., Korkusuz, F., Gursel I., Karkusuz, P., Ors, U., Hasirci, V. Sulbactam-cefoperazone polyhydroxybutyrate-co-hydroxyvalerate (PHBV) local antibiotic delivery system: in vivo effectiveness and biocompatibility in the treatment of implant-related experimental osteomyelitis. *J. Biomed. Mater. Res*. **1999**. 46 (4). 494–503

40. Shrivastav, A., Kim, HY., Kim, YR. Advances in the Applications of Polyhydroxyalkanoate Nanoparticles for Novel Drug Delivery System. *Biomed. Res. Inter.* **2013**.

41. Pramual, S., Assavanig, A., Bergkvist, M., Batt, C.A., Sunintaboon, P., Lirdprapamonhgkol, K., Svasti, J., Niamsiri, N. Development and Characterization of Bio-Derived Polyhydroxyalkanoate Nanoparticles as a Delivery System for Hydrophobic Photodynamic Therapy Agents. *J. Mater. Sci. Mater. Med.* **2016**. 27 (2)

42. Chen, GQ., Zhang, J. Microbial Polyhydroxyalkanoates as medical implant biomaterials. *Artific. Cell. Nanomed. Biotechnol.* **2018**. 46 (1). 1-18

43. Lim, J., You, M., Li, J., Li, Z. Emerging bone tissue engineering via polyhydroxyalkanoate (PHA)-based scaffolds. *Mate. Sci. Eng. C.* **2017**. 79. 917-929

44. Wang, Y.W., Wu, Q., Chen, GQ. Attachment, proliferation and differentiation of osteoblasts on random biopolyester poly(3-hydroxy- butyrate-co-3-hydroxyhexanoate) scaffolds. *Biomater*. **2004**. 25. 669–675

45. Deng, Y., Zhao, K., Zhang, X.F., Hu, P., Chen, GQ. Study on the three-dimensional proliferation of rabbit articular cartilage-derived chondrocytes on polyhydroxyalkanoate scaffolds. *Biomater*. **2002**. 23. 4049–4056.

46. Sodian, R., Hoerstrup, S.P., Sperling, J.S., Daebritz, S.H., Martin, D.P., Schoen, F.J., Vacanti, J.P., Mayer Jr, J.E. Tissue engineering of heart valves: in vitro experiences. *Ann. Thorac. Surg.* **2000**. 70. 140-144

47. Apte, S.S., Paul, A., Prakash, S., Shum-Tim, D. Current developments in the tissue engineering of autologous heart valves: moving towards clinical use. *Fut. Cardiol.* **2011**. 7 (1).

48. Wang, L., Wang, Z.H., Shen, C.Y., You, M.L., Xiao, J.F., Chen, G.Q. Differentiation of human bone marrow mesenchymal stem cells grown in terpolyesters of 3-hydroxyalkanoates scaffolds into nerve cells. *Biomater*. **2010**. 31 (7). 1691–1698

49. Novikova L.N., Pettersson, J., Brohlin, M., Wilberg, M., Novikov, L.N. Biodegradable poly- beta-hydroxybutyrate scaffold seeded with Schwann cells to pro- mote spinal cord repair. *Biomater*. **2008**. 29. 1198–1206

50. Young, R.C., Wiberg, M, Terenghi, G. Poly-3-hydroxybutyrate (PHB): a resorbable conduit for long-gap repair in peripheral nerves. *Br. J. Plast. Surg*. **2002**. 55. 235–240.

51. Rostovtsev, V.V., Green, L.G., Fokin,V.V., Sharpless, K.B,. A Stepwise Huisgen Cycloaddition Process: Copper(I)-Catalyzed Regioselective “Ligation” of Azides and Terminal Alkynes. *Angew. Chem. Int. Ed*. **2002**. 41. 2708-2711

52. Totobenazara, J., Burke, A.J., New click-chemistry methods for 1,2,3-triazoles synthesis:recent advances and applications. *Tetrahedron Let*. **2015**. 56. 2853-2859

53. Thirumurugan, P., Matosiuk, D., Jozwiak, K. Click chemistry for drug development and diverse chemical-biological applications. *Chem. Rev.* **2013**. 113. 4905-4979

54. Rodionov, V.O., Fokin, V.V., Finn, M.G. Mechanism of the ligand-free Cu(1)-catalyzed azide-alkyne cycloaddition reaction. *Agnew. Chem. Int. Ed.* **2005**. 44. 2210-2215

55. Rodionov, V.O., Presolski, S.I., Diaz, D.D., Fokin, V.V., Finn, M.G. Ligand-accelerated Cu-catalyzed azide-alkyne cycloaddition: a mechanistic report. *J. Am. Chem. Soc*. **2007**. 129. 12705-12712

56. Presolski, S.I., Hong, V., Cho, S.H., Finn, M.G. Tailored Ligand Acceleration of the Cu-Catalyzed Azide-Alkyne Cycloaddition Reaction: Practical and Mechanistic Implications. *J. Am. Chem. Soc.* **2010**. 132 (41). 14570-14576

57. Kai, D., Loh, X.J. Polyhydroxyalkanoates chemical modifications toward biomedical applications, *ACS Sustain. Chem. Eng*. **2014**. 2. 106–119

58. Tortajada, M., da Silva, L.F., Prieto, M.A. Second-generation functionalized medium-chain-length polyhydroxyalkanoates: the gateway to high-value bioplastic applications. *Int. Microbiol.* **2013**. 16. 1–15

59. Nkrumah-Agyeefi, S., Scholz, C. Chemical modification of functionalized polyhydroxyalkanoates via “Click” chemistry: A proof of concept. *Inter. J. Biol. Macromol.* **2017**. 95. 796-808

60. Carey, F.A. *Organic Chemistry*, 7th ed, McGraw Hill: Boston, 2008, 162-165

61. Sparks, J., Scholz, C. “Synthesis and characterization of a cationic poly(-hydroxyalkanoate)” *Biomacromol*. **2008**. 9(8). 2091-2096

62. Hein, J.E., Fokin, V.V. Copper-catalyzed azide–alkyne cycloaddition (CuAAC) and beyond: new reactivity of copper(I) acetylides. *Chem. Soc. Rev.* **2010**. 39 (4). 1302-1315

63. Gao, J., Wang, Z., Xu, D., Zhang, R. Solubilities of Triphenylphosphine in Ethanol, 2-Propanol, Acetone, Benzene, and Toluene. *J. Chem. Eng. Data*. **2007**. 52. 189-191

64. Nkrumah-Agyeefi, S., Pella, B.J., Singh, N., Mukherjee, A., Scholz, C. Modification of polyhydroxyalkanoates: Evaluation of the effectiveness of novel copper(II) catalysts in click chemistry. *Inter. J. Biol. Macromol.* **2019**. 128. 376-384